The Geological Society of America
Special Paper 480
2011

Geochemical mapping of the Kings-Kaweah ophiolite belt, California—Evidence for progressive mélange formation in a large offset transform-subduction initiation environment

J. Saleeby*
Division of Geological and Planetary Sciences, California Institute of Technology, Pasadena, California 91125, USA

ABSTRACT

The Kings-Kaweah ophiolite belt of the southwestern Sierra Nevada Foothills was generated in two pulses of mid-oceanic-ridge basalt (MORB) magmatism. The first was in the Early Ordovician, which resulted in the generation of a complete abyssal crust and upper mantle section. The crustal section was rendered from convecting mantle whose Nd, Sr, and Pb isotopic systematics lie at the extreme end of the sub-Pacific mantle regime in terms of time integrated depletions of large ion lithophile (LIL) elements. Semi-intact fragments of this Early Ordovician oceanic lithosphere sequence constitute the Kings River ophiolite. Following ~190 m.y. of residence in the Panthalassa abyssal realm, a second pulse of MORB magmatism invaded the Early Ordovician lithosphere sequence in conjunction with intensive ductile shearing and the development of ocean floor mélange. This Permo-Carboniferous magmatic and deformational regime produced many of the essential features observed along spreading ridge–large-offset transform fracture zones of the modern ocean basins. During this regime, Early Ordovician upper mantle–lower crustal rocks were deformed in the ductile regime along what appears to have been an oceanic metamorphic core complex, as well as along steeply dipping strike-slip ductile shear zones that broke the ophiolite into semi-intact slabs. Progressive deformation led to the development of serpentinite-matrix ophiolitic mélange within the abyssal realm. This (Kaweah) serpentinite mélange constitutes the majority of the ophiolite belt and encases fragments of both disrupted Early Ordovician oceanic lithosphere and crustal igneous-metamorphic assemblages that were deformed and disrupted as they formed by diffuse spreading along the fracture zone. An ~190 m.y. hiatus in abyssal magmatism cannot be readily accommodated in the current configuration of Earth's ocean basins, but it was possible during the mid- to late Paleozoic Panthalassa regime, when the proto-Pacific basin occupied over half of the Earth's surface.

The transform history of the ophiolite belt can be directly linked to the late Paleozoic transform truncation of the SW Cordilleran passive margin. Following juxtaposition of the transform ophiolite belt with the truncated margin a change in relative

*jason@gps.caltech.edu

Saleeby, J., 2011, Geochemical mapping of the Kings-Kaweah ophiolite belt, California—Evidence for progressive mélange formation in a large offset transform-subduction initiation environment, *in* Wakabayashi, J., and Dilek, Y., eds., Mélanges: Processes of Formation and Societal Significance: Geological Society of America Special Paper 480, p. 31–73, doi:10.1130/2011.2480(02). For permission to copy, contact editing@geosociety.org.

plate motions led to the inception of east-dipping subduction, and the en masse accretion of the ophiolite belt to the hanging wall of the newly established subduction zone. Structural relations and isotopic data on superimposed igneous suites show that the ophiolite belt was not obducted onto the SW Cordilleran continental margin. The accreted ophiolite belt formed the proto-forearc of the newly established active margin. The ophiolite belt never saw high-pressure/temperature (P/T) metamorphic conditions. Rare small blocks of high-pressure metamorphic rocks were entrained from the young subduction zone by serpentinite diapirs and emplaced upward into the ophiolitic mélange within a proto-forearc environment. An Sm/Nd garnet-matrix age on a high-pressure garnet amphibolite block suggests subduction initiation at ca. 255 Ma. This timing corresponds well with the initiation of arc magmatism along the eastern Sierra Nevada region. In Late Triassic to Early Jurassic time proximal submarine mafic eruptions spread across and mingled with hemipelagic and distal volcaniclastic strata that were accumulating above the accreted ophiolite belt. These lavas carry boninitic to arc tholeiitic and primitive calc-alkaline geochemical signatures. By Middle Jurassic time siliciclastic turbidites derived from early Paleozoic passive margin strata and early Mesozoic arc rocks spread across the primitive forearc. In late Middle to Late Jurassic time tabular plutons and dike swarms of calc-alkaline character invaded the ophiolite belt in a transtensional setting. Deformation fabrics that developed in these intrusives, as well as cleavage that developed in the cover strata for the ophiolite belt, imparted components of superimposed finite strain on the ophiolitic mélange structure but did not contribute significantly to mélange mixing. By ca. 125 Ma, copious gabbroic to tonalitic plutonism of the western zone of the Cretaceous Sierra Nevada batholith intruded the ophiolite belt and imparted regional contact metamorphism. Such metamorphism variably disturbed U/Pb systematics in rare felsic intrusives of the ophiolite belt but did not significantly disturb whole rock Sm/Nd systematics. Age constraints gained from the Sm/Nd and U/Pb data in conjunction with Nd, Sr, and Pb isotopic and trace element data clearly define the polygenetic abyssal magmatic history of the ophiolite belt. The variation of Nd and Sr radiogenic isotopes over time from the Paleozoic abyssal assemblages, through early Mesozoic supra-subduction zone volcanism to Early Cretaceous batholithic magmatism, record the geochemical maturation of the underlying mantle wedge without the involvement of SW Cordilleran continental basement.

INTRODUCTION

Mélanges are characterized by the encasement of coherent blocks of rock within a pervasively deformed less competent rock matrix (Hsü, 1968). The blocks may be exotic or native to the hosting matrix, although the inclusion of exotic blocks is the most commonly cited feature interpreted to indicate extreme disruption in the formation of mélange. The common occurrence of mélanges as tectonically bounded units within exhumed active margin assemblages has led to the common assumption that tectonic disruption leading to mélange formation is, a priori, the direct result of subduction megathrust movements. In colloquial usages the term *subduction mélange* is commonly used in place of what should be the descriptive term *mélange*. Subduction megathrust environments are well suited for mélange formation, but this chapter takes the position that a number of alternative mechanisms for mélange formation exist, and that such mélange units may form and then be subsequently accreted into active margin assemblages en masse.

This chapter integrates structural, geochronological, and geochemical data for the resolution of the temporal relations and environment of formation of the regional mélange structure of the Kings-Kaweah ophiolite belt of the southwestern Sierra Nevada Foothills metamorphic belt. Similar Paleozoic ophiolitic mélange and related tectonite units occur along the entire length of the Sierra Foothills (see Saleeby, 1990, for a review). Mesozoic overprints have obscured many of the critical relations and have been emphasized in the literature, thereby obscuring the importance of Paleozoic ophiolitic tectonics in terms of the first order shaping of the SW Cordilleran margin. Within the Kings-Kaweah ophiolite belt, several different mechanisms for late Paleozoic and possibly Early Triassic mélange formation are recognized that are not directly related to subduction megathrust motions. Moreover, these processes in conjunction with components of superimposed finite strain account for the entire mélange structure, with no compelling evidence that subduction megathrust motions directly contributed to the mélange mixing process. An abundance of literature documents such disruptive processes, yet they are rarely taken into account in the literature on mélanges. For example, vast tracks of severely disrupted abyssal crust and upper mantle are known to have developed at spreading center–transform intersections and are thereby packaged into abyssal crust along fracture zones (Aumento et al., 1971; Bonatti et al., 1971, 1973; Van Andel et al., 1971; Melson and Thompson, 1971; Melson et al., 1972; Bonatti and Honnorez, 1976; Fox et al., 1976; DeLong et al., 1977; Schreiber and Fox, 1977; CAYTROUGH, 1978; Karson and Dick, 1983; MacDonald et al., 1986; Pockalny et al., 1988; Johnson and Dick, 1992). Furthermore, thick and expansive accumulations of severely disrupted sediment that formed by massive submarine landslides are known to form in modern transform valley troughs as well as along both active and passive margins (cf. Moore et al., 1970, 1976; Jacobi, 1976; Johnson and Dick, 1992; Deplus et al., 2001) but are only rarely recognized as such after their emplacement and metamorphism within active margin belts (cf. Cox and Pratt, 1973; Schweickert et al., 1977). Thirdly, serpentinite diapirism with the inclusion of exotic metamorphic blocks and related seafloor extrusion of serpentinite debris flows are known to be important processes in oceanic transform and forearc environments (Lockwood, 1971; Bonatti et al., 1973, 1974; Fryer et al., 2000; Johnson and Dick, 1992). A major challenge in the analysis of active margin belts lies in the recognition of these less familiar mélange formation mechanisms, and the resolution of their role within the regional tectonic history.

The ophiolitic mélange problem in the Sierra Foothills belt, and arguably at global scale, encompasses transform tectonics of the abyssal realm as well as subduction zone initiation and primitive forearc evolution. Intimately related to this problem is the possibility that true abyssal lithosphere evolves in geodynamic settings that are not likely to render ophiolite emplacement into continental margin orogens (cf. Stern, 2004). The position taken in this chapter is that subduction initiation along a large offset transform juncture is a viable mechanism for such abyssal ophiolite emplacement along continental margin orogens. This mechanism does not necessarily entail ophiolite obduction onto continental crust, in that fragments of abyssal lithosphere may be accreted to the hanging wall of the newly established subduction zone and thereby form parts of the resulting proto-forearc. For example, tectonic relations along the Izu-Bonin-Mariana arc system indicate that the system originated in the Eocene by subduction initiation along a large offset oceanic transform (Hilde et al., 1977). Fragments of the Pacific plate were accreted to the hanging wall of the young subduction zone (De Bari et al., 1999), to be subsequently joined by proto-forearc assemblages formed by in situ igneous rifting with the eruption of boninitic to arc tholeiitic magma series rocks (Stern et al., 1991; Stern and Bloomer, 1992). The Macquarie Ridge–Puysgur trench–Fiordland plate juncture system represents a case of ongoing subduction initiation along a transform system where abyssal lithosphere is being actively accreted to part of the newly established hanging wall (Varne and Rubenach, 1972; Casey and Dewey, 1984). The Kings-Kaweah ophiolite belt records a petrotectonic evolutionary sequence and lies in a paleogeographic setting that entails elements of both of these Cenozoic subduction initiation systems.

Specific challenges in interpreting the geologic history of the Kings-Kaweah ophiolite belt, beyond its mélange structure, arise from its intruded and contact metamorphosed state. Subsequent to its tectonic disruption and emplacement into the SW Cordilleran margin the ophiolite belt was invaded by copious gabbroic to tonalitic plutons of the Sierra Nevada batholith (Mack et al., 1979; Saleeby and Sharp, 1980; Chen and Moore, 1982; Clemens-Knott and Saleeby, 1999). Contact metamorphism in albite-epidote to hornblende hornfels facies is near pervasive, leaving only minor lower-grade domains as areas to focus on ophiolite protolith features. Regardless, pre-batholithic features are locally preserved well enough to decipher the geochemical heritage and early tectonic development of the belt. Previous detailed structural and petrographic studies characterized the structural and metamorphic state of the ophiolite belt in detail (Saleeby, 1975, 1977, 1978, 1979), and geochronological studies have provided a number of age constraints on the igneous development of the belt and the complexities of polyphase igneous and thermal overprints (Saleeby and Sharp, 1980; Saleeby, 1982; Shaw et al., 1987). This paper presents additional isotopic and geochronological data, and coupled major and trace element data from sample sites representative of the principal units of the ophiolite belt exhibiting the lowest grade metamorphic overprints observed, as well as on sample sites preserving critical structural and stratigraphic relations that unfortunately possess relatively high-grade metamorphic overprints. Special focus is placed on isotopic and trace element data in terms of the discrimination of MORB igneous suites from subsequent suites having formed within a supra-subduction zone environment. Major and trace element data are further used as a means to evaluate the potential severity of disturbances in the radiogenic isotopic systems of Nd, Pb, and Sr, as these systems most clearly record the early MORB history of the belt. An overview of the critical structural relations of the ophiolite belt is presented first, and then the geochemical data are integrated with the structural relations as a mapping tool. The results of this integrated structural-geochemical mapping procedure are then integrated with regional tectonic relations in the formulation of a model for progressive ophiolitic mélange development followed by continental margin emplacement in a large offset transform-subduction initiation environment.

GEOLOGIC OVERVIEW

Regional Structure

The Kings-Kaweah ophiolite belt extends for ~130 km along the western Sierra Nevada Foothills between 35.9° N and 37° N (Fig. 1). It constitutes the southern segment of the Foothills metamorphic belt, where the Foothills belt is more highly intruded by the Sierra Nevada batholith than to the north. Basement core data (May and Hewitt, 1948; Wentworth et al., 1995; Saleeby, 2007, and unpub. data) indicate that rocks typical of

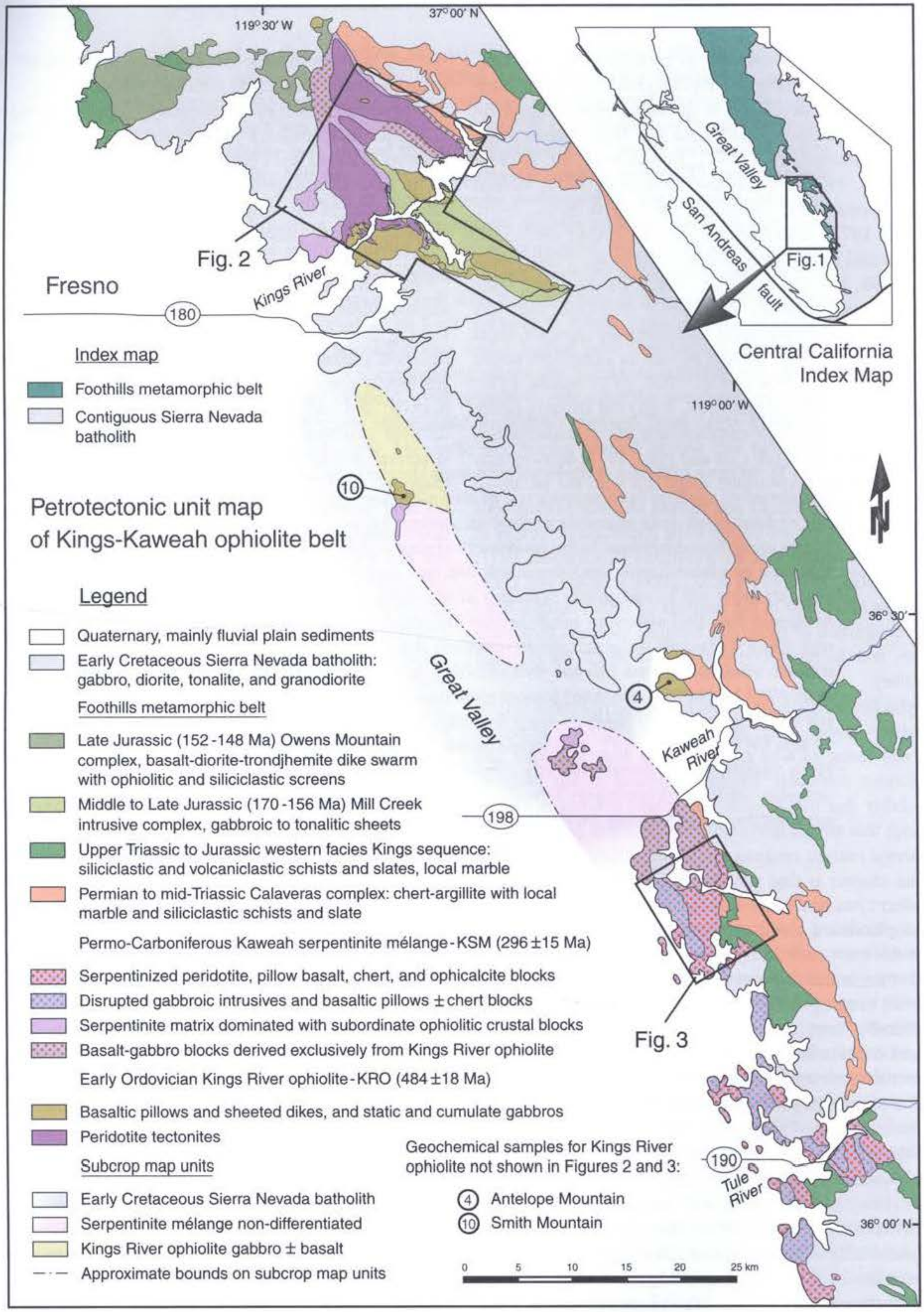

Figure 1. Petrotectonic unit map of the Kings-Kaweah ophiolite belt and related metasedimentary rocks. Geology after Saleeby (1977, 1978, and 1979), and subcrop mapping of Great Valley margin from gravity-magnetic modeling (Saleeby, 1975; Oliver and Robbins, 1978) and basement core data (Saleeby, 2007, and unpub. data).

the Kings-Kaweah ophiolite belt and its metamorphosed lower Mesozoic cover strata, as well as crosscutting Sierra Nevada batholith plutons, occur at least as far west as ~30 km beyond the Foothills basement exposures, and that such rocks continue in the Great Valley subsurface at least as far south as 35.4° N. Figure 1 depicts the Kings-Kaweah ophiolite belt in terms of its constituent petrotectonic units: some units characterized as large polylithologic slabs, and others as mélange units characterized by distinct block assemblages. Pre–Sierra Nevada batholith metamorphic wall rocks that lie directly east of the Kings-Kaweah ophiolite belt consist of chert-argillite and marble of the Permian to Middle Triassic Calaveras complex, which are locally intergradational with siliciclastic schists, mafic to felsic metavolcanic rocks, and marble, which constitute the western facies of the Upper Triassic–Jurassic Kings sequence (Saleeby et al., 1978; Saleeby and Busby, 1993). These metasedimentary rocks are in ductile-brittle fault contact along the east margin of the Kings-Kaweah ophiolite belt (Figs. 1 and 2), but also, at least locally, sit nonconformably above the belt (Fig. 3). In this structural setting these rocks are referred to as cover strata for the ophiolite belt. Cleavage that is axial planar to meso- and map-scale folds within the cover strata crosses the folded nonconformity with the ophiolite belt, and re-deforms the basement mélange structure by imparting additional components of finite strain. Structural and temporal relations of cleavage development in the cover strata, and ductile deformation fabrics in relatively low-volume early Mesozoic intrusions that crosscut the ophiolite belt, are discussed in Saleeby (1979) and Saleeby and Dunne (2011).

The central segment of the Kings-Kaweah ophiolite belt (36.5° N to 36.7° N) is in part cut out by a series of Early Cretaceous gabbroic to tonalitic plutons of the Sierra Nevada batholith (Saleeby and Sharp, 1980; Clemens-Knott and Saleeby, 1999) and is in part buried beneath Quaternary deposits of the southeastern Great Valley (Fig. 1). A buried pendant of the ophiolite belt lies directly west of the edge of the Foothills between 36.45° N and 36.7° N. The pendant and adjacent buried Sierra Nevada batholith plutons are shown in subcrop in Figure 1 based on gravity and magnetic modeling (Saleeby, 1975, 2007; Oliver and Robbins, 1978), geologic observations of small isolated hills that expose basement rocks, and on basement core data (Saleeby, 2007, and unpub. data). The central segment of the ophiolite belt sits between two distinct, yet closely related, segments that are relatively well exposed along steep sided grassy hills. The northern segment consists of the Kings River ophiolite, and the southern segment consists of the main exposures of the Kaweah serpentinite mélange. The Kings River ophiolite and the Kaweah serpentinite mélange are closely related. Serpentinite mélange zones of Kaweah affinity extend into and disrupt the Kings River ophiolite, whereas mélange blocks derived from this ophiolite occur as one of the distinct inclusion assemblages within the Kaweah serpentinite mélange.

Serpentinite-matrix mélange zones of the Kings-Kaweah ophiolite belt appear to have formed by at least four distinct mechanisms (Saleeby, 1978, 1979). These consist of the following:

1. Focused ductile shear strain that developed under high-grade, retrogressing to medium-grade, metamorphic conditions, and that resulted in the progressive disruption and mixing of the original ophiolite stratigraphy. Where such strain penetrated upper mantle levels the resulting peridotite mylonites underwent domainal hydration to form antigorite ± talc ± tremolite schist zones that concentrated subsequent shear strain, resulting in the entrainment of blocks derived from crustal rocks.

2. The progressive disruption and abrasion of completely serpentinized peridotite blocks with the marginal entrainment of exotic blocks, probably during diapiric rise. Vestigial ultramafic blocks in these cases commonly possess a distinct blocky fracturing, which, based on textural relations, developed prior to Sierra Nevada batholith contact metamorphism. Such blocky fracturing is common in the core areas of serpentinite diapirs (Moiseyev, 1970; Lockwood, 1971).

3. The emplacement of foliated serpentinite sheets along extensional and dilational shear fractures in otherwise coherent mafic rocks.

4. Mixing of debris flow and detrital serpentinites with various ophiolitic slide blocks on the seafloor. Such sedimentary mixtures readily acquired a strong shape fabric during the superposing of finite strain, thereby attaining a structure resembling that of tectonic mélange. Direct links between the later three mechanisms are suggested by their intergradational relationships, and by the logic of sourcing detrital and debris flow serpentinites from surfaced diapiric serpentinites.

The four serpentinite mélange formation mechanisms described above account for the majority of the mélange structure of the Kings-Kaweah ophiolite belt. An additional fifth mechanism was locally important, consisting of deeply sourced diapiric serpentinites that entrained rare high-pressure metabasite blocks that are exotic relative to the mafic crustal rocks of the Kings-Kaweah ophiolite belt. Structural, metamorphic, and age data presented below show that this subordinate mechanism significantly postdates the principal activity of the four main serpentinite mélange formation mechanisms.

Kings River Ophiolite

The Kings River ophiolite is exposed in a series of tectonic slabs that are as long as ~20 km and are separated by serpentinite-matrix mélange zones and crosscutting plutons of the Sierra Nevada batholith (Figs. 1 and 2). The principal slabs of the Kings River area consist of the depleted peridotite-cumulate-gabbro Red Mountain–Tivy Mountain slab, sheeted dike–pillow lava slabs of Hughes Mountain and Dalton–Bald Mountain, and the depleted peridotite-mafic tectonite slabs of Hog Mountain and upper Hughes Creek. Additional slabs of cumulate and static textured gabbro and pillow basalt with local sheeted dike sets occur at Smith and Antelope Mountains, respectively, within the highly intruded central segment of the ophiolite belt (Fig. 1). Within the tectonic slabs, various intervals of the original ophiolite succession are preserved. Homogeneity within the various

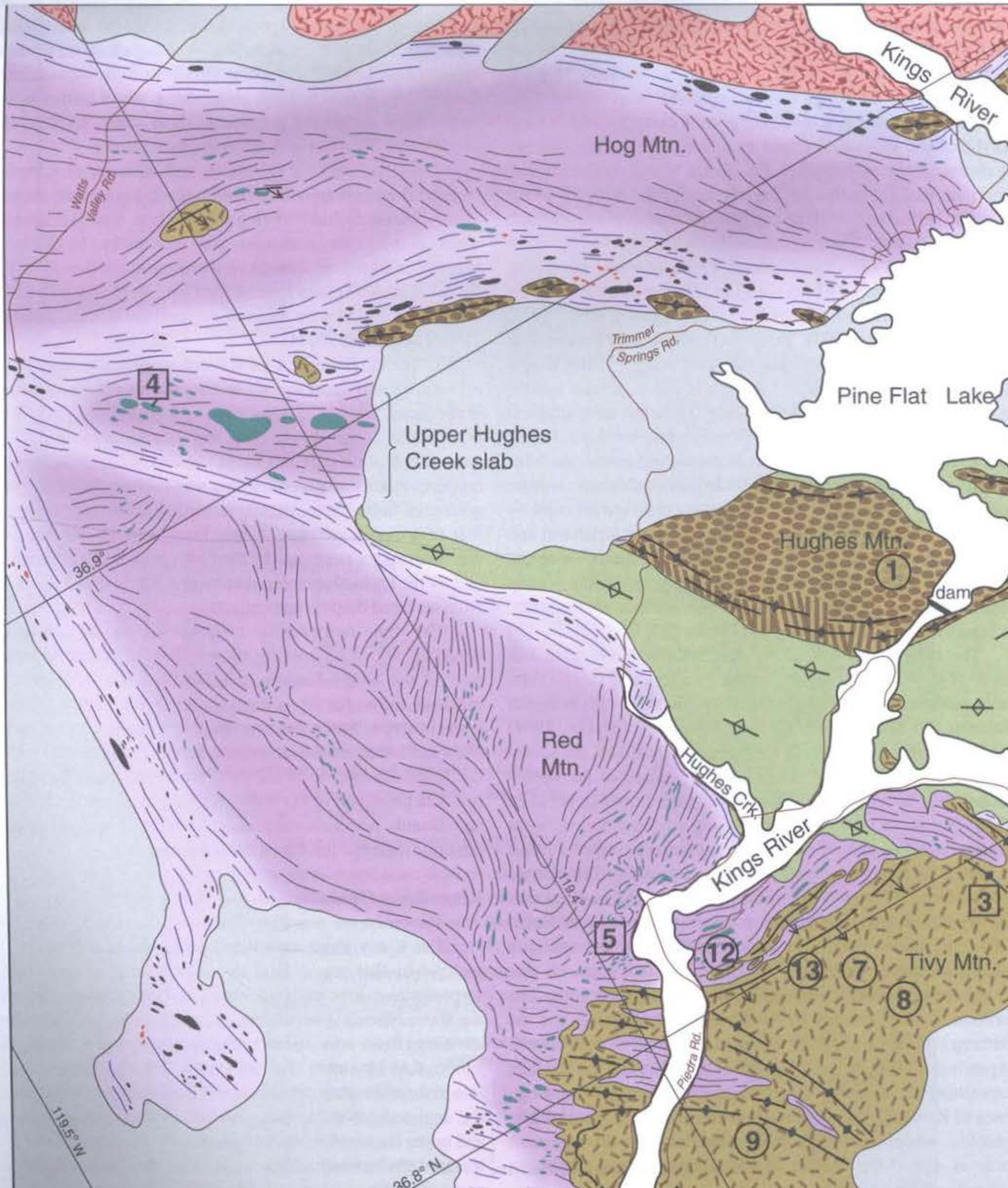

Figure 2 (*Continued on facing page*). Geologic map of the Kings River ophiolite, showing localities of geochemical samples (geology after Saleeby, 1978, and unpub. data).

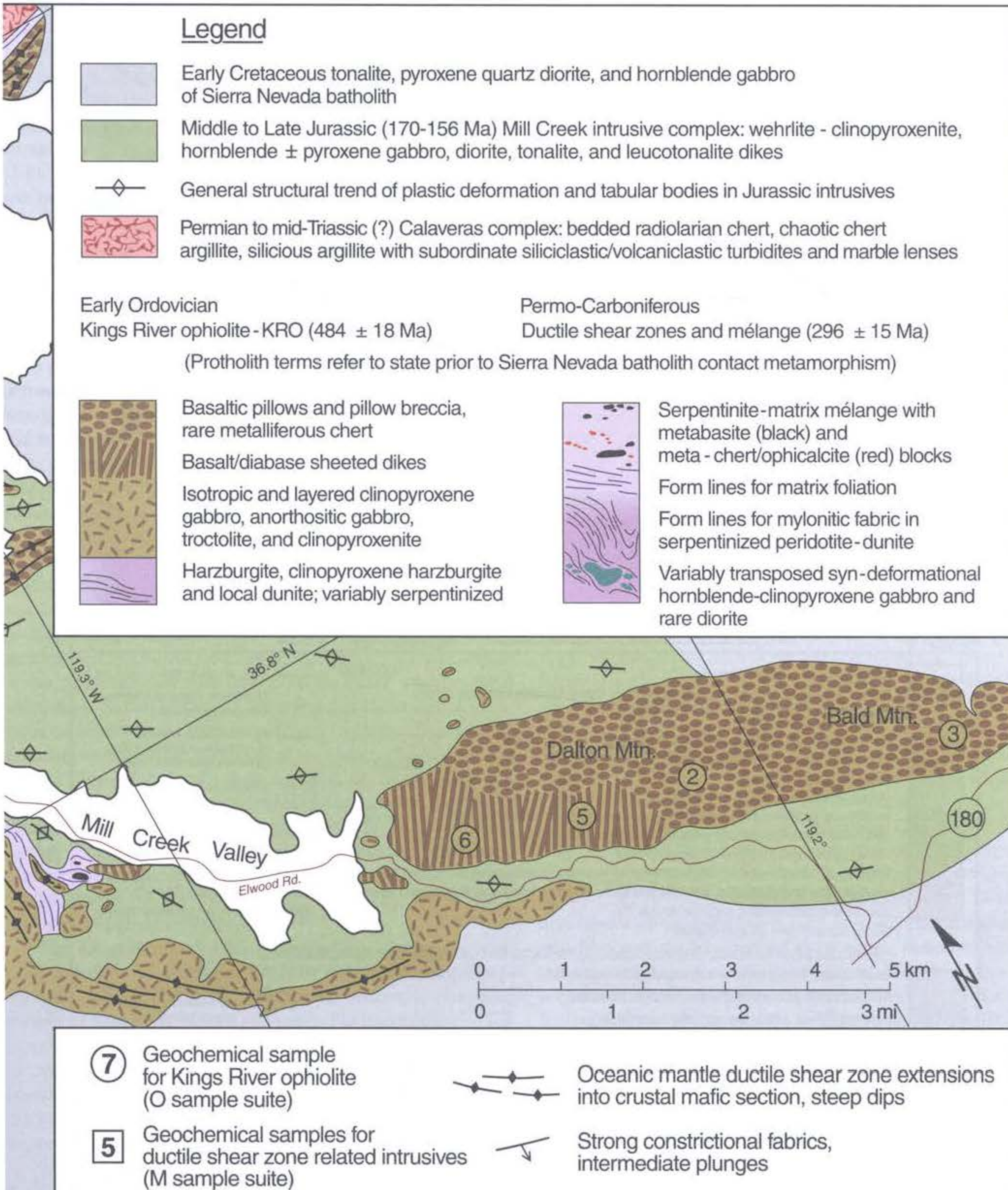

Figure 2 (*Continued*).

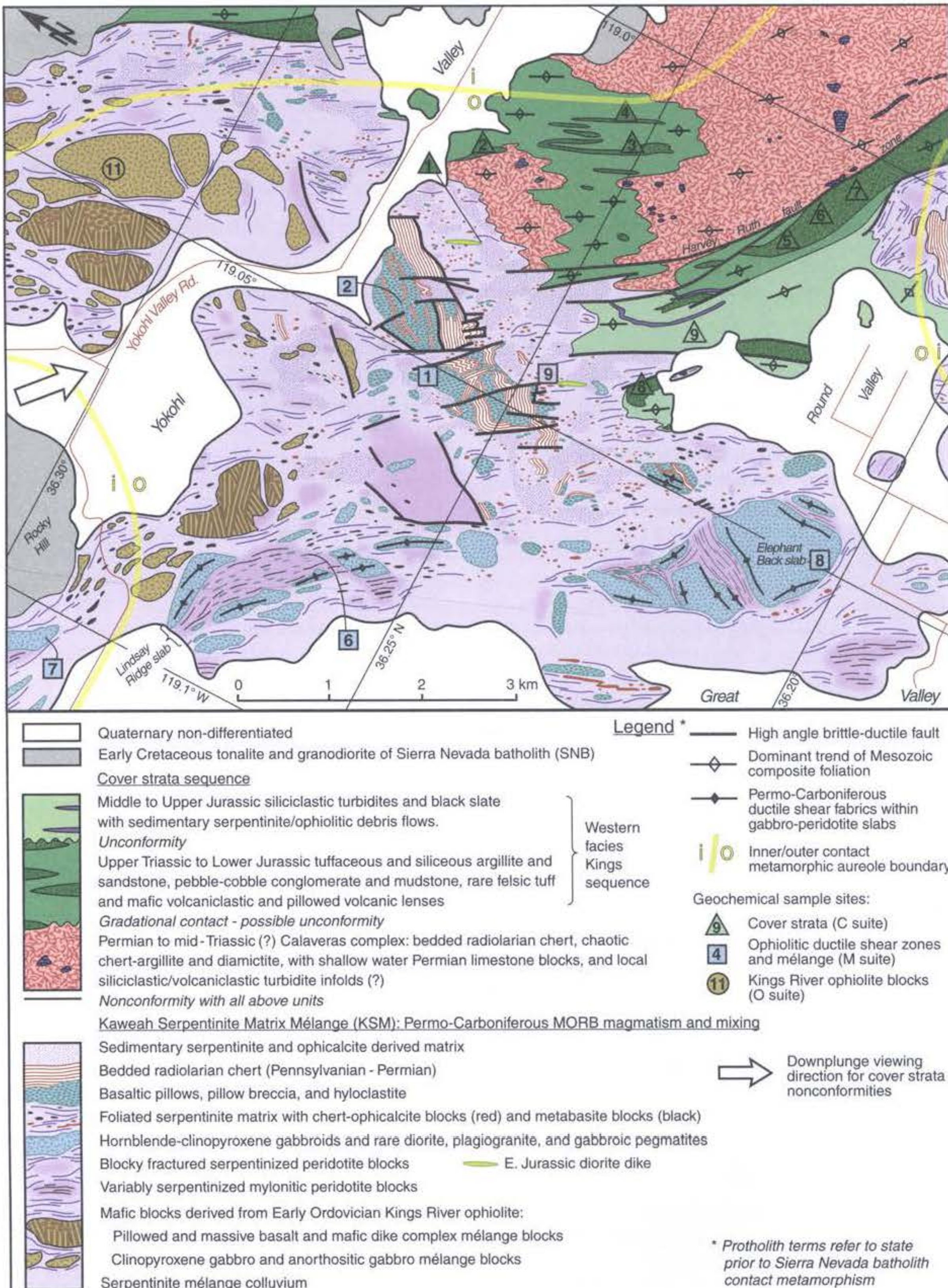

Figure 3. Geologic map of the Yokohl Valley area of the Kaweah serpentinite mélange, showing critical relations with cover strata and localities of geochemical samples (geology after Saleeby, 1979, and unpub. data).

lithologic zones, as well as overlap in the various lithostratigraphic intervals of the original succession that are preserved in adjacent slabs, facilitates the reconstruction of the original lithostratigraphic section (modified after Saleeby, 1978). From the base upward the reconstructed section consists of (1) a variably serpentinized tectonitic harzburgite, clinopyroxene harzburgite, and dunite that are >~6 km thick; (2) cumulate to static textured gabbros (~2 km thick); (3) mafic sheeted dikes (up to ~1 km thick); and (4) pillow basalt (up to ~2 km thick). The pillow basalt locally includes meter-scale lenses of metalliferous radiolarian chert, although a stratigraphic top has not been determined for the pillowed section. All principal exposures of pillow basalt (Hughes, Dalton-Bald, and Antelope Mountain slabs) consist of exceedingly homogeneous pillows, local pillow breccia, and local basaltic feeder dikes. Likewise the sheeted dikes are exceedingly homogeneous basaltic dikes with rare diabase dikes and screens. Basaltic pillows and dikes are either aphyric or modestly plagioclase phyric. The gabbroic rocks are also quite homogeneous with coarse locally layered clinopyroxene gabbro and anorthositic gabbro strongly dominating, and layered troctolite and minor plagioclase ± olivine clinopyroxenite present near the base of the gabbroic section. Wehrlitic and resolvable dunitic cumulates are rare, as are chromite pods concentrated along what is interpreted as the base of the cumulate section, although strong plastic deformation has obscured the primary relations. Much of the Tivy Mountain section is composed of coarse-grained, massive clinopyroxene-plagioclase rock suspected to be adcumulates, although primary textural relations are obscured by contact metamorphism. Igneous textures appear to fine southeastward with transitions into finer static textured and coarse diabasic zones, which, along with the basal ultramafic cumulates to the northwest, suggest a general facing to the cumulate section in the direction of the Dalton–Bald Mountain sheeted dike-pillow basalt sequence (Fig. 2). Smith Mountain (Fig. 1) preserves rocks lithologically identical to the coarse cumulates and finer static-textured gabbros of Tivy Mountain. Gravity-magnetic and basement core data indicate that a large mass of the Smith Mountain gabbro extends in the subsurface northwestward toward Tivy Mountain (Saleeby, 1975, 2007; Oliver and Robbins, 1978).

The Kings River ophiolite contrasts from many or perhaps most ophiolites (cf. Coleman, 1977) by an apparent lack of significantly fractionated rocks. The crustal section is composed entirely of basalt and various gabbroids. No intermediate to felsic-composition plutonic, hypabyssal, or volcanic rocks as part of the principal ophiolitic igneous suite have been discovered. Such fractionated rocks are common in the younger igneous suites that have been superposed across the exclusively MORB affinity Kings River ophiolite mafic crustal section.

Near pervasive contact metamorphism has inhibited detailed petrogenetic studies of the Kings River ophiolite. All primary minerals of the basaltic pillows and dikes are completely overprinted, and only traces of olivine, pyroxenes, and spinel are preserved in the ultramafic rocks. Remnants of igneous plagioclase and clinopyroxene are more widely preserved in gabbros and locally in coarse diabases. Olivine is completely replaced by chlorite, serpentine, and magnetite in troctolites and gabbros but is commonly preserved as grain core remnants in ultramafic rocks.

One of the outstanding features of the Kings River ophiolite is the transposition of the base of the gabbroic section and the continuation of such high plastic strain fabrics downward through much of the depleted peridotite section (Saleeby, 1978). Such strain is of much greater magnitude and encompasses a wider range of retrogressing conditions than what is typical of depleted peridotite sections of many well-preserved ophiolites (cf. Coleman, 1977). Structural form lines are shown in Figure 2 for pervasive mylonitic fabrics in the peridotites. Such widespread ductile shear in the mantle section extends into the mafic crustal section along more discretely defined ductile shear zones, shown in generalized form in Figure 2. Small mafic intrusions consisting of transposed dikes, and folded and boudinaged lenses that are petrologically distinct from the Tivy and Smith Mountain type gabbros, were magmatically emplaced into the shear zones during the principal phase of high-temperature plastic deformation. The shear zones coalesce and penetrate through much of the Red Mountain peridotite, leaving only local vestigial domains where higher temperature, upper-mantle-flow fabrics remain (i.e., Carter and Ave Lallemant, 1970; Boudier and Coleman, 1981). In the Hog Mountain peridotite slab the shear zones are more domainal, leaving larger vestigial domains with the remnants of high-temperature, mantle flow fabrics. The upper Hughes Creek slab is pervasively mylonititc along steep foliation surfaces. The shear zones represent high distributed shear strain within the sub-oceanic mantle that penetrated the crust along more concentrated zones, but they are not mélange. There are two types of shear zones on the basis of their orientations relative to the original ophiolite lithostratigraphy: (1) a basal zone that runs along the sub-oceanic Moho level of the ophiolite, as exposed along the lower Kings River Valley (Fig. 2); and (2) steeply dipping, longitudinal shear zones that cut at high angles across the ophiolite section, and which commonly grade into serpentinite-matrix mélange zones. Deformation fabrics of the basal shear zone are both cut by and merge into fabrics of the longitudinal shear zones, indicating that the two types of shear zones are partly coeval. The basal shear zone is characterized by strong constrictional fabrics with stretch factors typically >~10 that render a rodding structure to many of the transposed intrusions within the peridotites as well as corrugated separation planes in the mylonitic fabric of the peridotites. A relatively well-defined maximum in the principal stretch direction along the basal shear zone plunges at intermediate angles southward beneath the Tivy Mountain gabbro section (Fig. 2). Conflicting non-coaxial shear fabrics distributed within this shear zone appear to integrate into a coaxial component of the principal stretch (Saleeby, 1978). The longitudinal shear zones, where expressed in the peridotite sections, grade into serpentinite mélange zones with the inclusion of rock types exotic to the mantle section, such as pillow basalt, chert, and ophicalcite. Deformation fabrics in the longitudinal shear zones and their transitions into serpentinite mélange zones typically reflect a stronger flattening component than the constrictional fabrics that characterize the basal shear zone.

Ductile shear zones of the Kings River ophiolite developed during the intrusion of a series of distinct brown hornblende-bearing plagioclase-clinopyroxenites, clinopyroxene gabbros with local dioritic fractionates, and sets of solitary diabase dikes. High-temperature hydrothermal veins characterized by mixtures of antigorite, Cr-chlorite, talc, tremolite, and rare anthophyllite developed in the peridotite host during shearing and intrusive activity. These veins were variably transposed along with the mafic intrusive bodies. The intrusive bodies are pervasively mylonitic to ultramylonitic and blastomylonitic with some grading into coarse-banded clinopyroxene amphibolite. They underwent limited fractionation during deformation and crystallization to form variably transposed veins of mylonitic diorite. Embrittlement of the mafic bodies late in the ductile deformation regime is recorded by hornblende ± Na scapolite veining along extensional fractures that are oriented normal to the principal stretch direction. Locally such veins are also transposed into the principal stretch direction by late-stage ductile shear bands. Veining and hydration of the ultramafic host and mafic intrusive lenses are interpreted to have resulted from the influx of ocean water during ductile shearing. Attempts to confirm this by stabile isotope data are foiled by the effects of near pervasive Sierra Nevada batholith contact metamorphism.

Mélange units and ductile shear zones of the Kings River ophiolite are crosscut by a series of Middle to Late Jurassic tabular plutons and dike swarms (Saleeby and Sharp, 1980; Wolf and Saleeby, 1995; Saleeby and Dunne, 2011). These intrusions consist of the Mill Creek and Owens Mountain complexes (Figs. 1 and 2) and numerous small isolated dikes that are most readily observed where they cut ultramafic rocks. The Mill Creek complex consists of NW-trending lenticular gabbroic, dioritic, and tonalitic plutons containing modest to strong ductile deformation fabrics. The Mill Creek complex is structurally coherent. The Owens Mountain complex consists of basaltic, gabbroic, dioritic, and trondhjemitic dikes and small lenticular stocks that intrude and include as screens the western serpentinite mélange zone of the Kings River ophiolite (Fig. 1). The Owens Mountain complex is also deformed but structurally coherent, like the Mill Creek complex. A critical feature of the Mill Creek and Owens Mountain complexes is that they crosscut and thus postdate serpentinite mélange formation, yet they are plastically deformed. Thus they provide age constraints on both mélange development and on finite strain superimposed across the mélange structure. The ductile deformation fabrics of the Mill Creek and Owens Mountain intrusive complexes, as well as those of the Kings-Kaweah ophiolite belt mélange structure, are truncated by Lower Cretaceous plutons of the Sierra Nevada batholith (Figs. 1 and 2), which, for the most part, lack ductile deformation fabrics.

Kaweah Serpentinite Mélange

The Kaweah serpentinite mélange consists primarily of a foliated serpentinite matrix in which ophiolitic blocks of a wide range of sizes, shapes, and compositions are dispersed. The serpentinite matrix was derived from tectonitic peridotite, diapiric serpentinite, and serpentinitic debris flows and detrital rocks. The mélange blocks consist mainly of serpentinized peridotite, gabbro, diabase, basalt, chert, and ophicalcite. The blocks in many localities are oriented with long axes parallel to the matrix foliation, and they range in size from centimeters to kilometers. Relict primary features are preserved within the blocks, such as bedding, pillows, dikes, and cumulate layering. Ophicalcites occur as bedded carbonates with dispersed serpentinite ± basalt ± chert clasts, as submarine regoliths developed on serpentinites and serpentinized peridotites, and as vein networks along submarine faults and extensional fractures within ultramafic rocks.

Outcrop mapping reveals clustering of mélange blocks into several lithologic associations (Saleeby, 1977, 1979). The associations are defined as mélange units (Fig. 1), some of which appear to represent internally mixed vestiges of once intact ocean-floor sections. Four principal types of mélange units are recognized: (1) serpentinite matrix-rich, with highly dispersed blocks typically of mafic tectonite, chert, and ophicalcite; (2) dense block clusters derived almost solely from the mafic crustal rocks of the Kings River ophiolite; (3) block and block-like bodies of distinctive gabbroids and diabases that were intruded into variably deformed and serpentinized peridotite, and adjacent blocks consisting of pillow basalt, pillow breccia, and hyloclastite, as well as local chert; and (4) completely serpentinized peridotite, basalt, and chert, commonly with ophicalcite blocks and/or matrix disseminations. The first two units represent variably disrupted remnants of the Kings River ophiolite peridotite section and its crustal section, respectively. The third type of mélange unit represents "abnormal" abyssal crust composed of crustal-level serpentinized peridotite that was intruded by variably fractionated gabbroids and diabases, and which sat beneath pillowed eruptions and pelagic sediments. The fourth type also represents "abnormal" abyssal crust consisting of serpentinite diapirs and debris flows, detrital serpentinite, ophicalcite, chert, and pillowed eruptions. Relationships discussed below indicate that serpentinite diapirism and surface level extrusion were progressive through time, spanning residence in the abyssal realm as well as in the proto-forearc realm following accretion of the Kings-Kaweah ophiolite belt to the SW Cordilleran margin. A severe problem in interpreting these later mélange units is that hypabyssal dikes and pillow lava–breccia mounds having primary contacts with surfaced serpentinites readily broke into mélange block-like inclusions, and hosting detrital serpentinite textures were severely deformed upon superimposed folding and cleavage development. Also, examination of Figure 3 reveals a number of chert "blocks" that are oriented at high angles to the matrix foliation. These bedded bodies are commonly cross-cleaved parallel to the matrix foliation, and many could be the remnants of chert intervals that were interbedded with detrital serpentinite matrix materials. These "mélange" units may in fact not be mélange but instead be highly strained remnants of bedded and diked primary sequences for which strain localization in hosting serpentinites resulted in a serpentinite matrix, mélange-like assemblage.

Age constraints and geochemical data, covered below, as well as stratigraphic relations, reveal two distinct series of MORB pillowed eruptions that constitute the Kings-Kaweah ophiolite belt. The older series formed the upper crustal levels of the Kings River ophiolite abyssal lithosphere section, and sat above a coherent interval of basaltic sheeted dikes. The younger series was erupted during the tectonic disruption of the seafloor and the extrusion of serpentinite. Locally such pillow basalts, pillow breccias, and hyloclastites are interbedded with ophicalcite and sedimentary serpentinite, but in most localities such flows into serpentinitic sediments were broken into blocks or intergradational lenses with matrix material by subsequent deformation. Pillow lavas erupted over the highly disrupted ophiolitic substrate are commonly interbedded with and overlain by radiolarian chert, with the thickest and most continuous chert section increasing upward in siliceous argillite laminae. Such cherts and interbedded pillow flows form diagonal and transverse outcrop belts that cross the structural trend of the mélange. One such outcrop belt that is well preserved runs NE-SW across the central part of the Yokohl Valley map area (Fig. 3). The chert section of this belt is faulted and cross-cleaved parallel to the matrix foliation. The remnants of radiolarian tests are common in thin sections from this belt but are too recrystallized for paleontologic study.

Chert and siliceous argillite of the Calaveras complex lies along a complexly deformed nonconformity above serpentinite mélange, where the matrix was derived primarily from serpentinitic debris flows and detrital rocks (Fig. 3). Much of the chert-argillite possesses a chaotic fabric, which commonly grades into diamictites in areas of relatively low superimposed strain. Limestone clasts and blocks ranging up to ~500 m in diameter are encased in the chaotic chert-argillite. These rocks are most readily interpreted as olistostromes or submarine landslides (Saleeby 1979). Some of the larger limestone olistoliths contain Permian shallow-water benthic foraminifers (Saleeby et al., 1978). The remnants of radiolarian tests are common in thin sections of the chaotic cherts but are everywhere too recrystallized for paleontologic study. The stratigraphic thickness of the Calaveras complex is poorly constrained, whereas structural thickness ranges up to ~3 km where it sits on the Kaweah serpentinite mélange (Fig. 3), and up to ~5 km in the outcrop belt east of the Kings-Kaweah ophiolite belt (Fig. 1). It seems likely that the Calaveras complex of the study region in its entirety once sat above the disrupted Kings-Kaweah ophiolite belt, but currently much of it is dislodged from its original basement by Sierra Nevada batholith magmatism, or alternatively, Kings-Kaweah ophiolite belt basement remnants lie concealed beneath the eastern outcrop belt. The upper stratigraphic levels of the Calaveras chert-argillite grade into siliciclastic, volcaniclastic, and mafic flows of the Upper Triassic–Jurassic western facies Kings sequence (Saleeby, 1979; Saleeby and Busby, 1993). These strata possess a cleavage but are structurally intact except where they are adjacent to local basement-derived serpentinite dikes (Fig. 3). Except for such dikes and their derivative submarine debris flows, the lack of ophiolitic lithologies mixed into the Calaveras or western Kings sequence places a pre–early Mesozoic relative age constraint for mélange mixing, analogous to the structural chronology posed by Jurassic intrusive complexes that cut the Kings River ophiolite ductile shear and serpentinite mélange zones.

Structural complexity and severity of contact metamorphic overprinting require an iterative approach in the structural and petrologic analysis of the Kaweah serpentinite mélange and its relations with the Kings River ophiolite. We now turn to the use of geochemical techniques as a mapping tool in this analysis.

GEOCHEMICAL MAPPING AS A STRUCTURAL AND TECTONIC TOOL

The Kings-Kaweah ophiolite belt presents a unique problem in its tectonic analysis relative to many ophiolites in that numerous generations of mafic intrusive and submarine volcanic units are associated with the ophiolite belt with ages that span much of Paleozoic and Mesozoic time. As demonstrated below, only the Paleozoic assemblages constituted consanguineous abyssal lithosphere, with a variety of Mesozoic assemblages having formed in a supra-subduction zone environment. The Kings-Kaweah ophiolite belt is also unique relative to numerous ophiolites (cf. Mattinson, 1976; Hopson et al., 1981, 2008; Tilton et al., 1981; Harper et al., 1994) in that cogenetic felsic intrusives are exceedingly rare. The paucity of such intrusives, the severity of structural and metamorphic overprints, and multiple generations of crosscutting dikes and plutons have inhibited high-precision dating of the ophiolite belt's principal igneous suite. Zircon-bearing felsic rocks that can be shown by structural relations and geochemical data to be consanguineous with the Kings River ophiolite crustal sequence have not been discovered. Meter-scale plagiogranite bodies occur in three gabbroic mélange blocks from the southern segment of the Kings-Kaweah ophiolite belt. Zircon from these, along with a decimeter-scale diorite-mylonite layer from a transposed gabbro rod within the Kings River ophiolite basal shear zone, yielded disturbed U/Pb zircon systematics, indicating Permo-Carboniferous igneous generation (Saleeby and Sharp, 1980). These rare felsic rocks and their hosting mafites were erroneously interpreted as remnants of the Kings River ophiolite crustal section, leading to an initial erroneous Permo-Carboniferous age assignment for this ophiolite section. Likewise, early Mesozoic (ca. 200 Ma) U/Pb zircon ages on additional felsic dikes interpreted to be part of the Kings River ophiolite crustal section are shown to be members of a superimposed supra-subduction zone igneous suite (Saleeby and Dunne, 2011; and below). The polygenetic nature of the ophiolite belt, and the age range over which magmatism has

TABLE 1. INFORMATION ON FIELD SETTINGS AND PROTOLITHS* OF GEOCHEMICAL SAMPLES

Sample†	Protolith	Latitude (°N)	Longitude (°W)
O1	Pl phyric pillow basalt	36.84122	119.32083
O2	Pl phyric pillow basalt	36.75606	119.21613
O3	Aphyric pillow basalt	36.74280	119.16774
O4	Pl phyric pillow basalt	36.43381	119.06870
O5	a. Pl phyric basaltic dike	36.75947	119.23226
	b. Ophitic diabase screen		
O6	Aphyric basaltic dike	36.76591	119.25207
O7	Cpx gabbro layered cumulate	36.79389	119.36019
O8	Cpx gabbro	36.78779	119.35648
O9	Cpx gabbro	36.78092	119.39213
O10	Cpx gabbro layered cumulate	36.58867	119.34355
O11	Cpx gabbro	36.31176	119.04746
O12	Pl-ol clinopyroxenite layered cumulate	36.81609	119.38025
O13	Troctolite layered cumulate	36.79847	119.36898
M1	Aphyric pillow basalt	36.26122	119.05173
M2	Aphyric pillow basalt	36.26874	119.04552
M3	Hb-cpx diabase dike	36.79389	119.33611
M4	a. Hb-cpx gabbro mylonite	36.91908	119.41852
	b. Hb diorite mylonite		
M5	a. Hb-cpx anorthositic gabbro mylonite	36.81626	119.39012
	b. Hb-cpx gabbro mylonite	36.81625	119.39011
	c. Hb-qtz diorite mylonite		
M6	a. Hb-cpx gabbro mylonite	36.26424	119.07985
	b. Hb-qtz diorite mylonite		
M7	a. Plagiogranite screen	36.28164	119.09680
	b. Hb-cpx diabase dike		
M8	Pegmatitic hb gabbro pod	36.20322	119.04899
M9	Gt amphibolite	36.24600	119.03976
C1	Uralitic diorite dike	36.26199	119.03341
C2	Px phyric basaltic tuff breccia	36.26875	119.02265
C3	a. Px phyric basaltic tuff breccia	36.25436	119.01481
	b. Pl phyric dacite block in basaltic breccia	36.25438	119.01483
C4	Px phyric basaltic broken pillow breccia	36.25401	119.01088
C5	Px-pl phyric massive basaltic-andesite	36.22072	119.01531
C6	Px phyric pillowed basaltic-andesite	36.22425	119.01029
C7	Px phyric basaltic pillow breccia	36.22175	119.00516
C8	Aphyric pillow basalt	36.23575	119.03929
C9	Graded siliciclastic turbidite	36.23172	119.03088

*Protolith refers to pre–Sierra Nevada batholith contact metamorphic state. Key mineral symbols: Cpx—clinopyroxene; Gt—garnet; Hb—hornblende; ol—olivine; Pl—plagioclase; Px—pyroxene; qtz—quartz.
†O—Kings River ophiolite; M—ophiolitic ductile shear zones and Kaweah serpentinite mélange; C—cover strata.

affected it, require detailed iteration between field, geochronological, and geochemical techniques for its proper age analysis.

The strategy of this study is to build on the existing geochronological and radiogenic isotopic data (Saleeby and Sharp, 1980; Shaw et al., 1987), and to use it in conjunction with geological relations to guide additional sampling and analyses to (1) constrain the igneous generation age of the abyssal lithosphere section preserved in the KRO; (2) constrain its age of ductile shearing and its disruption to form ophiolitic mélange; (3) constrain in time the emplacement of the ophiolite belt into the SW Cordilleran continental margin; (4) utilize geochemical discriminate analyses to further test the MORB origin of the Kings-Kaweah ophiolite belt, as suggested by Shaw et al. (1987); (5) constrain in time the transition from abyssal MORB magmatic growth to supra-subduction zone magmatic growth; and (6) use the above in conjunction with structural and stratigraphic relations to better resolve the tectonics of ophiolite generation, disruption, and emplacement into the SW Cordilleran margin. The principal new data sets that are presented include Nd and supporting Sr and Pb isotopic data, major and trace element data for the same sample suite, and additional U/Pb zircon ages. The field setting and protolith information on the samples studied are presented in Table 1. The samples are separated into three suites that are differentiated by letter modifiers such that O represents those of the Kings River ophiolite crustal section; M represents those associated with serpentinite mélange formation, including igneous emplacement into high-temperature, ophiolitic ductile shear zones; and C represents those associated with the lower Mesozoic cover sequence. Analytical procedures used for the new data sets are presented in the Data Repository[1] along with

[1]GSA Data Repository Item 2011260, Geochemical data tables and presentation of analytical techniques, is available at www.geosociety.org/pubs/ft2011.htm, or on request from editing@geosociety.org, Documents Secretary, GSA, P.O. Box 9140, Boulder, CO 80301-9140, USA.

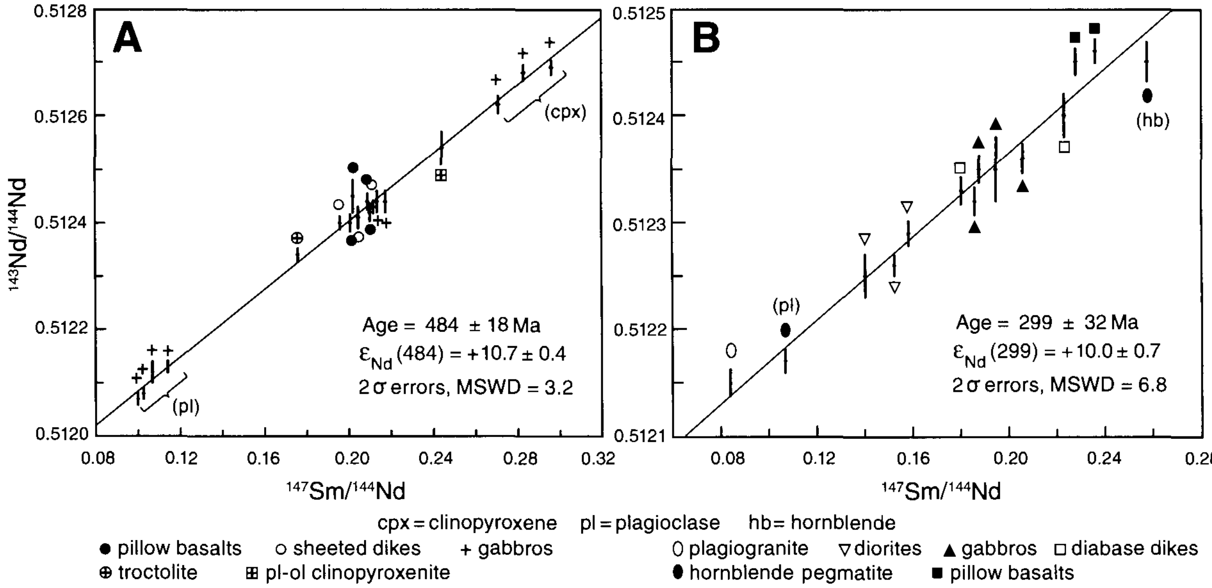

Figure 4. Isotopic evolution diagrams of $^{143}Nd/^{144}Nd$. (A) Kings River ophiolite samples. (B) Ophiolitic ductile shear zone and Kaweah serpentinite mélange samples. Isochron solution after Ludwig (2001). Data in Table DR1 (see footnote 1).

the tabulation of the new and previously published data. The focus is first on the Kings River ophiolite, followed by the Kaweah serpentinite mélange, and then topics regarding ophiolite emplacement and supra-subduction zone residence are pursued.

Kings River Ophiolite: Early Ordovician Abyssal Lithosphere

Homogeneity of the lithologic zones that make up the Kings River ophiolite facilitates the broad characterization of the ophiolite by geochemical techniques. Based on petrography, field relations, and geochemical data presented below, the principal slabs of the KRO, and the Smith Mountain and Antelope Mountain slabs as well as the cluster of petrographically similar mélange blocks of the northern Yokohl Valley area (Figs. 1 and 3), are all considered to be consanguineous members of the Kings River ophiolite. Fifteen samples were selected from these rocks for Sm-Nd whole rock and mineral isochron techniques, as well as major and trace element abundance studies. The samples include plagioclase-olivine clinopyroxenite, troctolite, anorthositic gabbro, clinopyroxene gabbros, ophitic diabase, sheeted basaltic dikes, and pillow basalts. Except for the clinopyroxenite, sample selection was based on the field sites as being highly representative of the principal crustal rocks of the Kings River ophiolite, and the sites being non-proximal to crosscutting plutons. Clinopyroxenites are somewhat rare in this ophiolite, and one was chosen for analysis in the hope of generating a large Sm-Nd spread to the whole-rock analyses. Coarse-grained gabbroids, including the clinopyroxenite sampled, are the only Kings River ophiolite crustal rocks that have not been completely recrystallized by Sierra Nevada batholith contact metamorphism. Careful attention was given to gabbros in search of relatively fresh clinopyroxene and plagioclase remnants for Sm-Nd mineral analyses as a means of better constraining isochron age relations. Our focus first is on the isotopic systematics, and then on the elemental abundance relationships.

The Kings River ophiolite Sm-Nd data are presented in Table DR1 (see footnote 1) and are plotted on a $^{143}Nd/^{144}Nd$ isotopic evolution diagram in Figure 4A. For most samples, metamorphic recrystallization prohibited mineral separate analyses, but for samples O8, O9, O11, and O12, igneous plagioclase, and for samples O9, O11, and O12, igneous clinopyroxene, these were sufficiently preserved for separation and analysis. The Sm-Nd array for the Kings River ophiolite mineral–bulk rock data define a fairly well constrained isochron age of 484 ± 18 Ma, with $\varepsilon_{Nd}(484) = +10.7 \pm 0.4$. The inclusion of clinopyroxene and plagioclase mineral data provides a considerable $^{147}Sm/^{144}Nd$ spread, facilitating age significance to the isochron, and rules out the possibility of such an array representing a mixing line. The MSWD (mean square of weighted deviates) of 3.2 indicates that scatter about the best-fit line is larger than expected on the basis of analytical errors alone, and indicates minor isotopic heterogeneities or minor disturbance during metamorphism. These results confirm the preliminary work of Shaw et al. (1987), suggesting that the Kings River ophiolite crustal section is distinctly older than the Permo-Carboniferous U-Pb zircon ages originally reported for plagiogranites and diorite mylonite of the ophiolite belt (Saleeby and Sharp, 1980).

The initial ε_{Nd} value of +10.7 ± 0.4 indicates derivation of the Kings River ophiolite crustal section from a source that lies near the end member composition of the depleted MORB mantle

(Zindler and Hart, 1986; Hoffman, 2004). The range of initial $^{87}Sr/^{86}Sr$ (Sr_i) and initial Pb isotopes determined for a subset of the Kings River ophiolite Sm-Nd samples further suggest such an end member composition for this ophiolite's mantle source. Sr_i ranges over 0.7023–0.7030 (Table DR1), and for initial Pb α = 17.14–17.82, β = 15.38–15.52, and γ = 36.80–37.38 (Table DR2). The dispersion of these values is notably greater than that which is recorded by the coherence of the Sm-Nd systematics. This is evident in initial ε_{Nd}-Sr_i, initial $^{206}Pb/^{204}Pb$-Sr_i, initial $^{207}Pb/^{204}Pb$-$^{206}Pb/^{204}Pb$, and initial $^{208}Pb/^{204}Pb$-$^{206}Pb/^{204}Pb$ variation diagrams (Fig. 5). These plots show the Kings River ophiolite data in relation to the field of East Pacific Rise MORB (Hoffman, 2004). As discussed below, trace-element concentration data further suggest that the Sr and Pb systems have been disturbed relative to Nd, and thus the range of initial Sr and Pb values shown in Figure 5 is a range of maximum values, with the minimum values for each system taken as approximations of primary values. The extreme positions of the initial Pb fields are consistent with primitive mantle-normalized La/Sm ratios (data in Table DR3) versus initial ε_{Nd} for Kings River ophiolite basalts, also plotted relative to modern Pacific MORB in Figure 5E (after Sun and McDonough, 1989; and Hoffman, 2004). The normalized La/Sm values of <1 at high initial ε_{Nd} values parallel the initial Pb data, showing the effects of pronounced long-term LILE (large ion lithophile element) depletions in the Kings River ophiolite mantle source regime.

Major and trace element abundance data for the Kings River ophiolite sample suite further define a MORB association (Tables DR3 and DR4; see footnote 1). Major element variations as a function of SiO_2 (Fig. 6A) show limited scatter, suggesting only modest alteration by seafloor and/or supra-subduction zone metamorphism. Basaltic pillows and dikes from the Kings River ophiolite plotted as CaO versus MgO indicate minimal effects of seafloor metamorphism (after Humphris and Thompson, 1978; Mottl, 1983). Alterations discussed below for mobile trace elements are thus considered to be dominated by supra-subduction zone fluid fluxing and/or Sierra Nevada batholith contact metamorphism. Focusing first on major element data, the four Kings River ophiolite pillow basalt samples that were taken from widely spaced localities are tightly grouped around SiO_2 = 50% and show major element compositions that are typical of N-MORB (normal mid-oceanic-ridge basalt) except for possible K_2O enrichment, although K_2O contents are within the range of geographic variation patterns of modern MORB (Sun and McDonough, 1989; Hoffman, 2004). Sheeted dike and gabbro samples show more scatter, but without K_2O enrichment. The gabbro compositions appear reasonably grouped, considering their widely spaced sample sites and implicit fractionated state, whereas the plagioclase-olivine clinopyroxenite and troctolite cumulates show expected dispersions from the gabbro cluster.

Major element variation patterns permit a common liquid line of descent for the basalts and gabbroids (Fig. 6A). Not represented in the data, but of importance, are dunite cumulates. On Al_2O_3-MgO and MgO-SiO_2 variation diagrams, tie lines between Fo90 olivine and the centroid of the basaltic dike data points are shown, and on Al_2O_3-MgO and CaO-SiO_2 diagrams,

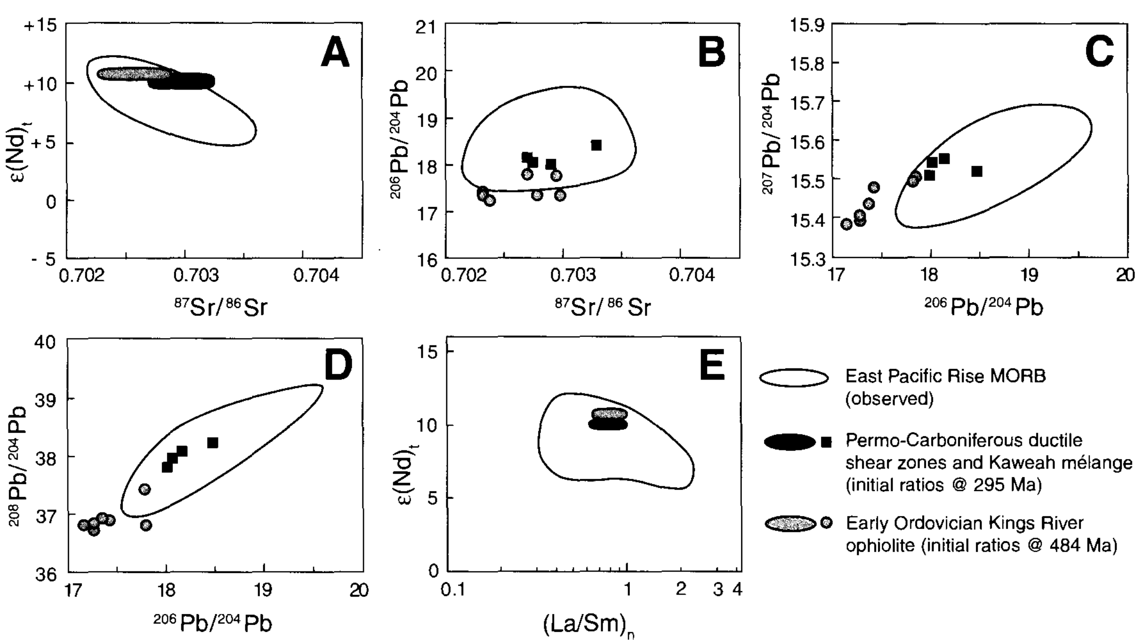

Figure 5. Initial radiogenic isotopic variation diagrams for the Kings-Kaweah ophiolite belt in relation to modern Pacific MORB compositions (after Hoffman, 2004). (A) ε_{Nd}-$^{87}Sr/^{86}Sr$. (B) $^{206}Pb/^{204}Pb$-$^{87}Sr/^{86}Sr$. (C) $^{207}Pb/^{204}Pb$-$^{206}Pb/^{204}Pb$. (D) $^{208}Pb/^{204}Pb$-$^{206}Pb/^{204}Pb$. (E) ε_{Nd}-primitive mantle normalized La/Sm (after Sun and McDonough, 1989). Data in Tables DR1, DR2, and DR3 (see footnote 1).

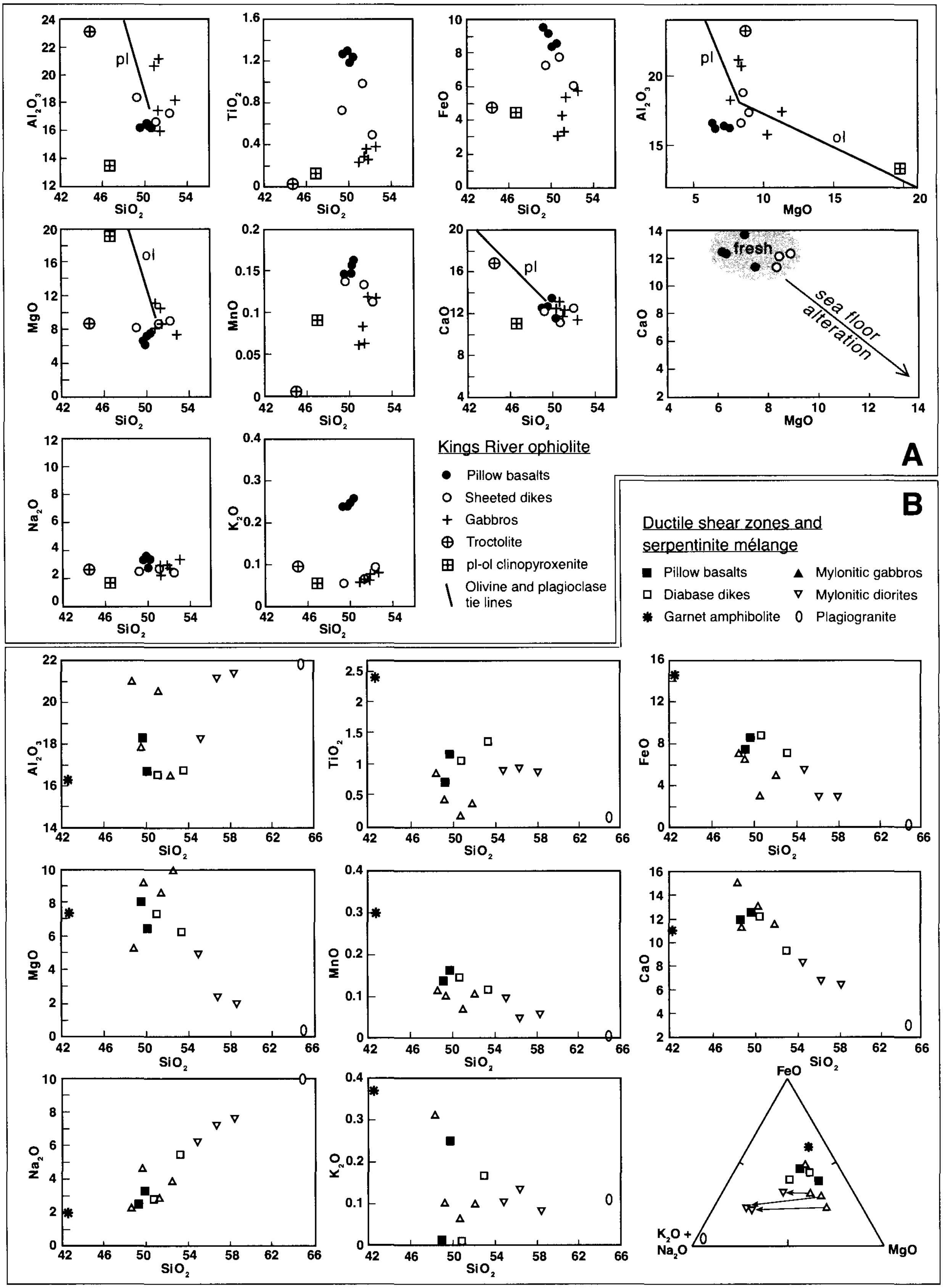

Figure 6. Major element variation diagrams for the Kings-Kaweah ophiolite belt. (A) Kings River ophiolite samples. (B) Ophiolitic ductile shear zones and Kaweah serpentinite mélange samples. Data in Tables DR4 and DR6 (see footnote 1). Fresh MORB and seafloor alteration fields in A, after Humphris and Thompson (1978) and Mottl (1983).

tie lines between An90 plagioclase and the centroid are shown. Perhaps most definitive are the Al_2O_3-MgO relations, which suggest a parental liquid composition similar to the dikes, with plagioclase and olivine fractionation rendering the cumulates and pillow basalts. The potential role of clinopyroxene fractionation is unclear, and of possible second order importance, although concentration of clinopyroxene in cumulate gabbros could have slightly depleted the residual melt in SiO_2 as observed in the pillow basalts. Enrichments of Mn, Ti, Fe, and possibly K in the pillow basalt data can also be explained by minor fractionation of a sheeted dike-like parental liquid.

Trace element data for the pillow basalts and sheeted dikes of the Kings River ophiolite are normalized to N-MORB in Figure 7A (after Sun and McDonough, 1989). The general displacement of the pillow basalt data array from the sheeted dike array parallels the fractionation pattern suggested by the major element data. Also shown in the plot is the compositional trend of E-MORB (enriched mid-ocean-ridge basalt) relative to N-MORB (normal mid-oceanic-ridge basalt) (after Sun and McDonough, 1989). Much of the Kings River ophiolite basalt data fall into the field bounded by N-MORB and E-MORB, although distinct positive spikes occur for Ba, Pb, and Sr, and, for some samples, Cs and K. These trace elements are known to have considerable compositional variation with geographic position in modern MORB (Hoffman, 2004), although the spread in the Figure 7A data is greater than that observed and indicates that these trace elements have undergone at least some enrichments relative to MORB. In that CaO-MgO relations in the basalts show no evidence for significant seafloor metamorphic alteration (Fig. 6A), such enrichment is interpreted to have occurred in the supra-subduction zone environment by a combination of fluid fluxing through the mantle wedge and/or more proximally driven Sierra Nevada batholith contact metamorphism. The trace elements of Cs, Ba, K, Pb, and Sr are typically enriched in supra-subduction zone fluids (cf. Pearce et al., 1995). In contrast, Nb of the Kings River ophiolite basalts has retained coherency with the MORB pattern, consistent with its negligible mobility in supra-subduction zone fluids (Pearce et al., 1995). The Figure 7A data also show that the rare earth elements (REEs) have not been enriched by such fluid interactions, which is consistent with the minor mobility of Nd in supra-subduction zone fluids, lending further confidence to the Sm-Nd isochron age and initial ε_{Nd} values of Figure 4A.

The range of initial Sr and Pb isotopic ratios determined for the Kings River ophiolite, in light of the coherency of the REE data, are interpreted to reflect differential alteration of the samples by the influx of exotic Sr and Pb by supra-subduction zone fluid fluxing and/or Sierra Nevada batholith contact metamorphism. Figure 8 shows Rb/Sr and $^{235}U/^{207}Pb$ evolution diagrams for samples for which initial isotopic ratios were determined. The samples consist of bulk rock data for basalts and gabbros, and plagioclase data for two coarse-grained gabbros exhibiting only grain-boundary metamorphic overprints. The Rb/Sr and $^{235}U/^{207}Pb$ systems were chosen for this analysis because that during alteration, potential parent nuclide enrichments for these systems are minimal relative to daughter nuclide enrichments, in contrast to the $^{238}U/^{206}Pb$ and $^{232}Th/^{208}Pb$ systems. In each diagram the plagioclase data plot closest to the origin and yield the lowest initial ratios, calculated for 484 Ma, based on the Sm-Nd isochron age (Fig. 4A). A 484 Ma reference isochron is passed through the plagioclase data points in Figures 8A and 8B, and on each plot the isochron also passes through the O7 gabbro sample, which shows little or no enrichment of Sr or Pb relative to N-MORB. Comparison of trace element abundances of

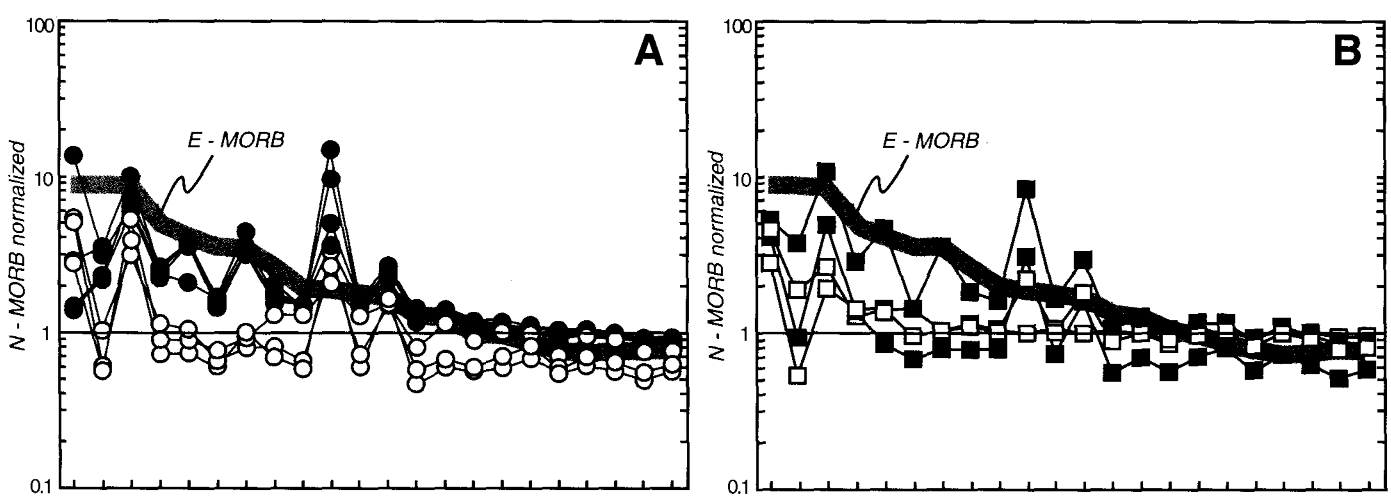

Figure 7. Trace element normalization plots for basaltic rocks of the Kings-Kaweah ophiolite belt normalized to idealized N-MORB and in comparison with idealized E-MORB (after Sun and McDonough, 1989). (A) Kings River ophiolite basaltic pillow lavas and sheeted dikes. (B) Basaltic pillow lavas and diabase dikes related to the Kaweah serpentinite mélange. Data in Table DR3 (see footnote 1). Symbols are the same as in Figure 6.

O7 with those of N-MORB is provisional in that O7 is a cumulate of probable MORB derivation, and depletions of LIL trace elements relative to erupted MORB is expected on the basis of crystal-liquid elemental partitioning and the implicit fractionated state of a cumulate. Nevertheless, in comparison with the O9 cumulate gabbro data point in each diagram, enrichments in Sr and Pb correlate with divergence from the 484 Ma isochron. This is shown to the right of the two isotopic evolution diagrams by plots of δ, defined as the divergence of given $^{87}Sr/^{86}Sr$ and $^{207}Pb/^{204}Pb$ ratios from the respective reference isochron versus (Sr or Pb) E_{NM}, defined as the respective elemental enrichments relative to N-MORB (after Sun and McDonough, 1989). In the δ versus E_{NM} plots the position of the O9 gabbro is shown relative to N-MORB by the light cross, and relative to Sr and Pb concentrations of sample O7 by the darker cross. This is done in order to help see through the effects of O7 and O9 as cumulates. There is clearly a positive correlation between δ and E_{NM}, and such a correlation, albeit noisy, is indicated for the basaltic samples as well. The correlation between the divergence of the initial isotopic ratios and the elemental enrichments of Sr and Pb argue strongly for a secondary origin for the enrichments of Sr and Pb, relative to N-MORB, and by analogy the trace element enrichments of Cs, Ba, and possibly K in Figure 7A. Lead and Sr isotopic data for the Sierra Nevada batholith (cf. Chen and Tilton, 1991) show a range of radiogenic compositions for which similar composition fluids could have profound alteration effects superposed over the relatively non-radiogenic ratios of the Kings River ophiolite. The Figure 8 relationships also lead to the interpretation that the plagioclase and/or the most primitive gabbro initial isotopic ratios most accurately reflect those of the Kings River ophiolite mafic crustal section, indicating Sr_i = 0.70225, and for Pb α = 17.139, β = 15.384, and γ = 37.384. In Figure 5 it is clear that these initial Sr and Pb isotopes lie at, or even beyond, the extreme long-time integrated LILE depletions typical of the Pacific MORB mantle source regime. In Figure 7A it is clear that the removal of the secondary spikes for Cs, Ba, K, Pb, and Sr results in an N-MORB to slightly enriched MORB profile for the Kings River ophiolite basalts.

The major and trace element abundance data in conjunction with Nd, Sr, and Pb isotopic data clearly point to an N-MORB, or perhaps a slightly enriched MORB, source for the Kings River ophiolite. Reconstructed stratigraphic thicknesses for the various lithologic zones of the ophiolite agree well with the seismic velocity structure of "normal" abyssal crust. The widespread occurrence of sheeted basaltic dikes, virtually devoid of significantly fractionated members, is also consistent with an abyssal ridge-crest origin for the ophiolite (cf. Robinson et al., 2008). Based on geochemical data, lithostratigraphic relations, and

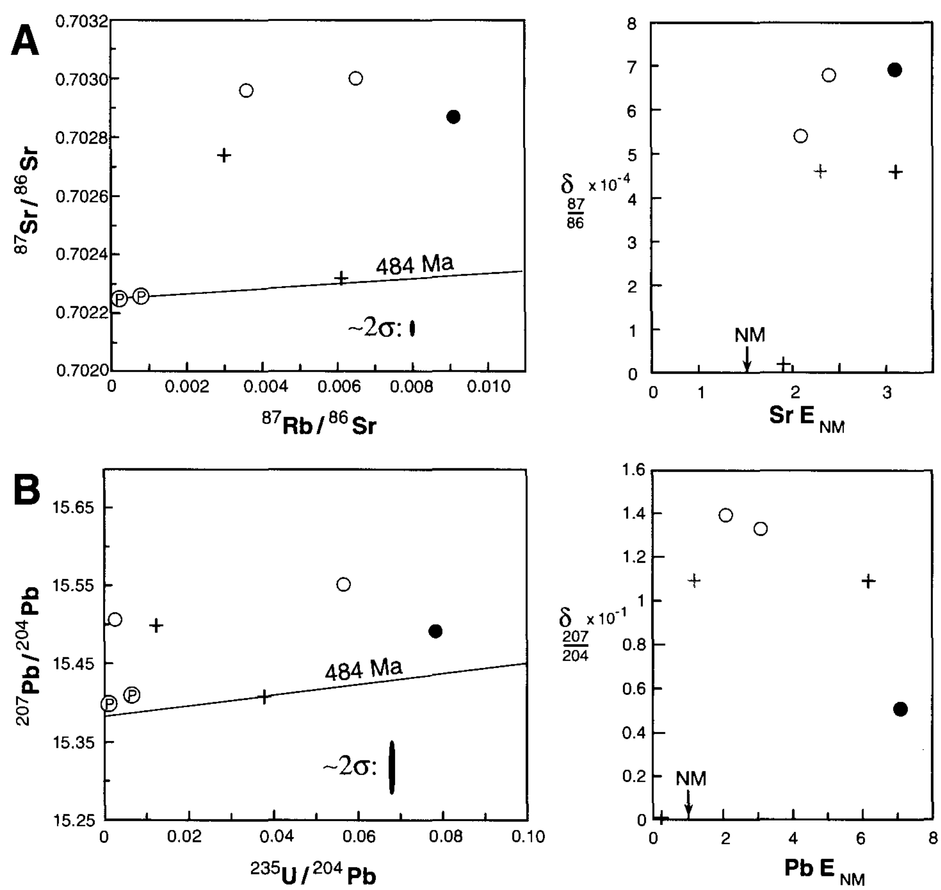

Figure 8. Isotopic evolution diagrams for $^{87}Sr/^{86}Sr$ (A) and $^{207}Pb/^{204}Pb$ (B), each showing 484 Ma reference isochron (after Fig. 4A) forced through samples with most primitive initial ratios at t (time) = 484 Ma. Symbols are same as in Figure 6A, but with an encircled p symbol denoting gabbro plagioclase separates. Shown to the right of each isotopic evolution diagram are plots of the divergences of the respective isotopic ratios off of reference isochrons (δ) versus respective elemental enrichments (E_{NM}) of samples relative to N-MORB (after Sun and McDonough, 1989). These plots show that secondary Sr and Pb enrichments correlate with disruption of primary initial isotopic ratios. Data in Tables DR1, DR2, DR3, and DR4 (see footnote 1).

petrography, the Kings River ophiolite is the clearest example of a complete abyssal crust and upper mantle lithosphere sequence preserved in the North American Cordillera. We now focus on a distinctly younger abyssal igneous event resolved within the Kings River ophiolite, and its relationships with the development of the Kaweah serpentinite mélange.

Permo-Carboniferous Ductile Shear Zones and Kaweah Serpentinite Mélange

The Yokohl Valley area (Fig. 3) was chosen for the principal analysis of the Kaweah serpentinite mélange because of its relatively low thermal metamorphic overprint, as compared with all other areas of the Kings-Kaweah ophiolite belt, and for the preservation of a number of important primary relationships. The Yokohl Valley map area is unique to the Kings-Kaweah ophiolite belt in that a textural (±index mineral) "isograd" may be resolved, which corresponds to what is defined here as inner versus outer contact metamorphic aureole positions. The inner aureole position is defined by near-pervasive actinolitic hornblende + sodic-plagioclase ± clinozoisite or epidote static overprinting in mafic assemblages, black-wall skarn domains and vein networks, and nematoblastic antigorite overprints in ultramafic assemblages, and the occurrence of andalusite ± sillimanite in cover strata pelites. Outer aureole positions are defined by a lack of these indices and also the widespread preservation of primary igneous phases and/or pre–Sierra Nevada batholith metamorphic assemblages. As displayed in Figure 3, a large central area lies within an outer aureole position, encompassing a number of important primary relationships.

Primary relationships that are relatively well preserved in the Yokohl Valley map area include the intrusion and eruption of abyssal igneous rocks through disrupted and actively shearing Kings River ophiolite–related abyssal lithosphere, pelagic sedimentation across the resultant polygenetic basement complex, and nonconformable overlap by hemipelagic strata of the Calaveras complex and in sequence siliciclastic and volcanogenic strata of the Kings sequence. This area also displays the internal complexity of the Kaweah serpentinite mélange, as it covers three well-defined mélange units (Fig. 1) characterized by assemblages derived as tectonic blocks from the Kings River ophiolite, variably deformed intrusive bodies emplaced into serpentinized peridotites that had ascended to crustal levels, and surfaced serpentinites that mingled with pillowed eruptions and pelagic sediments.

Pillow basalts sampled from the Kaweah serpentinite mélange (samples M1 and M2) were taken from the NE-SW–trending belt of interbedded basalt and chert that extends across the center of the Yokohl Valley area (Fig. 3). This partially disrupted stratified belt was deposited on a serpentinite substrate. It contrasts in field setting from the thick homogeneous pillow basalt sections of the Hughes, Dalton-Bald, and Antelope Mountain slabs of the Kings River ophiolite by the intercalation of radiolarian chert, hyaloclastite, and ophicalcite, and the absence of an underlying sheeted dike complex. All pillowed flows of the observed Kaweah serpentinite mélange are aphyric. Local, isolated feeder dikes for the pillowed flows are typically highly altered, having interacted with serpentinite host rocks, and most have been broken into relatively non-deformed, angular "mélange blocks." Some feeder dikes are pepperitic, suggesting that they were emplaced into non-lithified sedimentary serpentinite (cf. Kokelaar, 1982). The Kaweah serpentinite mélange–related mafic dikes grade in texture from aphyric basalts to coarser diabases, microgabbros, and gabbros, with the coarser varieties not having been observed to be directly linked to pillowed basalts. Where not highly recrystallized from contact metamorphism the coarser rocks appear distinct from intrusive rocks of the Kings River ophiolite by the common occurrence of subordinate brown igneous hornblende along with clinopyroxene. Solitary and non-sheeted sets of igneous hornblende–bearing diabases are widespread along the Kings-Kaweah ophiolite belt, cutting mafic and ultramafic levels of the Kings River ophiolite, dispersed as "mélange blocks" and within intrusive complex blocks within the Kaweah serpentinite mélange. One such dike, with the best remnants of an igneous texture observed (sample M3), was taken directly adjacent to the margin of the longitudinal ductile shear zone that cuts the eastern margin of the Tivy Mountain gabbro (Fig. 2). This dike was chosen for its texture and its field setting of lying proximal to a shear zone that variably transposes dikes of similar composition.

More extensive sampling was performed on gabbroic mylonites and their dioritic fractionates that occur within the ophiolitic ductile shear zones. Based on contradictory intrusive and mylonitization relationships, igneous emplacement within the shear zones is shown to have been coincident with high-temperature ductile shearing (Saleeby 1977, 1978). Because ductile shearing instigated tectonic disruption of the Kings-Kaweah ophiolite belt, the age of such shearing places important time constraints on the initial phases of serpentinite mélange development. The gabbroic and dioritic intrusives of the shear zones are distinct from the thick cumulate sections of Tivy and Smith Mountains, which are characterized by intermediate to calcic plagioclase and coarse diopsidic augite with local olivine. The mylonitic gabbros of the ductile shear zones are characterized by a similar compositional range in plagioclase and clinopyroxene, but they commonly contain brown hornblende that is igneous in origin and that appeared early in the crystallization sequence. Protolith compositions of the deformed intrusive bodies include hornblende ± plagioclase-clinopyroxenite, hornblende-clinopyroxene gabbro, and anorthositic gabbro, and small volumes of hornblende ± quartz diorite. Large clinopyroxene and hornblende grains commonly form porphyroclasts in a finely laminated blastomylonitic matrix, locally with millimeter to decimeter scale dioritic veins that are variably transposed. Olivine bearing gabbroids have not been recognized as part of this distinctive suite of ophiolitic intrusives. Sampling of the shear zone gabbros and diorites focused on the upper Hughes Creek slab (samples M4a and M4b), and samples M5a, M5b, and M5c from the Kings River ophiolite basal shear zone along the lower Kings River (Fig. 2). Vestigial lenses and blocks of serpentinized mylonitic peridotite with mylonitic gabbros are dispersed through the Kaweah serpentinite mélange, the largest of which recognized is the Lindsay Ridge slab in Figure 3. Samples M6a and M6b were taken from mylonitic gabbro and diorite of this slab.

Serpentinized peridotite also forms the host for shallow-level mafic intrusive swarms that are not penetratively sheared along with their hosts. These intrusives consist of basaltic dike rock, hornblende-clinopyroxene diabase and static textured gabbro, and rare pegmatitic hornblende gabbro and plagiogranite. Sample M7a is from a plagiogranite body, and sample M7b is from a set of diabase dikes that crosscut the plagiogranite and its gabbroic host. The plagiogranite and diabase dikes are subordinate members of vari-textured gabbroids that form a series of composite intrusive sheets lying within an antigorite ± talc ± tremolite schist matrix within the Yokohl Valley area (Fig. 3). The Elephant Back slab of the Yokohl Valley area (Fig. 3) consists of composite hornblende-clinopyroxene gabbro and microgabbro intrusive bodies that are marginally sheared along with serpentinized peridotite host rocks. Local pegmatitic hornblende gabbro segregations are well preserved within the Elephant Back intrusive bodies, one of which yielded a 250 Ma K/Ar hornblende age (Saleeby and Sharp, 1980) and which is included here as sample M8.

Figure 4B is a $^{143}Nd/^{144}Nd$ isotopic evolution diagram for the entire Kaweah serpentinite mélange suite of gabbros, diorites, basalts, diabases, and plagiogranites, including those that intrude the Kings River ophiolite. All of the data on the neodymium evolution diagram are bulk rock, except for the coarse hornblende from the pegmatite and its partially recrystallized plagioclase matrix. The widespread tectonitic fabrics and near pervasive metamorphic overprints of the Kaweah serpentinite mélange sample suite otherwise prohibit mineral separate analyses. The Figure 4B data define an apparent linear array corresponding to an isochron age of 299 ± 32 Ma with ε_{Nd} (299) = +10.0 ± 0.7. The isochron age is consistent with U/Pb zircon ages on plagiogranites and the mylonitic diorites discussed further below, although the scatter about the isochron line is considerable (MSWD = 6.8). The scatter could reflect small disturbances related to metamorphism and/or supra-subduction zone fluid fluxing, or to minor variations in the initial isotopic compositions of the various samples. Some component of the later mechanism seems likely, considering the large array of field settings for the samples compounded by the large area over which they were taken. The isochron age is thus considered a rough approximation for the igneous age of the suite.

One of the essential features of the Sm-Nd results for the Kaweah serpentinite mélange suite of samples is the correspondence of the isochron "age" with U/Pb zircon ages on plagiogranites and mylonitic diorites. As mentioned above, published zircon ages for the three dispersed plagiogranite-bearing blocks from the Kaweah serpentinite mélange, and the sample M5c mylonitic diorite, suggest a Permo-Carboniferous igneous age with substantial Cretaceous thermal disturbance (Saleeby and Sharp, 1980). Zircon was extracted from the sample M4b and M6b mylonitic diorites and re-extracted from the M5c mylonitic diorite and M6a plagiogranite, and analyzed in conjunction with this study (Table DR5 [see footnote 1]). These samples were subjected to stepwise chemical leaching procedures similar to those used in Mattinson (1994) in order to remove labile components of U and Pb (GSA Data Repository[1]). The new data are plotted along with the original data for samples M5c and M6a in the Figure 9 concordia diagram. The new data form a tight array adjacent to the original published upper intercept, reflecting the removal of highly labile discordance bearing U and Pb components. The two original samples included in this analysis yield much lower precisions, reflecting improved analytical techniques, and cascade down concordia considerably reflecting the isotopic signature of their labile components. The upper intercept age of 296 ± 15 Ma for the entire suite corresponds well with the isochron "age" of the Kaweah serpentinite mélange sample suite, which is scaled onto concordia in Figure 9. Also scaled onto concordia are K/Ar hornblende ages from Kings-Kaweah ophiolite belt basites, differentiated as lying in inner versus outer contact-aureole field positions, and concordant U/Pb zircon ages from dike swarms and Sierra Nevada batholith plutons that crosscut and contact metamorphosed the Kings-Kaweah ophiolite belt. The K/Ar ages from inner contact aureoles are completely reset to proximal

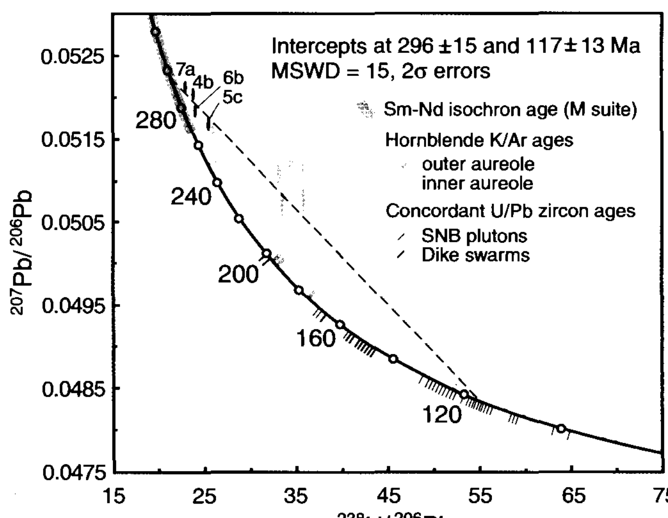

Figure 9. Concordia diagram based on $^{207}Pb/^{206}Pb$ versus $^{238}U/^{206}Pb$ (after Terra and Wasserburg, 1972) for plagiogranite and mylonitic diorites of ophiolitic ductile shear zones and Kaweah serpentinite mélange (data in Table DR5; see footnote 1). Also plotted along concordia are concordant U/Pb zircon ages from dike swarms and batholithic plutons that crosscut and contact metamorphosed the ophiolite belt, K/Ar hornblende ages from ophiolite-belt mafic rocks differentiated as from inner versus outer contact aureole positions (after Saleeby and Sharp, 1980; Clemens-Knott and Saleeby, 1999; Saleeby and Dunne, 2011), and M suite Sm-Nd isochron age with a 2σ error envelope (after Fig. 4B). MSWD—mean square of weighted deviates; SNB—Sierra Nevada batholith.

Sierra Nevada batholith ages, whereas those from outer aureole positions are partially disturbed. The 117 ± 13 Ma lower intercept for the plagiogranite and dioritic mylonites clearly corresponds with the thermal metamorphic maxima as reflected in the Sierra Nevada batholith U/Pb zircon and reset K/Ar hornblende ages. Scatter in the more discordant ophiolitic zircon data points, as well as in the data for the other plagiogranite zircon populations not presented here (Saleeby and Sharp, 1980), are interpreted to reflect multiple pulses of thermal overprinting, which began in the Jurassic and intensified into the Early Cretaceous. Considering both the Sm/Nd isochron age and the U/Pb zircon ages, and the overlap of their uncertainties, ca. 295 Ma is considered a reasonable approximation for the age of the Kaweah serpentinite mélange suite, and is used for initial Pb and Sr isotopic composition corrections discussed below.

The initial ε_{Nd} value of +10.0 ± 0.7, derived above for the Kaweah serpentinite mélange suite, also indicates derivation from a source that lies near the end member composition of the depleted MORB mantle (Hoffman, 2004). Moreover, Sr_i from the Kaweah serpentinite mélange suite ranges over 0.7027–0.7033 (Table DR1), with initial ε_{Nd} versus Sr_i for the suite lying within the field of modern Pacific basin MORB (Fig. 5A) except for the highest Sr_i value, which, as discussed below, is considered to have been altered in the supra-subduction zone environment. Initial Pb values for the Kaweah serpentinite mélange suite are notably more radiogenic than for the Kings River ophiolite suite, with α = 17.962–18.493, β = 15.511–15.600, and γ = 37.663–38.211 (Table DR2). Nevertheless, the Kaweah serpentinite mélange suite Pb values plot within the field of Pacific MORB on initial $^{206}Pb/^{204}Pb$-Sr_i, $^{207}Pb/^{204}Pb$-$^{206}Pb/^{204}Pb$, and $^{208}Pb/^{204}Pb$-$^{206}Pb/^{204}Pb$ variation diagrams (Fig. 5). As discussed below, trace element concentration data further suggest that the Sr and Pb systems have been disturbed relative to Nd, and thus the range of Sr and Pb values shown in Figure 5 is a range of maximum values as with the range of Kings River ophiolite values. As with the Kings River ophiolite basaltic samples, the Kaweah serpentinite mélange basalts yield a primitive mantle normalized La/Sm versus initial ε_{Nd} field that lies toward the pronounced long-term LILE depletion domain of the field for modern Pacific MORB (Fig. 5E).

Major and select trace-element abundance data are presented for the Kaweah serpentinite mélange sample suite in Table DR6 (see footnote 1), except for the extremely coarse-grained hornblende pegmatite. Major element variations as a function of SiO_2 (Fig. 6B) show a distinctly wider range than for the Kings River ophiolite sample suite. The two pillow basalt samples (M1 and M2) are at SiO_2 = 49–50 wt% and show major element compositions that are typical of N-MORB (Sun and McDonough, 1989). The fact that all of the gabbros analyzed are from scattered, relatively small intrusive bodies that were emplaced into serpentinized peridotite leads to the expectation that coherent fractionation trends would not be evident in the overall major-element variation patterns, and that a common liquid line of descent is highly unlikely. In aggregate, however, the variation of Na_2O, K_2O, and CaO with SiO_2, and the array on the AFM plot, point to local silica-alkali enrichment. On the AFM plot, tie lines are shown between proximally related mylonitic gabbros and diorites. The plagiogranite and dioritic samples show Na_2O enrichment relative to K_2O, typical of oceanic felsic associations (Coleman and Peterman, 1975). The low-volume diorites and plagiogranites appear to represent local closed-system fractionation products derived from adjacent gabbroids.

Trace element data for the M1 and M2 basaltic pillows and the M3 and M7b diabase dikes (Table DR3) are normalized to N-MORB in Figure 7B (after Sun and McDonough, 1989). Also shown on the plot is the compositional trend of E-MORB (after Sun and McDonough, 1989). The Kaweah serpentinite mélange data are similar to the Kings River ophiolite basalt data, mainly in the field bounded by N-MORB and E-MORB, and some samples show distinct positive spikes for Cs, Ba, Pb, and Sr. The Figure 7B data also show that REEs for the Kaweah serpentinite mélange basalts were not influenced significantly by such mobilization, lending further confidence to the Sm/Nd isochron age and initial ε_{Nd} values derived in Figure 4B. The similarity of some positive spikes for Cs, Ba, Pb, and Sr to the Kings River ophiolite data suggests that the implicit enrichments in these elements occurred in the common supra-subduction zone fluid fluxing and/or Sierra Nevada batholith contact metamorphic environment that the Kaweah serpentinite mélange and Kings River ophiolite underwent. As with the Kings River ophiolite, Pb has clearly been mobilized in the bulk rocks during contact metamorphism, considering that radiogenic Pb is partially disturbed in the plagiogranite and mylonitic diorite zircon populations (Fig. 9). As with the Kings River ophiolite suite, the Sr_i and initial Pb values for the Kaweah serpentinite mélange suite are interpreted as a range of maximum values, with the least radiogenic ratios conceivably approximating true initial values. This leads to the interpretation of the Kaweah serpentinite mélange suite having an approximate primary isotopic composition of Sr_i = 0.7027, and for initial Pb α = 17.962, β = 15.511, and γ = 37.663.

The radiogenic isotopic data, as well as the major and trace element abundance data, indicate that the Kaweah serpentinite mélange suite of intrusions and pillow basalts is also of MORB affinity. Field relations and the age data indicate that these Permo-Carboniferous MORB affinity magmas were emplaced and erupted into the Early Ordovician Kings River ophiolite abyssal crust and mantle lithosphere during high-magnitude shear strain of the hosting lithosphere, and its progressive disruption to form serpentinite mélange on the seafloor. Basaltic magmas of the Permo-Carboniferous suite erupted across the serpentinitic substrate as mélange was forming, and such lavas were interbedded with sedimentary serpentinite, ophicalcite, and radiolarian ooze. The widespread stabilization of early igneous hornblende in many of the Kaweah serpentinite mélange intrusives is consistent with their emplacement along a major transform fracture zone (Melson et al., 1972; Engle and Fisher, 1975; Bonatti and Honnorez, 1976; Honnorez et al., 1984; Johnson and Dick, 1992; Schroeder and John, 2004; Cipriani et al., 2009). One possibility is that water was sequestered out of the variably serpentinized peridotites that hosted the intrusive masses. Geochemical studies and modeling of partially serpentinized peridotite of the Feather River massif of the northern Sierra Foothills, a likely correlative of the Kings-Kaweah ophiolite belt ultramafics and mafic tectonites as discussed below, suggest that the respective abyssal serpentinization front reached ~40-km depths, possibly along a transform fault (Li and Lee, 2006). Given a MORB magma extraction depth of 30–50 km (Lee et al., 2009), the Kaweah serpentinite mélange suite of intrusives conceivably ascended through ≥30 km of partially hydrated ultramafic wall rocks prior to stalling out within ductile shear zones, tensile fractures, or relatively small plutons within the disrupted Kings River ophiolite abyssal crust and upper mantle section. This would yield ample opportunity for minor sequestering of water and the stabilization of early igneous hornblende. The ~190 m.y. hiatus in abyssal MORB magmatism indicated by the age data presented above is profound relative to abyssal magmatic patterns of the modern ocean basins, and requires attention.

Polygenetic Abyssal Lithosphere

The Kings River ophiolite consists of a complete abyssal spreading-ridge crust and upper mantle sequence of Early Ordovician age. The homogeneity of this mafic crustal section, extensiveness of sheeted dikes, and lack of differentiated rocks suggests spreading ridge genesis above a steady-state magma chamber, which further suggests genesis along a fast-spreading ridge like the East Pacific Rise (i.e., Babcock et al., 1998). The coherency of the Sm-Nd systematics and uniformity of bulk compositions for the Kings River ophiolite sample suite suggest a common source and liquid line of descent for the principal slabs and mélange blocks. The along-strike extent of voluminous Kings River ophiolite mafic rocks, minus small transverse zones of crosscutting Sierra Nevada batholith intrusions, is ~50 km (Fig. 1). Geochemical studies of the East Pacific Rise show that distinct domains of magma source regime and liquid line of descent can exceed 40 km along strike (Reynolds et al., 1992). Thus the principal mafic slabs of the Kings River ophiolite and their derivative mélange blocks are interpreted as the products of one source, ascent, and crystallization domain along a fast-spreading ridge in the early Paleozoic Panthalassa basin. Pelagic sedimentation across the Kings River ophiolite abyssal basement is feebly recorded in small metalliferous radiolarian chert lenses within the pillow basalt section, and as dispersed blocks of similar metalliferous chert within the Kaweah serpentinite mélange. The greatest stratigraphic thicknesses measured for such metalliferous chert blocks are typically ~30 m. Such blocks are devoid of argillaceous, serpentinitic lute or tuffaceous components, which contrasts with local thin laminae present in thicker chert sections that lie above the Permo-Carboniferous pillow basalts of the Kaweah serpentinite mélange. Sedimentation rates for radiolarian oozes in the early Paleozoic are not constrained, and in conjunction with the disruption of the Kings River ophiolite chert section into dispersed mélange blocks this ophiolite's pelagic sedimentation history is obscured. This has resulted in an ~190 m.y. hiatus in the geologic history recorded in the Kings-Kaweah ophiolite belt.

The Early Ordovician abyssal lithosphere of the Kings River ophiolite underwent an intense phase of tectonic disruption in the Permo-Carboniferous. The association of high-temperature ductile shearing coincident with MORB magmatism, the surfacing of variably serpentinized depleted peridotites on the seafloor, and the mingling of serpentinitic detritus with pelagic deposits are typical of the intersection zones of slow-spreading ridges and large offset transforms (cf. Bonatti et al., 1973; Karson and Dick, 1983; Johnson and Dick, 1992; Cannat, 1996; Rommevaux-Jestin et al., 1997; Schroeder and John, 2004; Cipriani et al., 2009). The profound relationship recorded for the Kings-Kaweah ophiolite belt, however, is that this distinctive deformational and magmatic regime was superposed across MORB igneous crust and abyssal mantle lithosphere after the ~190 m.y. hiatus of geologic history. This seems profound, given that the oldest known abyssal lithosphere currently residing in an ocean basin is ca. 168 Ma (Ogg and Smith, 2004). The potential notion that the Permo-Carboniferous petrotectonic regime occurred in a supra-subduction zone environment is rejected on the basis of the pelagic and hemipelagic sedimentation history of the Kaweah serpentinite mélange as well as the geochemical data presented above. The thickest radiolarian chert sections that lie depositionally on Permo-Carboniferous pillow basalts are in several areas ~100 m thick (cf. Fig. 3). Pelagic sedimentation rates for radiolarian oozes in the late Paleozoic are somewhat better constrained than for the early Paleozoic. For example, a post compaction rate for radiolarian cherts studied in the Permian Dalong Formation of southwest China are ~0.4 cm/10^3 yr (Gu et al., 2007). Such a rate, if applicable, would imply an ~30 m.y. accumulation of predominantly clean radiolarian chert commencing in the Permo-Carboniferous, or ca. 295 Ma, prior to the onset of Calaveras hemipelagic sedimentation. Calaveras chert-argillite does not appear to have much, if any, volcanic input, and as discussed below the products of supra-subduction zone volcanism were not expressed in the cover strata until well into Middle Triassic time, at the earliest.

CONDITIONS AND SETTINGS OF METAMORPHISM, DEFORMATION, AND MÉLANGE MIXING

Petrographic data and map relations for the Kings River ophiolite indicate that geographically focused thermal metamorphism and cleavage development related to Jurassic plutonism and tectonism, and regional thermal metamorphism related to Early Cretaceous Sierra Nevada batholith plutonism, were superimposed on (1) regional low to medial grade static textures within the coherent mafic crustal section of the Kings River ophiolite and its derivative mélange blocks, (2) high-temperature upper-mantle flow fabrics of the peridotite section of this ophiolite and its derivative mélange blocks, (3) mylonitic fabrics of the Permo-Carboniferous ductile shear zones, and

(4) matrix schistosity in serpentinite mélange zones. Similar textural relations are recorded for the Kaweah serpentinite mélange with thermal overprints affecting matrix schistosity as well as regional low to medial grade assemblages or mylonitic fabrics within mélange blocks. Rocks of the Kings-Kaweah ophiolite belt did not undergo high P-T metamorphic conditions, nor was this ophiolite belt subjected to intermediate- to high-pressure conditions during Sierra Nevada batholith metamorphism. Petrologic constraints on depth of emplacement for Sierra Nevada batholith plutons that intrude the Kings-Kaweah ophiolite belt indicate relatively shallow levels (Putman and Alfors, 1969; Ague and Brimhall, 1988; Liggett, 1990; Clemens-Knott et al., 2011), consistent with the predominance of andalusite and only local andalusite + sillimanite in meta-pelites of the cover strata. The regional low-grade conditions are most readily attributed to a combination of ocean floor metamorphism and subsequent burial metamorphism and cleavage development beneath lower Mesozoic cover strata. Widespread mylonitization and tectonic disruption clearly occurred during the invasion of the Early Ordovician abyssal lithosphere by the Permo-Carboniferous abyssal magma series, and are not related to subduction megathrust tectonics.

The association of high-strain mylonitic gabbros and peridotites with serpentinite diapirs and extrusions, sedimentary serpentinite, and ophicalcite is typical of the intersections of slow-spreading ridge segments with large transform offsets on the ocean floor (Aumento et al., 1971; Melson and Thompson, 1971; Melson et al., 1972; Bonatti et al., 1971, 1973; Bonatti and Honnorez, 1976; Johnson and Dick, 1992). Metamorphic tectonites that developed in such environments typically exhibit deformation proceeding in a retrogressing P-T regime, commencing with basaltic solidus conditions in parallel with such deformational conditions as are recorded in the Kings-Kaweah ophiolite belt. Submarine studies of ridge-transform intersection environments at slow- to intermediate-rate spreading ridges also indicate that deep mafic crustal and upper mantle rocks are exposed as metamorphic core complexes, particularly when magma production rates lagged behind spreading rates (CAYTROUGH, 1978; Cannat, 1996; Baines et al., 2003; Schroeder and John, 2004; Ildefonse et al., 2007; Tucholke et al., 2008). The sub-oceanic Moho transition zone of the Kings River ophiolite possesses intense structurally concordant constrictional deformation fabrics developed during relatively low flux Permo-Carboniferous MORB magma injection that rendered structural and fabric relations like those developed by upper mantle corner flow off of spreading axis shoulders beneath oceanic core complexes (cf. Schroeder et al., 2007). Mylonitic fabrics developed in the Kings River ophiolite in this structural setting merge into and are cut by steep mylonitic fabrics of the longitudinal shear zones, which are interpreted to be transform shears, or ridge crest discontinuity shears, that evolved into major strike-slip fault and serpentinite mélange zones during large-magnitude transform displacement of the Kings-Kaweah ophiolite belt.

The upper age boundary for significant mélange mixing is provided by the nonconformable overlap relations of lower Mesozoic volcaniclastic and siliciclastic strata, as discussed below. Such nonconformable overlap occurred in a supra-subduction zone environment within the SW Cordillera. The age and structural setting of rare high-pressure mafic metamorphic blocks that occur within the Kaweah serpentinite mélange further constrain the tectonic events that occurred between mélange development in the abyssal realm, and depositional overlap by the active margin strata.

Cryptic High-Pressure Metamorphism

As discussed above, the Kings River ophiolite, as well as crustal blocks within the Kaweah serpentinite mélange, record metamorphic and deformational processes of the abyssal realm with the superposing of regional medial-grade burial conditions and thermal metamorphic overprints acquired in its subsequent supra-subduction zone setting. Two monolithologic mélange blocks of 5-m scale have been discovered that contrast with this pattern, demonstrating the existence of a once underlying high-P metamorphic environment. These two blocks are in mélange units from the southern segment of the ophiolite belt and occur in matrices for which textures and structures that suggest a diapiric and/or detrital origin are relatively well preserved. These rare high-P metamorphic blocks are clearly exotic to the Kings-Kaweah ophiolite belt relative to all other metabasites.

Sample M9 is from one of the two garnet amphibolite blocks discovered, located in the Yokhol Valley area (Fig. 3). The field setting of the block is such that it lies in an area where serpentinite diapirism is shown to have been polyphase, as evidenced by serpentinite "dikes" cutting the cover strata and feeding sedimentary serpentinites within the strata. These relations can be visualized by orienting Figure 3 in such a way as to place the clear arrow positioned along the left margin of the figure at the bottom facing up. In this orientation the folded nonconformity between the Kaweah serpentinite mélange and its cover strata may be viewed as down-plunge. A vertical dike-like body of remobilized sedimentary serpentinite penetrates the nonconformity and cuts into the cover strata along the Harvey Ruth fault zone. The "dike" connects to multiple sedimentary serpentinite-ophiolitic debris flow beds within the cover strata, indicating that it was a growth structure. To the southwest, another dike-like serpentinite body extends southward into the cover strata, with its southeast terminus covered by Quaternary sediments of Round Valley. The M9 garnet amphibolite block is situated in the apparent core area of this "dike."

The M9 garnet amphibolite block records a deformation-metamorphic regime that is distinct from that which characterizes the Kings-Kaweah ophiolite belt. The sample possesses a simple mineralogy and a well-preserved crystalloblastic texture. Hornblende is highly annealed and is embayed by euhedral garnet porphyroblasts. Zoning is not present in the hornblende or garnet grains. Small rutile, albite, and apatite grains are dispersed throughout the hornblende-rich matrix. Fine inclusions within garnet porphyroblasts consist of quartz, augite, and albite. Retrograding and/or contact overprinting is restricted to chlorite sheaths lying along some grain boundaries, and apatite grains that are partially replaced by calcite. Calcite occurs as sub-millimeter-thick veins within the mélange block, and is disseminated in the proximal serpentinite matrix as grain boundary coatings and ophicalcite vein networks. Calcite veining and retrograding in the block are interpreted to represent fluid exchange with the serpentinite matrix.

The equilibrium pressure and temperature conditions of metamorphism for the M9 garnet amphibolite block were calculated using the internally consistent average P-T mode in THERMOCALC, version 3.26 (Powell and Holland, 1994; Holland and Powell, 1998). Critical phase compositions used in the calculation (garnet, hornblende, and plagioclase) are given in Table DR7 (see footnote 1). A value of 802 ± 65 °C and 15.9 ± 2.5 kb is derived. The thermobarometric results place the garnet amphibolite nominally within the high-temperature eclogite facies field (Spear, 1993). Such is not the case, as this sample contains albite and augite. There is no textural evidence of the amphibolite being a retrograded eclogite unless the albite grains are a product of jadeite breakdown in the presence of quartz. However, no jadeite component was detected within the augite inclusions, and the texture and mineralogy of the sample are interpreted to reflect ascent to, and subsequent rapid descent from, the determined P-T conditions without the growth of eclogite facies phases.

Sample M9 was chosen for Sm-Nd geochronology because it shows only minimal textural evidence for a thermal metamorphic overprint, in contrast to the other block that was discovered that lies in an inner contact aureole position and shows a greater textural overprint. Figure 10 is a $^{143}Nd/^{144}Nd$ evolution diagram that shows data for sample M9 garnet and its hornblende-rich matrix, which yield a two point "isochron" corresponding to an age of 255 ± 20 Ma with ε_{Nd} (255) = +8.6 ± 0.4. This age is taken as the approximate time of peak metamorphic conditions for the amphibolite. A K/Ar age of 195 ± 5 Ma was reported for the M9 hornblende (Saleeby and Sharp, 1980). This age is interpreted as a minimum age, considering that the amphibolite is partly retrograded; it sits in an outer contact aureole position, and unfortunately it also sits adjacent to a large Early Jurassic dioritic dike that cuts the Kaweah serpentinite mélange (Fig. 3).

Major element data for the garnet amphibolite suggest that it was derived from a Ti-rich ferrogabbro (Table DR4 [see footnote 1] and Fig. 6B). The high positive initial ε_{Nd} value suggests that it could be of MORB derivation, but major element compositions are too rich in Fe, Ti, and K, and too poor in Si, for typical MORB derivation. Titanium-rich ferrogabbros are present along transform fracture zones from all major ocean basins (cf. Engle and Fisher, 1975; Bloomer et al., 1989; Constantin et al., 1996). A number of these ferrogabbros also show alkali enrichment relative to MORB, like sample M9. The silica depletion of sample M9 is comparable to the most primitive ferrogabbros dredged from fracture zones. In terms of bulk composition, sample M9 also resembles the most primitive mafic eclogite recovered from the Voltri Group of the northern Apennines, also interpreted as a high-P metamorphic derivative of an oceanic ferrogabbro (Mottana and Bocchio, 1975).

Trace-element variation patterns of Ti, V, Zr, Cr, and Y for sample M9 (Fig. 11; data in Table DR6) are most consistent with a MORB derivation. Based on Sm-Nd systematics, derivation from Kings River ophiolite–like or Kaweah serpentinite mélange–like abyssal crustal rocks appears unlikely on the basis of the topologic relations of the respective isochrons (Fig. 10), unless sample M9 has undergone significant alteration in the metamorphic environment. Neodymium is enriched in the sample, compared with all other Kings-Kaweah ophiolite belt basalts and gabbroids (Tables DR3, DR4, and DR6), and small degrees of Nd mobilization are known to be important in at least some deep supra-subduction zone settings (Pearce et al., 1995). Small components of Nd enrichment from marine sediments would shift ε_{Nd} to less radiogenic values (Hoffman, 2004), thereby pulling the M9 Sm-Nd systematics down off a potential primary composition like that represented by the Kings River ophiolite or Kaweah serpentinite mélange Sm-Nd arrays. Phosphorus in sample M9 is also enriched relative to other Kings-Kaweah ophiolite belt basalts and gabbroids (Table DR6). Various degrees of chemical mixing are known to occur along with high-temperature tectonic abrasion and mixing in deep subduction zones (Bebout and Barton, 2002), and subducted hemipelagic sediments are a viable source for phosphorus enrichment (Ingall et al., 1990). Such chemical changes could also entail components of silica depletion, particularly for fluid fluxes subparallel to the subduction megathrust interface (Manning, 1997). Thus the extreme silica depletion of the putative ferrogabbro protolith need not be wholly a primary feature.

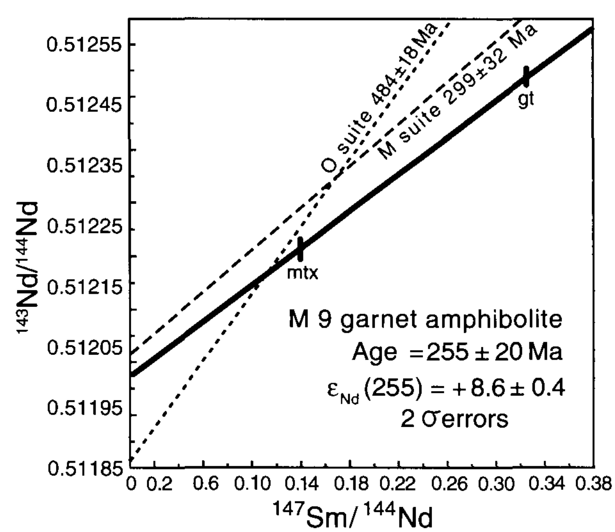

Figure 10. Isotopic evolution diagram of $^{143}Nd/^{144}Nd$ for garnet and hornblende-rich matrix for sample M9 garnet amphibolite showing a 255 ± 20 Ma "isochron" age (isochron solution after Ludwig, 2001). Also shown are isochrons from O and M suite samples from Figure 4. Data in Table DR1 (see footnote 1); gt—garnet; mtx—matrix.

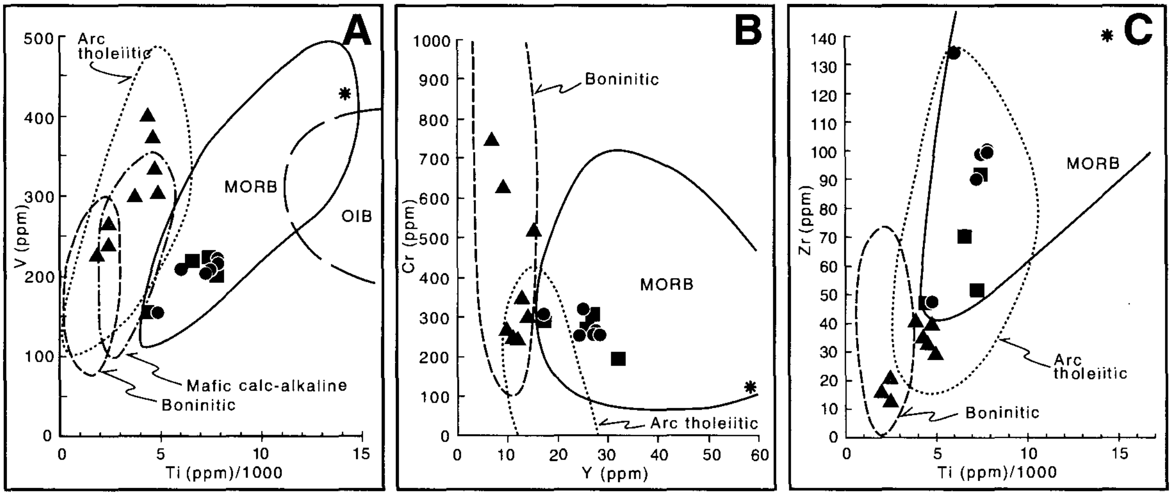

Figure 11. Trace element discriminate diagrams for Kings River ophiolite basalts (circles), Kaweah serpentinite mélange basalts and diabases (squares), and garnet amphibolite (star), and for cover-strata mafic volcanic rocks (triangles). Discriminate fields after Pearce (1982) and Shervais (1982). Data in Tables DR3, DR4, DR6, and DR8 (see footnote 1). MORB—mid-oceanic-ridge basalt; OIB—oceanic-island basalt.

Given the above rationale for metamorphic alterations of sample M9 in the deep subduction zone environment, the derivation of the sample M9 protolith from a Kings-Kaweah ophiolite belt–affinity ferrogabbro that has lost silica and gained a small Nd isotopic contaminant signal from underthrust sediments is favored. The widespread occurrence of relatively low-volume ferrogabbros along fracture zones may be attributed to lateral injection of relatively low-volume fractionated magmas from spreading axis environments into bounding transform walls (Bloomer et al., 1989). The scenario that is tentatively favored is that the ferrogabbro protolith was generated as part of an intrusive complex in conjunction with Middle Permian spreading adjacent to the outer transform wall that bounded the Permo-Carboniferous abyssal crust that was generated within the leaky transform system. The outer transform igneous complex entered a neo-subduction zone that nucleated beneath the Kings-Kaweah ophiolite belt while the intrusive complex was still warm from primary heat. Fragments of the complex were accreted to the hanging wall, where they underwent high P and T metamorphism as well as metasomatic changes that were driven by fluids liberated from underthrust oceanic crust and hemipelagic sediments. Rather than remaining for an extended period of time in the deep hanging-wall environment, and progressing through a complete counterclockwise P-T trajectory (cf. Wakabayashi, 1990), blocks of the complex were abruptly entrained and transported upward in serpentinite diapirs into the overlying Kings-Kaweah ophiolite belt, and possibly were erupted as clasts in serpentinite mud volcanoes. Rapid extraction from the peak metamorphic environment inhibited the development of zoning in the principal metamorphic phases, as contrasted with zoning patterns in major phases of high-P blocks from subduction complexes that have completed a counterclockwise path (cf. Wakabayashi, 1990).

COVER STRATA OF THE KAWEAH SERPENTINITE MÉLANGE

Cover strata related to the Kings-Kaweah ophiolite belt consist of the southern exposures of the Permian to Middle Triassic Calaveras complex, and the western facies of the lower Mesozoic Kings sequence. These cover strata occur primarily as pendant rocks structurally against the eastern margin of the Kings-Kaweah ophiolite belt and also as nonconformable infolds above the Kaweah serpentinite mélange (Figs. 1 and 3). We focus on these infolds, and specifically those of the Yokohl Valley area (Fig. 3). Viewing Figure 3 in down-plunge orientation (clear arrow at bottom, pointing up), an ~1.5-km-long segment of the nonconformity at the base of the Calaveras complex is seen folded about NW-striking axial surfaces. These folds and related cleavage deform the transitional contact with overlying siliceous argillite and siliciclastic-volcaniclastic strata of the Kings sequence, which occurs as a doubly plunging synformal keel within the Calaveras. This relationship is disrupted to the west by the Harvey Ruth fault zone, which bounds the western margin of the Calaveras exposures. The thicker, more intact intervals of bedded chert within the Calaveras complex resemble the upper-level cherts of the diagonal belt of pillow basalt and chert that extends NE-SW across the Yokohl Valley area, in terms of containing siliceous argillite laminar interbeds and overall bedding forms. This, in conjunction with Figure 3 map relations, suggests that bedded cherts of the diagonal belt, and others like it in the Kaweah serpentinite mélange, graded upward to chert and chert-argillite of the overlying Calaveras complex with increasing argillaceous components. During this hemipelagic sedimentation history the surfacing of serpentinite diapirs severely disrupted the then accumulating stratigraphic succession. The locus of diapiric emplacement was along a transverse fault, which cuts and defines the southeast margin of the diagonal pillow basalt–chert belt, and along the Harvey Ruth fault zone. The transverse fault has been deformed in conjunction with cleavage development in the cover strata. The Harvey Ruth fault zone is suggested to have formed a major submarine scarp in the Kaweah serpentinite mélange, with uplifted ocean floor mélange and serpentinized peridotite massifs bounding a trough to the northeast in which Calaveras hemipelagic sediments ponded. Calaveras complex rocks are not observed southwest of the Harvey Ruth fault zone, including the numerous basement cores of the southeastern Great Valley (May and Hewett, 1948; Saleeby, 2007). All cover strata exposures and basement cores from regions southwest of the fault zone are western Kings-sequence-affinity turbidites and volcaniclastic rocks. Thus the Harvey Ruth fault zone constitutes an important tectonic boundary within the Kaweah serpentinite mélange; it originated during deposition of the Calaveras hemipelagic strata, and it continued its activity during the supra-subduction zone residence of the Kings-Kaweah ophiolite belt as shown by its having cut arc volcanic–bearing units of the cover strata.

Western facies Kings sequence strata appear to have also been partly ponded into the down-dropped wall of the Harvey Ruth fault zone. Aside from the more massive mafic volcanic intervals that are discussed below, these strata consist at lower stratigraphic levels of siliceous and tuffaceous argillite and arenaceous and conglomeratic strata, much of which were derived from a chert-rich source like the Calaveras complex, and at upper levels from distally derived siliciclastic turbidites. The Harvey Ruth fault zone was remobilized during deposition of this sequence, at least in part as a conduit for renewed serpentinite diapirism. As evident in the down-plunge view of Figure 3, the serpentinite "dike" was a growth feature feeding multiple sedimentary serpentinite-ophiolitic debris flows within the turbidite section. In this setting the upthrown wall of the fault constituted a forearc ridge, which hosted the serpentinite diapirs that entrained small high-pressure metamorphic blocks that were emplaced into the Kaweah serpentinite mélange.

Supra-Subduction Zone Volcanism

Mafic- to intermediate-composition pillowed and volcaniclastic flows, and tuffaceous admixtures, occur within hemipelagic and siliciclastic cover strata for the Kings-Kaweah ophiolite belt. The stratigraphic positions of these volcanic rocks appear to be restricted to the interval between the cessation of Calaveras radiolarian chert deposition and the arrival of distal siliciclastic turbidites into the region. Unfortunately a vent complex for the volcanic rocks has not been discovered, although likely feeder dikes are observed cutting Kaweah serpentinite mélange basement rocks (Fig. 3). A suite of seven samples from mafic flows, a solitary possible feeder dike that cuts the Kaweah serpentinite mélange, and a dacite clast from a mafic flow were studied geochemically as a means of testing for supra-subduction zone petrogenesis. The more mafic rocks consist of aphyric pillow basalt (sample C8), and pyroxene ± plagioclase ± olivine phyric basalt and basaltic-andesite pillowed and volcaniclastic breccias (samples C2, C3a, C4, C5, C6, and C7). Pyroxenes are commonly pseudomorphed by green amphibole with remnants of only clinopyroxene observed. Rare olivine phenocrysts are pseudomorphed by chlorite ± serpentine ± magnetite. A possible feeder dike for the volcanic rocks, consisting of uralitic diorite, was also studied (sample C1). Major and select trace-element abundance data are presented for the suite in Table DR7 (see footnote 1) and Figures 11 and 12. Except for the dacite clast (sample C3b), silica ranges >52%–55%, with MgO ranging >4%–13%. The dispersed stratigraphic positions of the mafic units, lying within primarily argillaceous strata, raise the question as to the time interval over which the units were erupted. This raises further the question as to whether coherent differentiation trends should be expected for the suite as a whole. Major element variation (Fig. 12) shows some coherency, however. There is a general trend of Al_2O_3, CaO, and TiO_2 enrichment, and MgO depletion with SiO_2. There is no coherency to alkalis, and with the elevated K_2O value of 1.32% for sample C6, at least some alkali mobility is suggested. An iron enrichment trend is suggested for the entire suite on the basis of the FeO/MgO versus SiO_2 plot. On this plot the data straddle the boundary between island arc tholeiite and calc-alkaline–boninite lava series, as defined by Reagan and Meijer (1984) for the Island of Guam in the Mariana forearc. The three lowest stratigraphic level samples (C2, C3a, and C4) have some major element similarities to boninites, with MgO ranging from 9% to 13%, and with SiO_2 at ~52%. These samples also show elevated Ni and Cr contents, which is consistent with a boninitic affinity. In general, however, the suite more closely resembles an arc tholeiite association.

Trace element data for the cover-strata volcanic rocks are consistent with an arc tholeiite–transitional boninite lava series. Select trace element variation diagrams for the mafic volcanic members, as well as basalts from the Kings-Kaweah ophiolite belt, are presented in Figure 11 (after Pearce, 1982; Shervais, 1982). On the V versus Ti plot the cover strata suite spreads along the arc tholeiite–calc-alkaline–boninite field. For Cr versus Y the three high-Mg rocks plot in the boninite field, and the rest in the boninite-arc tholeiite transition. For Zr versus Ti the three high-Mg rocks again plot in the boninite field, and the rest in the arc tholeiite field. All Kings-Kaweah ophiolite belt basalts plot within the MORB field. The two cover-strata volcanic rocks with the lowest SiO_2 (samples C3a and C8) were analyzed for Nd and Sr isotopes (Table DR1). Initial isotopic composition corrections were made for a nominal age of ca. 215 Ma, which is justified below in the discussion of the age of the cover sequence. Initial ε_{Nd} for these samples is +8.2 (±0.4) and 7.9 (±0.4), respectively. The Sr_i values are 0.7036 and 0.7040, respectively. The Nd data point to a strong depleted mantle component, whereas the Sr data suggest a seawater component added to the depleted mantle component. The initial ε_{Nd} values fall within the upper range of values typically measured for arc tholeiite-boninite series rocks, whereas the Sr_i values lie at the lower range (Taylor et al., 1994;

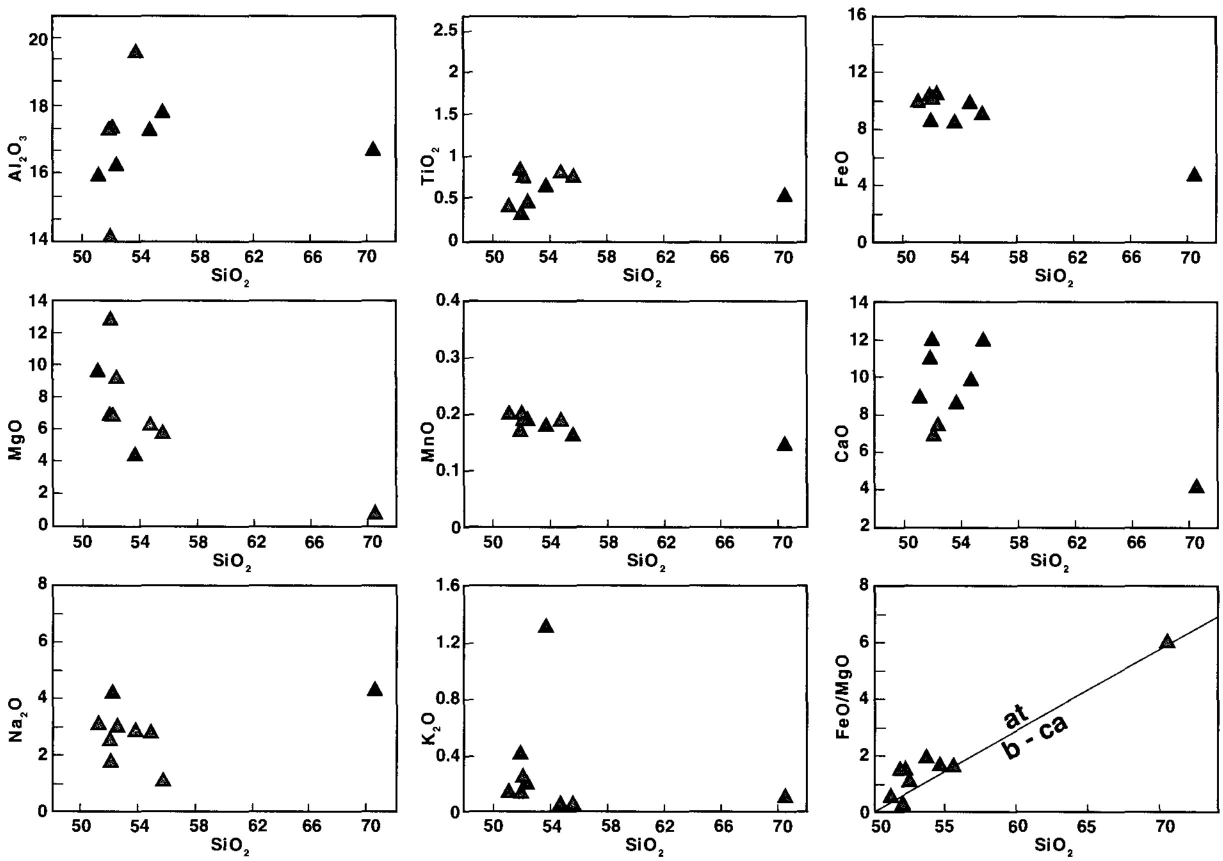

Figure 12. Major element variation diagrams for cover-strata volcanic rocks. Island arc tholeiite–calc-alkaline–boninite boundary on FeO/MgO versus SiO_2 diagram from Reagan and Meijer (1984). Data in Table DR8 (see footnote 1).

Stern et al., 1991). Thus the mantle source for these lavas appears to have been at the more highly depleted end of the spectrum for typical sources of such lavas.

The association of early-stage boninitic-affinity lavas, followed by arc tholeiites, is typical of the initial stages of supra-subduction zone magmatism following subduction initiation (Stern and Bloomer, 1992; Bloomer et al., 1995; Stern, 2004). Relatively shallow-level partial melting of partially serpentinized harzburgite, like that of the Kings River ophiolite, is a likely source for the earlier boninitic-affinity lavas with deeper melting of a similar depleted source that gave rise to the tholeiitic lavas. The relatively advanced state of time integrated LILE source depletion, as indicated by the Nd and Sr isotopic data, is consistent with abyssal mantle lithosphere akin to that of the Kings River ophiolite, forming the principal source rock in the mantle wedge that rendered the mafic lavas.

Stratigraphic Setting and Age Constraints of Proximal Supra-Subduction Zone Volcanic Rocks

The eruption of proximal volcanic rocks of the cover strata began at the cessation of radiolarian chert deposition in the Calaveras complex, and ceased by the time of siliciclastic turbidite deposition of the western Kings sequence. These relationships are exhibited for the sample C2 basaltic unit that lies along the Calaveras–Kings sequence contact, and the sample C8 basaltic unit that is mainly faulted against, but appears to be in local depositional contact with, the turbidites (Fig. 3). The local depositional contact is likely an angular unconformity, now transposed, representing an unknown hiatus. Age constraints for the cover strata are only quite broad, and thus the time interval over which proximal volcanism occurred is not well constrained. Accumulation of Calaveras chert-argillite began after a putative ~30 m.y. of radiolarian ooze deposition above ca. 295 Ma Kaweah serpentinite mélange pillow basalt. This suggests that Calaveras chert-argillite sedimentation began at ca. 265 Ma, or in the Middle Permian. The inclusion of Permian shallow-water-limestone slide blocks within chaotically deformed Calaveras chert-argillite (Saleeby, 1979) only constrains hosting chert-argillite deposition to the Permian or younger. Ammonoid remains from several localities within Kings sequence argillites indicate an early Mesozoic age (Saleeby et al., 1978). U/Pb zircon ages of 170 ± 1 Ma on a hornblende andesite dike that crosscuts the sample C3 volcanic unit (Saleeby and Sharp, 1980), and of 152 ± 1 Ma on a trondhjemitic dike that cuts the siliciclastic turbidites, further indicate an early Mesozoic age for much of the section (Saleeby and Dunne, 2011). The 255 ± 20 Ma Sm-Nd isochron age for the sample M9 garnet amphibolite putatively further constrains proximal supra-subduction zone volcanism to have initiated in early Mesozoic time.

Maximum age constraints for the sample C3 volcanic unit are provided by U/Pb zircon age data on sample C3b, an angular dacite clast of ~30 dm diameter that lies in a basaltic tuff breccia (sample C3a). The size and textural immaturity of the clast indicate that it probably underwent only one cycle of transport within the hosting submarine pyroclastic flow. This further suggests that its source was proximal to the vent complex for the mafic flow. In terms of bulk composition (Table DR7 and Fig. 12) and the presence of plagioclase microphenocrysts, completely recrystallized, the dacite clast is similar to silicic members of the boninite-arc tholeiite suites of Chichijima in the Bonin Islands forearc (Taylor et al., 1994). Possible consanguinity between the dacite clast and its mafic host suggests that the age of the clast could approximate the age of the sample C3 volcanic unit and other similar units proximal to the sample C3 site (Fig. 3). Sample 3b yielded a meager population of fine euhedral zircon. Figure 13A is an age frequency plot for $^{206}Pb/^{238}U$ ages determined by laser ablation ICP-MS (inductively coupled-plasma mass spectroscopy) techniques on 23 fine euhedral grains extracted from the clast. Analytical data are presented in Table DR9a. The data define a mean age of 219.1 ± 2.9 Ma. Ages for a number of grains range to as young as earliest Cretaceous, similar to the highly discordant zircon from the Kaweah serpentinite mélange plagiogranites (Saleeby and Sharp, 1980). The zircon grains of sample C3b, exhibiting the younger ages, are considered disturbed by Sierra Nevada batholith contact metamorphism and have been omitted from the Figure 13A analysis. The distribution of $^{207}Pb/^{206}Pb$ ages for those grains included in the age analysis (Table DR9a) suggests that most of these ages are concordant, and with the small scatter of the $^{206}Pb/^{238}U$ ages (MSWD = 1.4), 219 Ma is taken as the eruption age for the dacite clast source. U/Pb zircon data indicating an age of ca. 200 Ma was presented for the sample C1 dioritic "feeder" dike (Saleeby and Sharp, 1980). These age constraints suggest a Late Triassic to earliest Jurassic age for the principal phase of supra-subduction zone volcanism in the cover strata. The onset of supra-subduction zone volcanism in the Late Triassic in conjunction with stratigraphic relations (Fig. 3) places a Middle Triassic bound on the termination of hemipelagic sedimentation for the Calaveras complex.

Approximate age and sediment provenance constraints for the siliciclastic turbidite of sample C9 are provided by U/Pb ages of its detrital zircon population (Table DR9b and Figs. 13B and 13C). Sample C9 consists of a 10-cm-thick sandstone bed graded to medium sand size along its base, where it consists of ~60% quartz, ~20% feldspar, plagioclase dominant, and ~20% lithic fragments, both volcanic and metamorphic. Recrystallization inhibits the precision of the determined modes and may have skewed the analysis away from a higher lithic content. Figure 13B shows an age probability plot for back to 500 Ma on the basis of 37 $^{206}Pb/^{238}U$ ages. In terms of age constraints on the turbidite, the strong peak at 175–160 Ma suggests a late Middle Jurassic maximum depositional age. The minimum age of the turbidite section is constrained by it and its first cleavage being cut by a 152 ± 1 Ma trondhjemite dike swarm (Saleeby and Dunne, 2011). The 175–160 Ma peak corresponds to one of two major early Mesozoic magmatic flux events in the SW Cordilleran arc, the other being during the Triassic (Stern et al., 1981; Chen and Moore, 1982; Fiske and Tobisch, 1978; Busby-Spera, 1984; Barth et al., 1997; Ducea, 2001; Saleeby and Dunne, 2011). The sample C9 detrital zircon clearly reflects detrital inputs from both early Mesozoic arc belts. The full spectrum of $^{206}Pb/^{238}U$ detrital zircon ages for sample C9 is given in Figure 13C, with comparative plots from regional Paleozoic siliciclastic units that constituted proximal parts of the SW Cordilleran passive margin and overlying lower Mesozoic eolianites, which were possible sources for the ancient detrital zircon populations. Of particular interest are the spectra from continental slope-rise strata that occur in southern Sierra Nevada pendants as basement for the eastern facies of the Kings sequence (Saleeby and Busby, 1993; and unpub. data), and similar pendant rocks from the northern Mojave Desert region (A. Chapman and J.B. Saleeby, unpub. data). The spread of ages between ca. 0.95–2.1 Ga and 2.45–2.8 Ga corresponds to a series of peaks in the C9 turbidite. In contrast, lower Paleozoic passive-margin shelf rocks of the Snow Lake pendant of the east-central Sierra Nevada, the central Mojave Desert, and Death Valley (Grasse et al., 2001; Barbeau et al., 2005) do not yield spectra similar to the Late Archean-Proterozoic population of sample C9. Sample C9 peaks in the 390–640 Ma range are not readily explained with the southern Sierra–northern Mojave source spectra. Ages in the 390–400 Ma range could reflect fringing arc rocks emplaced into and erupted over lower Paleozoic (Shoo Fly) slope-rise strata of the northern Sierra Nevada (Saleeby et al., 1987), whereas detrital zircon with ages ranging from 390 to 640 Ma are abundant in lower Mesozoic eolianites that spread across the western reaches of the SW Cordilleran passive margin (Dickinson and Gehrels, 2003; Fig. 13C). The distribution of Paleozoic SW Cordilleran passive margin strata along the California region is pursued further below.

In summary, proximal supra-subduction zone submarine mafic volcanic rocks of the Kaweah serpentinite mélange cover strata were erupted in Late Triassic to earliest Jurassic time. Upper Middle to lower Upper Jurassic siliciclastic turbidites appear to rest unconformably on the youngest of these mafic flows. A vent complex has not been identified for the Late Triassic–earliest Jurassic flows. Intercalation of the flows with argillite-rich strata suggests episodic volcanism off the flanks of a vent complex within a basinal setting. Such a vent complex has been identified for Late Triassic–earliest Jurassic arc tholeiitic to transitional calc-alkaline submarine mafic volcanics of the Jasper Point–Penon Blanco Formation ~100 km north of the Kings-Kaweah ophiolite belt along the Sierra Foothills belt (Saleeby, 1982; Snow, 2007). This volcano-plutonic complex

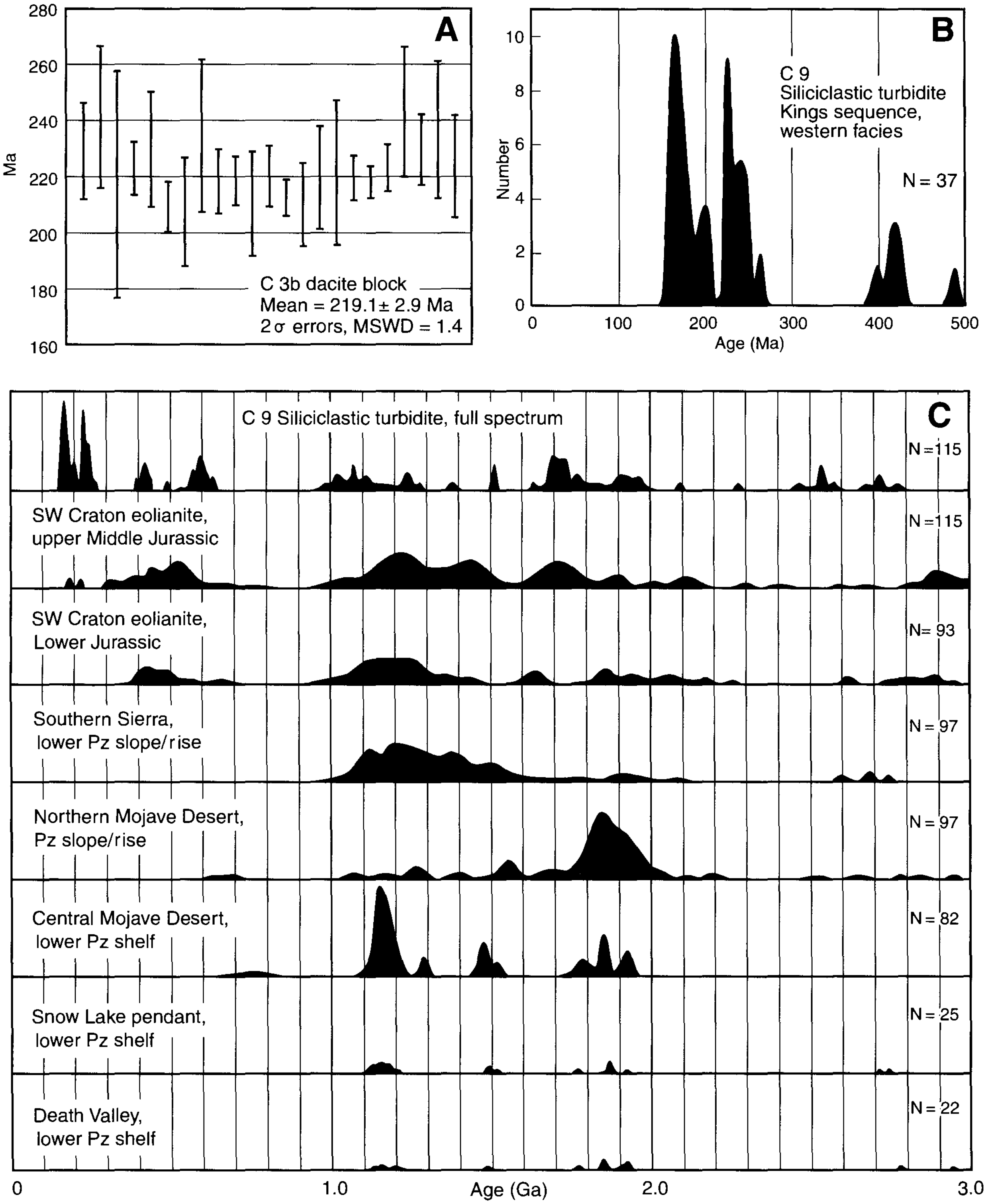

Figure 13. U/Pb zircon age data for cover strata samples. (A) Frequency plot of $^{206}Pb/^{238}Pb$ ages on single igneous zircon grains from sample C3b dacite block. (B) Probability plot of younger spectrum of $^{206}Pb/^{238}Pb$ ages for detrital zircon from sample C9 siliciclastic turbidite. (C) Probability plots of $^{206}Pb/^{238}Pb$ ages for detrital zircon of C9 siliciclastic turbidite in comparison to $^{206}Pb/^{238}Pb$ ages for detrital zircon populations from Paleozoic siliciclastic units of the southern Sierra Nevada region and for lower Mesozoic eolianites of the SW Cordillera, which were potential source components for the turbidites (after Grasse et al., 2001; Dickinson and Gehrels, 2003; Barbeau et al., 2005; Chapman et al., 2011). Data in Tables DR9a and DR9b (see footnote 1). MSWD—mean square of weighted deviates; Pz—Paleozoic.

was constructed on the Permo-Carboniferous Tuolumne ophiolitic mélange. The Jasper Point–Penon Blanco volcanic construct appears to have constituted a broad pillowed shield with hemipelagic sediment intervals followed by submarine volcaniclastic cone construction. The upper volcaniclastics interfinger northward along the Foothills belt with argillite-rich strata, producing a section similar to the principal stratigraphic section in which the Kaweah serpentinite mélange cover strata volcanics lie. It seems likely that the mafic flows in this serpentinite mélange cover strata likewise formed off the flanks of a major constructional center, presently not exposed. Thus the pattern of early Mesozoic supra-subduction zone mafic submarine volcanism constructed on a disrupted and accreted late Paleozoic ophiolitic substrate is a regional pattern along the Foothills belt. Furthermore, the Jasper Point–Penon Blanco construct, and part of its intrusive roots, rest unconformably beneath Upper Jurassic siliciclastic turbidites (Saleeby, 1982; Ernst et al., 2009), further attesting to a common early Mesozoic tectonic history along the Foothills belt.

TECTONICS OF MÉLANGE FORMATION IN A LARGE OFFSET TRANSFORM–SUBDUCTION INITIATION ENVIRONMENT

In this section a tectonic model is developed that accounts for the polygenetic abyssal magmatic history of the Kings-Kaweah ophiolite belt, its progressive disruption to form ocean floor mélange, and its accretion into the SW Cordilleran active margin and ensuing residence in a supra-subduction zone environment. A number of initial questions must be addressed in order for such a model to be seriously considered: (1) Was the Kings-Kaweah ophiolite belt "obducted" onto the Cordilleran margin? (2) Given up to an ~190 m.y. hiatus in abyssal magmatism, is the implied residence time within the abyssal realm reasonable within the physical constraints of seafloor spreading rates and characteristic sizes of major ocean basins? And (3) Given a major abyssal transform phase for the Kings-Kaweah ophiolite belt, did the plate kinematics of this plate juncture circuit directly into the plate kinematics of the Cordilleran margin? Or alternatively, was the abyssal transform phase decoupled from Cordilleran tectonics, and the transform assemblage merely accreted en masse, independent of its transform history? This question may also be posed as: Is there evidence within the SW Cordillera, independent of the transform history recorded in the Kings-Kaweah ophiolite belt, for late Paleozoic transform tectonics having affected the region?

Gross Emplacement Geometry

The Kings-Kaweah ophiolite belt was not obducted onto the SW Cordilleran margin. Regionally pervasive deformation structures and fabrics associated with the ophiolite belt are steep to vertical. West-dipping mid-crustal reflectors along the western Sierra Nevada–Great Valley transition directly north of the Kings River region (Miller and Mooney, 1994) are commonly cited as evidence for eastward obduction of the Foothills belt, including its ophiolitic basement, in the Late Jurassic. However, basement core, as well as surface map data, shows that such reflectors underlie voluminous Early Cretaceous Sierra Nevada batholith rocks and subordinate pendants of Foothills belt rocks (May and Hewett, 1948; Saleeby, 2007). The referenced reflectors are continuous and highly coherent, and would not survive in such a state after the intrusion of copious batholithic intrusions. Furthermore, these reflectors coincide with a patch of recent seismicity (Gilbert et al., 2007), and thus it is much more likely that the reflectors are young and potentially active structures related to ongoing mantle-lithosphere removal processes and related lower crustal flow beneath the region (Zandt et al., 2004; Le Pourhiet et al., 2006; Saleeby et al., 2003).

The emplacement geometry of the Kings-Kaweah ophiolite belt appears to have constituted a lithosphere-scale wedge that was accreted to the hanging wall of a newly established subduction zone. Serpentinite diapirs were sourced from deep enough below the accreted wedge to entrain high-pressure metamorphic blocks from underplated abyssal lithosphere, and the diapirs penetrated up through the accreted ophiolite belt without entrainment of hypothetical continental structural basement for the belt, assuming an obduction geometry. Early Mesozoic boninitic to arc tholeiitic volcanics that were erupted through the Kings-Kaweah ophiolite belt were likewise sourced within a mantle wedge composed of hydrous depleted peridotites with strong time integrated LILE depletions. Finally, Early Cretaceous members of the Sierra Nevada batholith that were intruded through the Kings-Kaweah ophiolite belt lack any evidence of having interacted with hypothetical continental structural basement for the ophiolite belt. The above is displayed in the Figure 14 plot of initial ε_{Nd} verses Sr_i for principal igneous suites of the southern Sierra Nevada (DePaolo, 1981; Pickett and Saleeby, 1994; Clemens-Knott et al., 2011; and data reported here). The plot shows data fields for the Kings-Kaweah ophiolite belt, cover strata mafic volcanics, shallow-level Early Cretaceous Sierra Nevada batholith rocks emplaced into the Kings-Kaweah ophiolite belt, deep-level Early Cretaceous Sierra Nevada batholith rocks emplaced south of, but along strike of, the Kings-Kaweah ophiolite belt, and Late Cretaceous Sierra Nevada batholith rocks emplaced into North American crustal rocks of the axial to eastern Sierra Nevada batholith. The plot also shows a representative field for Proterozoic sialic basement of the SW Cordillera region, an important component for the axial to eastern Sierra Nevada batholith suite. The western Foothills suites display a geochemical maturation of the underlying mantle wedge with time, starting with its proto-composition as depleted mantle of Kings-Kaweah ophiolite belt affinity. Progressive addition of slab-derived fluids and minor terrigenous sediment components to the mantle wedge with time progressively shifted the ε_{Nd} and Sr_i values progressing from the early Mesozoic supra-subduction zone mafic volcanics to the cross-cutting batholithic units (cf. DePaolo, 1981; Lackey et al., 2005; Stern et al., 1991; Clemens-Knott et al., 2011). In contrast, the entire axial to eastern Sierra Nevada batholith suite shows a strong Proterozoic North

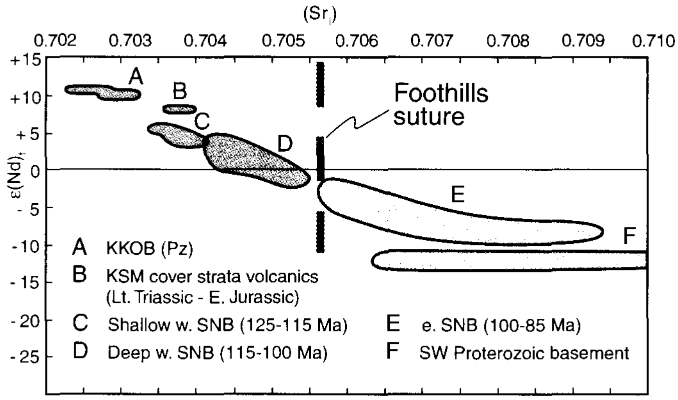

Figure 14. Plot of initial ε_{Nd} verses Sr_i for samples from the Kings-Kaweah ophiolite belt (KKOB), its cover strata mafic volcanics, crosscutting plutons of the Early Cretaceous Sierra Nevada batholith (SNB), axial to eastern batholithic rocks of the southern Sierra Nevada, and SW Cordilleran Proterozoic basement (DePaolo, 1981; Pickett and Saleeby, 1994; Clemens-Knott et al., 2011; data presented in Table DR1 [see footnote 1]). Also delineated is the geochemical expression of the Foothills suture. Pz—Paleozoic.

American lithosphere or crustal component that is consistent with the North American crustal host rocks for the inner Sierra Nevada batholith zones. The boundary between the distinctive eastern continental affinity and western oceanic affinity Sierra Nevada batholith coincides with a profound tectonic break in metamorphic framework rocks wherein Paleozoic ophiolitic rocks lie to the west, and early Paleozoic Cordilleran passive-margin-affinity rocks lie to the east. The pre-batholithic boundary is named the *Foothills suture,* shown by its expression in the Sierra Nevada batholith ε_{Nd} versus Sr_i in Figure 14, and discussed further below.

Aging of Oceanic Plates

As noted earlier, an ~190 m.y. hiatus in abyssal magmatism may not seem reasonable within the context of modern plate tectonics. The oldest known abyssal crust is ca. 168 Ma in the western Pacific, and it is nearing subduction into the Mariana trench (Ogg and Smith, 2004). However, the geometry of the continental masses and ocean basins was very different throughout the Paleozoic, as compared with the Cenozoic. During the Pangean supercontinent era the Panthalassa ocean basin occupied nearly two-thirds of Earth's surface (Murphy and Nance, 2008). Thus such an extended abyssal-realm residence for the Kings-Kaweah ophiolite belt does not appear to pose any problems that cannot be accounted for in our current understanding of plate tectonics through geologic time.

An interesting consideration regarding the abyssal magmatic hiatus is the implication of the residence of such old oceanic lithosphere in the Panthalassa basin. Based on simple principles of conductive cooling of oceanic lithosphere as it ages off its respective spreading axis, such old oceanic lithosphere should have carried strong negative buoyancy forces. Such strong negative buoyancy would have worked in favor of a subduction initiation event, given the correct tectonic circumstances. It appears that the SW Cordilleran margin and the adjacent Panthalassa basin presented such circumstances at the end of the Paleozoic.

Transform Tectonics and Subduction Initiation along the SW Cordilleran Margin

One of the definitive features of the SW Cordilleran margin is a regionally extensive zone of Permo-Carboniferous transform truncation that coincides with the pre-batholithic metamorphic framework of the Sierra Nevada (Davis et al., 1978; Walker, 1988; Kistler, 1990). Evidence supporting this event includes the high-angle truncation of NE-SW–trending facies boundaries and fold-thrust structures in the Neoproterozoic-Paleozoic passive margin sequence along the eastern Sierra Nevada region, and the truncation of the regional Paleozoic "McCloud" fringing arc-marginal basin system that ran outboard of the central to northern Cordilleran passive margin (Rubin et al., 1990). In conjunction with this truncation event was the transpressive accretion of NW-trending strike-slip ribbons along the truncation zone, which constitute the principal Paleozoic metamorphic framework units for the Sierra Nevada batholith. Figure 15 shows the distribution of Paleozoic metamorphic framework ribbons in the Sierra Nevada as well as the southern termination of the McCloud arc in the eastern Klamath Mountains. The Sierra Nevada batholith framework ribbons occur along the western Foothills, where they are variably covered by lower Mesozoic active margin strata as poly-metamorphosed pendants within this batholith, and as the eastern wall of the batholith along the Owens Valley region. The general distribution of the displaced ribbons relative to the zone of Permo-Carboniferous continental truncation is shown in the inset map of Figure 15.

Essential features of Figure 15 are the delineation of regional tectonic domains based on facies relations and petrotectonic assemblages of Paleozoic rock exposures. The domains include areas once occupied by Paleozoic rocks that have been intruded out by Mesozoic plutons or covered by Mesozoic or Cenozoic strata. The principal domains are the western North America craton margin, the passive margin shelf, its slope and rise, the McCloud fringing arc with remnants of its subduction complex, and Panthalassa lithosphere that was accreted to the SW Cordilleran margin. The principal Paleozoic rock exposures for the Sierra Foothills belt and the southeastern Klamath Mountains are differentiated within the context of the regional domains. Of critical importance in the western Sierra are exposures of Paleozoic ophiolitic mélange and metamorphic tectonites of the Feather River, Bear Mountain, and Tuolumne complexes, all of which have igneous and metamorphic age, and a number of structural relations that are similar to those of the ophiolitic ductile shear zones and serpentinite mélange of the Kings-Kaweah ophiolite belt (Saleeby, 1990). Co-extensive with these Paleozoic oceanic basement exposures are belts of Calaveras complex chert-argillite, all broadly constrained in age from

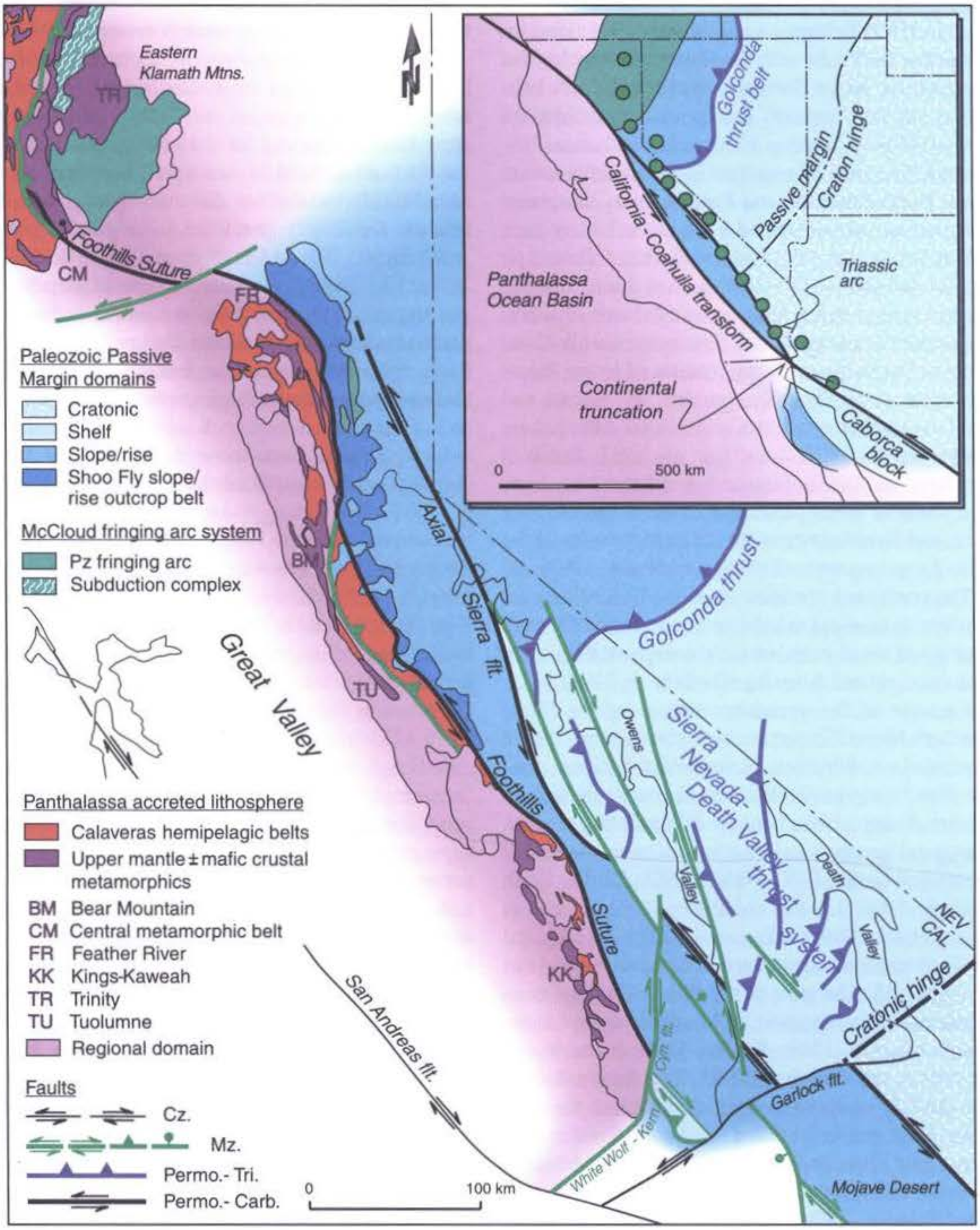

Figure 15. Maps showing principal Paleozoic tectonic elements and facies systems of the SW Cordillera in relation to the Permo-Carboniferous continental truncation zone, Sierra Foothills Paleozoic ophiolite and related (Calaveras) chert-argillite belts, and key Paleozoic tectonic elements of the eastern Klamath Mountains. Some of the larger isolated plutons and basal contacts of the lower Mesozoic overlap units of the Sierra Foothills and the Klamath Mountains are delineated for location purposes. No attempts were made to restore Basin and Range extension nor Middle Jurassic dextral drag along the Sierra Nevada and its proximal backarc region. The strike-slip ribbons of the Sierra Nevada are reconstructed from stratigraphic relations of metamorphic pendant belts. (Sources: D'Allura et al., 1977; Irwin, 1977; Schweickert et al., 1977; Saleeby et al., 1987; Kistler, 1990; Saleeby, 1990; Saleeby and Busby, 1993; Metcalf et al., 2000; Dickinson and Lawton, 2001; Glazner et al., 2005; Stevens and Green, 2000; Stevens et al., 2005; Stevens and Stone, 2005; Nadin and Saleeby, 2008; Saleeby and Dunne, 2011.) Pz—Paleozoic; Cz—Cenozoic.

Permo-Carboniferous to Permo-Triassic (Cox and Pratt, 1973; Schweickert et al., 1977; Behrman and Parkison, 1978; Watkins et al., 1987; Saleeby, 1979). As with the Calaveras complex that is spatially related to the Kings-Kaweah ophiolite belt, these belts are interpreted as mainly "Permian" hemipelagic accumulations that rested above, and were accreted along with, Panthalassa lithosphere fragments. The locus of accretion is the Foothills suture, the join between North American and Panthalassan lithosphere. The suture is hypothesized to have had a polyphase history, first, of Permo-Carboniferous sinistral transform motion, followed by latest Permian sinistral oblique thrust imbrication during subduction initiation, and then re-deformation within the axis of superposed early Mesozoic arc magmatism. The eastern wall of the suture in the central to northern Sierra consists of lower Paleozoic slope-rise strata of the Shoo Fly complex, and plutons and overlap strata of the southernmost McCloud arc (D'Allura et al., 1977; Schweickert et al., 1977; Saleeby et al., 1987; Rubin et al., 1990; Harding et al., 2000). Similar lower Paleozoic slope-rise strata lie in southern Sierra pendants east of the intruded-out Foothills suture, and form basement for the eastern facies of the lower Mesozoic Kings sequence (Saleeby and Busby, 1993; and unpub. data). The northward continuation of the Foothills suture is suggested below to have extended into the southern Klamath Mountains, but it has since been severely overprinted by early Mesozoic subduction-related thrusting (Davis et al., 1978).

The inner margin of the truncation zone along the Sierra Nevada and northern Mojave Desert has been completely intruded out by the Mesozoic batholithic belt. Nevertheless, the inner truncation boundary can be regionally delineated by stratigraphic and sedimentary facies discontinuities between NW-trending pendant belts and by regional geochemical discontinuities in the batholithic belt (Moore and Foster, 1980; Walker, 1988; Kistler, 1990; Dunne and Suczek, 1991; Saleeby and Busby, 1993; Greene et al., 1997; Stevens et al., 2005; Lackey et al., 2005; Saleeby and Dunne, 2011). The inner truncation structure is shown as the Axial Sierra fault in Figure 15. The trace of the Permo-Carboniferous Axial Sierra fault has been disrupted by Mesozoic dextral faults (Lahren and Schweickert, 1989; Kistler, 1990; Saleeby and Busby, 1993; Nadin and Saleeby, 2008). The distribution of passive-margin shelf facies rocks along and adjacent to the truncation zone has been further shuffled by Permo-Triassic and mid-Cretaceous thrust faults, and conceivably by early Mesozoic extensional faults (Stevens and Greene, 2000; Stevens and Stone, 2005; Nadin and Saleeby, 2008; Saleeby and Dunne, 2011). The principal superposed Mesozoic structures are shown in Figure 15 in green, some preserved in batholithic and pendant rocks, and some largely cut out by batholithic rocks. In the extreme southwestern Sierra Nevada and adjacent Mojave Desert, large-magnitude extensional structures of Late Cretaceous age that exhumed the Sierra Nevada batholith to lower crustal levels have obscured pre-batholithic pendant relationships (Nadin and Saleeby, 2008; Saleeby et al., 2007). Elsewhere in the Sierra Nevada, exhumation of the batholith has been limited to mid- to upper crustal levels, leaving pendant stratigraphy and batholith petrochemical patterns intact to the extent that the complex structural relations along the truncation zone can be reasonably constrained (Fig. 15).

The accreted Panthalassa lithosphere domain extends across the projected trace of the Foothills suture in the eastern Klamath Mountains region as the Trinity peridotite, which forms depositional basement for the southernmost McCloud arc, and the Klamath Central Metamorphic Belt that consists of Paleozoic MORB metabasites that were partly subducted eastward beneath the Trinity peridotite in mid-Paleozoic time (Wallin and Metcalf, 1998; Metcalf et al., 2000; Barrow and Metcalf, 2006). The Trinity peridotite consists of serpentinized harzburgite, dunite, and lherzolite that are similar to the long-term LILE-depleted mantle that rendered the crustal section for the Kings River ophiolite. Plagioclase lherzolite that equilibrated under shallow upper-mantle, diapiric conditions (Quick, 1981) yields an Sm-Nd mineral–bulk rock isochron and an initial ε_{Nd} that are indistinguishable from those determined for the Kings River ophiolite mafic crustal section (Jacobsen et al., 1984; Shaw et al., 1987). The high ε_{Nd} value indicates that the Trinity peridotite was derived from the Panthalassa-depleted MORB mantle. The Trinity peridotite was ascending and undergoing partial melting beneath a Panthalassa spreading center at the same time that the Kings River ophiolite crustal section was generated along a Panthalassa spreading center by the partial melting of a Trinity-like peridotite. Unfortunately, vestigial lenses of peridotites retaining the remnants of high-temperature mantle-flow fabrics in the Hog and Red Mountain slabs of the Kings River ophiolite are serpentinized and contact metamorphosed, so they are not well suited for mineral isotopic studies that could more directly test a Trinity peridotite affinity. The Trinity peridotite was incorporated into a supra-subduction zone environment during the Early Silurian initiation of the southern segment of the McCloud arc system (Metcalf et al., 2000), whereas the Kings River ophiolite remained in the Panthalassa abyssal realm until the Late Permian. This is consistent with the Kings River ophiolite being generated at a fast spreading ridge, as concluded above, which potentially generated large expanses of abyssal lithosphere, including that of the Trinity peridotite, capable of rendering highly divergent tectonic evolutionary paths of potentially derivative ophiolitic fragments.

The inset map of Figure 15 shows the southwest Cordillera truncation zone in a regional context. The truncation structure has been equated with the Mojave-Sonora megashear (Anderson and Silver, 1979), a zone of Late Jurassic sinistral shear that has produced little translation that can be documented. The term *California-Coahuila transform* has been adopted from Dickinson and Lawton (2001) as the Permo-Carboniferous truncation and translation zone, so as not to confuse this plate juncture for the superposed intraplate supra-subduction zone strain of the "megashear." The Caborca block is shown in the northwestern Mexico region astride the transform. This block corresponds to a fragment of the passive margin shelf that was translated 500–800 km along the transform from the truncated shelf at Sierra Nevada latitudes (Stevens et al., 2005). Stratigraphic relations along the truncation locus indicate that the principal phase of sinistral translation was during the Pennsylvanian (Stevens et al., 2005). Isolated exposures of slope-rise strata along the northwest margin of the Caborca block could be facies changes across the margin of the block and/or additional strike-slip ribbons displaced within the transform zone. The inset map also shows the locus of Triassic arc magmatism, which runs inboard and along the trace of the transform zone (Stern et al., 1981; Chen and Moore, 1982; Busby-Spera, 1984; Barth et al., 1997; Saleeby and Dunne, 2011). The actual age range of this "Triassic" arc belt is from the latest Permian (ca. 248 Ma) into the Early Jurassic (ca. 200 Ma), with the highest flux of plutons occurring in Early to Middle Triassic time. The principal phase of transform truncation and displacement along the California-Coahuila system, and the onset of "Triassic" arc magmatism, are in accord with the transform phase of development, and the subduction initiation emplacement of the Kings-Kaweah ophiolite belt.

Translation and Emplacement of the Kings-Kaweah Ophiolite Belt

The favored hypothesis for the generation, displacement, and emplacement of the Kings-Kaweah ophiolite belt is shown in Figure 16, and an overview of the critical phases of geologic history recorded in this ophiolite belt are summarized in Table 2. Lacking definitive constraints, a simple approach is adopted for the initial plate configuration whereby the genesis of the Kings River ophiolite along a fast-spreading ridge is depicted to have been proximal to a large offset transform roughly aligned with the future California-Coahuila transform (Fig. 16A). The fracture zone is shown extending into the Cordilleran passive margin as a marginal offset in the Neoproterozoic rifted margin. The marginal offset is shown as the outer edge of what was to become the Caborca block in the Permo-Carboniferous. The configuration of the passive margin to the south of the Caborca block native site (present geographic coordinates) is poorly constrained owing to subsequent tectonic overprints (Dickinson and Lawton, 2001; Nance and Linnemann, 2008). The possible existence of additional continental ribbons displaced from the outer edge of the Caborca block is also poorly constrained, with one possibility being the older continental basement elements within the Chortis block of the Central America isthmus (Rogers et al., 2007).

Vast tracts of new abyssal lithosphere are shown to have been generated in Early Ordovician time (Fig. 16A), capable of rendering highly divergent evolutionary paths of its potential ophiolitic fragments, as indicated by the contrasting histories of the Kings River ophiolite and the Trinity peridotite. Considering the distribution of the continents and major ocean basins in the early Paleozoic (Murphy and Nance, 2008), the seafloor spreading kinematics of Figure 16A could have circuited directly into Iapetus plate motions. A hypothetical site for the Early Ordovician ascent of the Trinity peridotite beneath a Panthalassa ridge segment is shown adjacent to the "Kings River ophiolite" ridge segment, across a major transform fracture zone. The "Trinity" ridge-transform segments are considered likely nucleation sites for the initiation of east-dipping intra-oceanic subduction that rendered the southern segment of the McCloud arc, which was formed by Early Silurian time as recorded in the Klamath Mountains (Wallin and Metcalf, 1998). Once subduction initiated for the McCloud arc, the plate configuration depicted requires that the oceanic transform zone separating the Kings River ophiolite and Trinity ridge segments became active as a boundary transform, possibly analogous to the modern South Sandwich transform that bounds the southern Scotia Arc (British Antarctic Survey, 1985). Devonian–Early Mississippian fold and thrust belt structures developed along the southern McCloud backarc and adjacent Cordilleran shelf region suggest an early phase of McCloud arc impingement along the Cordilleran margin (cf. Smith and Miller, 1990) the details of which are not treated here.

Figure 16B shows the plate geometry in the Late Pennsylvanian (295–290 Ma), entailing the initiation of the California-Coahuila transform, and intra-oceanic rifting along the Kings-Kaweah ophiolite belt–hosting transform. The initiation of a transform-spreading geometry similar to the Cayman Trough is adopted (CAYTROUGH, 1978; Rosencrantz et al., 1988) whereby ephemeral short spreading-center segments lie nested between transform walls with metamorphic core complex segments. The b–b′ cross section diagrammatically shows Ordovician MORB crust and mantle lithosphere (Kings River ophiolite) along the edge of the transform deforming into a metamorphic core complex and being entrained into the reactivated leaky transform zone. The geometry and kinematics of the putative core complex differ from oceanic core complexes that have been described in the literature (cf. Baines et al., 2003; Schroeder and John, 2004; Tucholke et al., 2008) in that the driving transtensional deformation is affecting the edge of an aged oceanic plate along an intra-oceanic rift, as opposed to transform plate edges developed proximal to more or less steady-state abyssal spreading centers. In this cross section a detachment fault similar to that imaged at the mid-Atlantic Ridge–Atlantis fracture zone intersection (Canales et al., 2004) is shown disrupting the Kings River ophiolite crustal section and rooting into a neovolcanic rift along which new oceanic lithosphere is generated. The Kings River ophiolite Moho ductile shear zone is shown forming along the asthenospheric corner flow zone off the shoulder of the neo-rift zone (after Baines et al., 2008). Entrainment of the Kings River ophiolite into the rift system requires the nucleation of a transform segment between this ophiolite and its native abyssal plate, as shown in the Figure 16B inset.

Figure 16C shows the plate geometry in the Early Permian (285–260 Ma), with the growth of an oceanic microplate within the dilational transform system. The microplate is named the *Foothills ophiolite belt* microplate for its current expression as the principal ophiolitic exposures of the Sierra Foothills, including the Feather River, Bear Mountains, Tuolumne and Kings-Kaweah sub-belts and the co-extensive Calaveras hemipelagic belts. The Foothills ophiolite belt microplate was composed primarily of "abnormal" oceanic crust with an abundance of surfaced serpentinized upper mantle rocks, mafic metamorphic

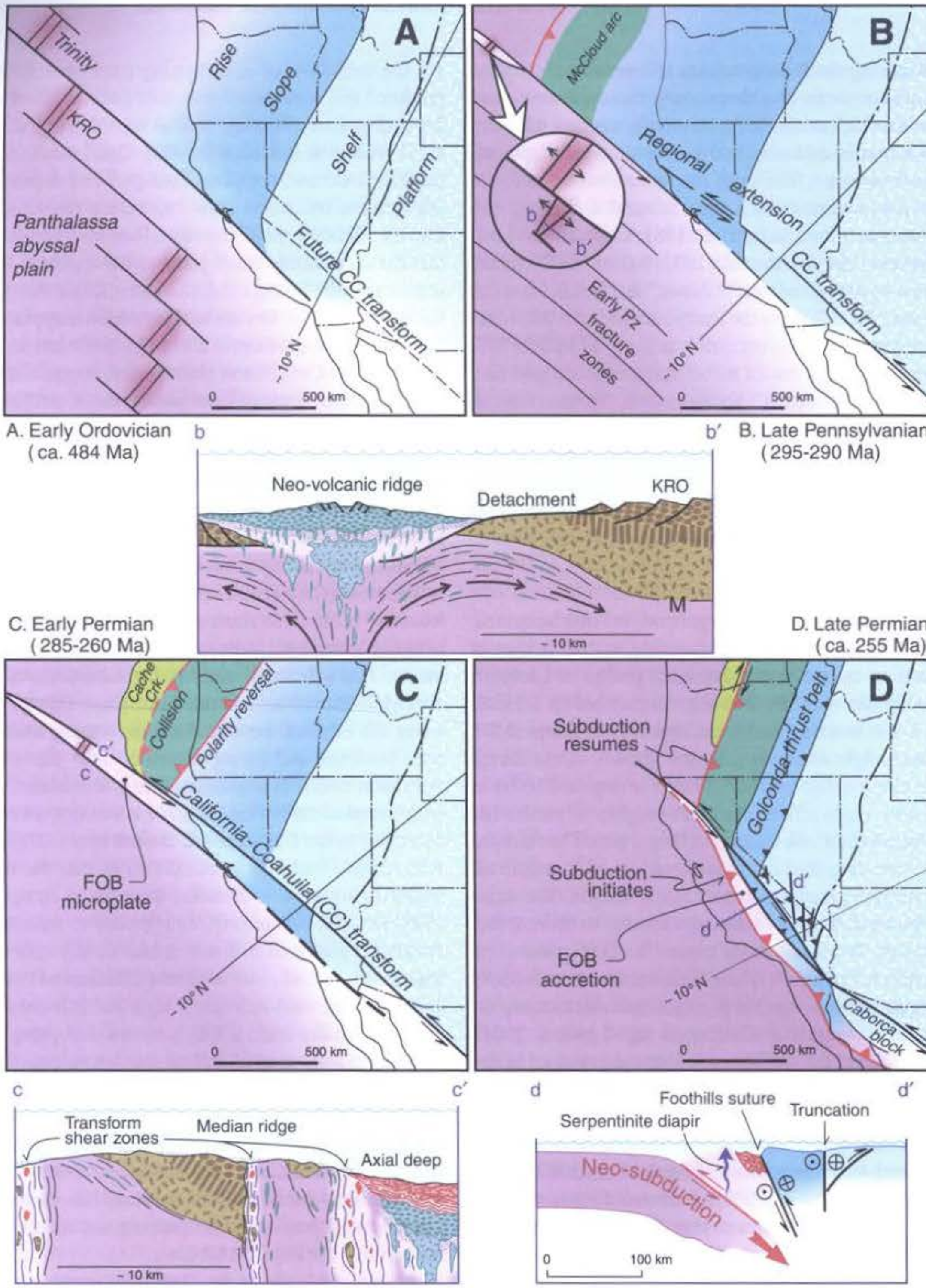

Figure 16. Generalized plate tectonic model for the generation of the Kings River ophiolite along a fast-spreading ridge in the Early Ordovician Panthalassa ocean basin, followed by the generation of the Kaweah serpentinite mélange in a Permo-Carboniferous leaky transform–slow-spreading-ridge system like that of the Cayman Trough, and the emplacement of the Kings-Kaweah ophiolite belt along the Foothills suture during subduction initiation. Insets show diagrammatic cross-sectional relationships at key time intervals. The Foothills ophiolite belt (FOB) consists of the Feather River, Bear Mountains, and Tuolumne sub-belts, in addition to the Kings-Kaweah ophiolite belt and the overlying and co-extensive Calaveras chert-argillite belts. Color-coding for details of the Kings-Kaweah ophiolite belt is the same as in Figures 2 and 3, and for other regional features (Fig. 15). Paleolatitude and orientation of the southwest North American craton are after Cocks and Torsvik (2002) and Nance and Linneman (2008). See text for details. KRO—Kings River ophiolite; Pz—Paleozoic.

TABLE 2. OUTLINE OF PETROGENETIC AND TECTONIC EVENTS RECOGNIZED IN THE KINGS-KAWEAH OPHIOLITE BELT (KKOB)

Geologic time* (Ma)	Tectonic regime
125–100	Intrusion of gabbroic to tonalitic plutons of western zone Sierra Nevada batholith and resulting contact metamorphism.
152–125	Second slaty cleavage formed in cover strata turbidites.
157–148	Intrusion of tonalitic intrusive sheets and basalt-trondhjemite solitary and sheeted dike sets with sinistral shear, and local dynamothermal contact metamorphism.
160–152	Nonconformable deposition of siliciclastic turbidites, serpentinite diapiric dike emplacement, and formation of first cleavage in turbidites.
170–157	Intrusion of gabbroic to tonalitic sheets with longitudinal dextral shear and local dynamothermal contact metamorphism, and local basalt to andesite solitary dike emplacement.
190–175	Early cover strata erosion, possible surfacing of serpentinite diapirs.
205–195	Intrusion of dioritic and trondhjemitic solitary dikes.
225–190	Submarine eruption of boninitic to arc tholeiitic pillowed and volcaniclastic flows, local submarine dacite dome-tuff eruption, deposition of tuffaceous and siliceous argillite, and sandstones-conglomerates derived from chert-rich source.
265–225	Deposition of Calaveras chert-argillite, near pervasive soft sediment deformation and inclusion of Permian shallow-water-limestone blocks.
ca. 255	Emplacement of KKOB to hanging wall of neo-subduction zone, and underlying high-pressure metamorphism with subsequent emplacement of derivative metamorphic blocks into KSM[†] by serpentinite diapirism.
295–255	Oceanic transform displacement of KKOB to SW Cordilleran transform margin.
295–265	Pelagic sedimentation of radiolarian oozes.
ca. 295	Diffuse oceanic spreading, transform generation of ophiolitic ductile shear zones, core complex deformation, and transform capture of KRO[§], and initiation of submarine serpentinite diapirism and ocean floor mélange formation.
484–295	Residence of KRO in Panthalassa ocean basin with sparse pelagic sedimentation of metalliferous radiolarian ooze.
ca. 484	Seafloor spreading generation of KRO at fast spreading center in Panthalassa ocean basin.

*Time intervals not shown lack resolvable geologic record. Italics denote approximate upper and lower bounds on time constraints.

[†]KSM—Kaweah serpentinite mélange.

[§]KRO—Kings River ophiolite.

tectonites deformed along transform shear zones and core complex segments, dispersed basaltic-hypabyssal carapaces, mafic and ultramafic rubble piles, and variably deformed pelagic oozes. The c–c′ cross section shows a diagrammatic profile across the transform zone with tectonic slabs of the Kings River ophiolite forming a median ridge that faced into an axial deep along which pelagic and hemipelagic oozes of the Calaveras complex accumulated. During this time interval the Kings-Kaweah ophiolite belt was undergoing progressive deformation into ophiolitic mélange by transform shearing and large-magnitude displacements, and progressive serpentinite diapirism. The Calaveras complex is also being progressively deformed from soft sediment to lithification states by transform shearing as well as by slumping driven by vertical tectonism and conceivably transform seismicity.

Viewing Figure 16C in a regional context, displacements related to the growth of the Foothills ophiolite belt microplate are shown circuiting into the California-Coahuila transform and displacing the Caborca block. Such transform motion conceivably continued farther into the Rheic suture zone that transected the interior of Mexico, and which accommodated the impingement of Gondwana with the southern margin of Laurentia (Nance and Linnemann, 2008). Ribbons of slope-rise facies strata of the Cordilleran passive margin and superimposed southernmost McCloud arc rocks were entrained in the transform zone and accreted along the continental truncation zone inboard of the encroaching abyssal lithosphere. The autochthonous slope-rise facies system lying inboard of the truncation zone, which also constituted part of a marginal basin behind the McCloud arc, underwent an unknown amount of shortening along the Golconda thrust belt during the later Permian phases of transform activity. This in part may account for the disproportionate along-strike dimensions of the strike-slip ribbons as compared with the current across-strike width of the slope-rise facies belt, compounded by additional dispersal of the ribbons along Mesozoic dextral faults (Fig. 15). Golconda thrust belt convergence is interpreted to have been driven by a reversal in the McCloud arc, which, based on the disruption of eastern Klamath arc activity and depositional overlap by the shallow-water reefal McCloud limestone, occurred in Early to Middle Permian time (Irwin, 1977; Stevens, 2009). A possible mechanism shown for driving the reversal was the collision of a major ocean island chain that formed in Panthalassa low latitudes, the remnants of which are dispersed along the northern Cordillera as the Cache Creek terrane, and from which shallow-water limestone blocks and clasts were derived and regionally reworked into early Mesozoic hemipelagic and volcaniclastic deposits (Davis et al., 1978; Ross and Ross, 1983).

A number of Permo-Carboniferous events along the inboard wall of the transform system reflect extensional and/or transtensional deformation interpreted to be kinematically linked to the California-Coahuila transform regime. These events include extensional exhumation of the southern end of the McCloud arc subduction complex (Barrow and Metcalf, 2006), the termination of McCloud arc–related volcanism in the northernmost Sierra Nevada with subsidence that promoted overlapping hemipelagic sedimentation (D'Allura et al., 1977), the development of a borderland facies belt oriented along the truncated edge of the passive margin shelf (Stone and Stevens, 1988), and widespread extensional tectonism in the passive margin east of the truncation zone (Smith and Miller, 1990). This extensional-transtensional regime was abruptly overprinted by Golconda thrust belt deformation, and then later by Permo-Triassic sinistral transpression, interpreted below to mark initiation of subduction along the transform zone.

The simplistic plate geometry adopted in Figure 16 offers an explanation for an enigma regarding the Calaveras complex belts of the Sierra Foothills. Permo-Carboniferous reefal limestones that formed on the Cache Creek ocean island chain are biogeographically distinct from the Permian McCloud arc capping reefal limestones, and both are distinct from coeval shelf limestones of the Cordilleran passive margin (cf. Ross and Ross, 1983). Blocks and slabs of the Cache Creek–type limestones are common in Permo-Triassic chert-argillite belts accreted to the margin of the McCloud arc, stretching from the Sierra Foothills to the southern Yukon (Davis et al., 1978). However, in the Calaveras complex belts of the Sierra Foothills blocks and clasts of both Cache Creek and McCloud-type limestones are present. This is the only region where fragments of both limestone types are present in the same rock assemblages, which is in line with the Figure 16C reconstruction whereby blocks of each were readily sourced in submarine landslides from the inboard wall of the transform system and delivered into the Calaveras depositional trough(s).

The Foothills ophiolite belt microplate appears to have been juxtaposed with the truncated SW Cordilleran margin in the latest Permian (Fig. 16D). As final juxtaposition progressed, Panthalassa lithosphere began converging with the truncated Cordilleran margin, and a new subduction zone nucleated. Permo-Carboniferous "abnormal" oceanic lithosphere of the Foothills ophiolite belt microplate was susceptible to accretion to the hanging wall of the new subduction zone owing to its buoyancy that resulted from widespread serpentinization. According to the Figure 16 model the majority of the impinging oceanic lithosphere was old (≥200 Ma) and consisted of "normal" ridge crest–generated lithosphere of Kings River ophiolite affinity. Juxtaposition of aged cold oceanic lithosphere with the buoyant "abnormal" oceanic lithosphere ribbon presented ideal circumstances for subduction initiation (cf. Stern, 2004). The ca. 255 Ma Sm/Nd age for the Kaweah serpentinite mélange garnet amphibolite block is taken as the approximate time of subduction initiation. High-pressure metamorphism is envisaged to have occurred along the neo-subduction megathrust with the high temperature (~800 °C) of metamorphism recorded in the garnet amphibolite block possibly reflecting the subduction of a warm mid-Permian segment of the Foothills ophiolite belt microplate outer edge. Fragments of the high-P metamorphic selvage that formed along the neo-subduction megathrust were entrained in serpentinite diapirs and transported up to crustal levels in the proto-forearc wedge, possibly erupting in mud volcanoes. The d–d′ cross section diagrammatically shows the en masse accretion of the Kings-Kaweah ophiolite belt to the hanging wall of a neo-subduction zone and its juxtaposition with the passive margin, para-autochthonous strike-slip ribbons along the Foothills suture. The Kings River ophiolite transform median ridge is shown hypothetically persisting as a bathymetric high forming a proto-forearc ridge, facing inward to the Calaveras axial deep sediment wedge that was likewise accreted en masse along the Foothills suture. Serpentinite diapirs are shown, sourced from the subduction megathrust zone where they entrained fragments of the high-P metamorphic selvage that formed along the neo-megathrust.

The upper plate of the neo-subduction zone responded to oblique convergence by sinistral transpression as recorded by Permo-Triassic east-directed thrusting of the Sierra Nevada–Death Valley thrust system (Stevens and Stone, 2005) and similar-age thrust structures of the Mojave Desert region (Miller and Sutter, 1982; Walker, 1988), now highly dispersed in the northwest Mojave region by large-magnitude Late Cretaceous extension (Chapman et al., 2011). Partly coincident with Permo-Triassic transpression, relatively low-volume arc plutonism initiated along the trace of the truncation zone (Stern et al., 1981; Chen and Moore, 1982; Barth et al., 1997; Saleeby and Dunne, 2011). Such arc plutonism is recorded for end of Permian–Early Triassic time, whereas Late Triassic and earliest Jurassic arc activity is recorded by widespread voluminous silicic ignimbrites, some of which were ponded in large submarine calderas that were nested in a regional arc graben system (Fiske and Tobisch, 1978; Busby-Spera, 1984, 1988; Schweickert and Lahren, 1989).

The temporal and spatial relations of supra-subduction zone magmatism, as presented in the Figure 16 model, seem at odds with the generalized subduction initiation model of Stern (2004).

In the Figure 16 model a relatively low-volume calc-alkaline to locally shoshonitic arc was established along the eastern Sierra region before Late Triassic–earliest Jurassic boninitic-arc tholeiitic volcanism occurred along the Foothills belt. In the Stern (2004) model, which is based on the Izu-Bonin–Mariana arc system, such proto-forearc volcanism develops in response to profuse slab rollback as negatively buoyant lithosphere founders during subduction initiation (cf. Hall et al., 2003) and the upper plate of the new subduction zone undergoes regional extension. This form of subduction initiation is termed *spontaneous* and in theory arises primarily from buoyancy contrasts across transform faults in abyssal lithosphere. Stern (2004) also presents an end member alternative to spontaneous initiation that is termed *induced,* which results from far-field plate forces rendering the necessary component of convergence for the initiation and sustenance of subduction. The Macquarie Ridge–Puysgur Trench–Fiordland plate juncture system is cited as an example of ongoing induced subduction initiation, and emphasis is placed on the importance of upper plate compressive deformation, opposed to extension, as the sign of induced initiation.

The Permo-Triassic subduction initiation event of the SW Cordillera resembles the induced subduction initiation regime that is occurring today along the Macquarie Ridge–Puysgur Trench–Fiordland system. There the transform system that is evolving into a new subduction zone extends from abyssal lithosphere into passive margin–type lithosphere of the Campbell-Challenger plateau, where transpressive deformation is in large part producing the New Zealand landmass. As of yet, however, this system has not produced any known boninitic-arc tholeiitic volcanic associations in an extensional proto-forearc setting. Returning to the Permo-Triassic event of the SW Cordillera, subduction initiation appears to have been in response to far-field oblique compressive forces, as evidenced by regional transpressive deformation of the upper plate. Perhaps as subduction progressed, the convergence trajectory changed to a stronger normal component, whereupon negative buoyancy forces in the aged downgoing slab began to dominate the dynamics of the system, and a phase of profuse slab rollback ensued. The result of this rollback was the inflow of asthenosphere into the forearc mantle wedge, promoting boninitic magma genesis at shallow levels and arc tholeiitic magma genesis at deeper levels. The already heated axial region of the arc responded to regional extension by changing the mode of arc magmatism to a series of dispersed large-volume submarine calderas, as opposed to a chain of calc-alkaline to shoshonitic plutons, which were conceivably overlain by andesitic strata-cones. The common occurrence of silicic ash components within the siliceous argillites that the Kaweah serpentinite mélange cover-strata mafic volcanics were erupted into is consistent with distal large-volume silicic eruptions occurring intermittently during the forearc region mafic volcanism. The relationships outlined above suggest that the Permo-Triassic subduction initiation regime along the SW Cordillera has elements of both induced and spontaneous initiation, as defined by Stern (2004), and thus appears to be a hybridization of the process as defined.

Initiation of Franciscan Subduction

The regional geology of California is distinguished by the late Mesozoic–early Cenozoic Franciscan subduction complex, which produced the California Coast Range basement regime. Regional tectonic relations, as well as the history of the Coast Range ophiolite and the initial high-pressure metamorphism recorded in the Franciscan complex, call for a subduction initiation event in the Middle Jurassic (Stern and Bloomer, 1992; Anczkiewicz et al., 2004; Shervais et al., 2005). The timing of this event corresponds well with the onset of a high–magmatic flux event of late Middle to Late Jurassic age that is recorded within the early-stage Sierra Nevada batholith and its metavolcanic pendants (Stern et al., 1981; Chen and Moore, 1982; Snoke et al., 1982; Ducea, 2001). Such a subduction initiation event calls for a major change in the plate tectonic regime of the SW Cordillera in the time interval between the production of the Triassic arc belt and the late Middle to Late Jurassic belt. This time interval corresponds to a distinct lull in early Mesozoic arc magmatism of the SW Cordillera (Stern et al., 1981; Chen and Moore, 1982; Barth et al., 1997; Saleeby and Dunne, 2011), dextral-sense transpression in the region (Saleeby et al., 1992; Saleeby and Dunne, 2011), and to unconformities in the forearc region as recorded in the Kaweah serpentinite mélange cover strata and the Jasper Point–Penon Blanco sequence. In absolute age this lull occurred between 200 and 175 Ma. The explanation favored here for these ill-defined events is that they record the dextral-sense oblique collision of the Insular Superterrane, a major composite arc terrane of peri-Gondwana affinity that impinged northward and accreted into the northern Cordillera region in the Middle to Late Jurassic, and which was progressively compressed and accreted into the northern Cordillera in the Early Cretaceous (Davis et al., 1978; McClelland et al., 1992; Getty et al., 1993). As the Insular Superterrane slid northward along the SW Cordilleran margin toward its northern Cordillera accretion site it left a leaky transform–spreading ridge system in its wake along which the Coast Range and other southern Cordillera Middle Jurassic ophiolites formed (Saleeby et al., 1992). Nucleation of Franciscan subduction followed in the wake of Insular Superterrane northward migration along the leaky transform system.

CONCLUSIONS

The Kings-Kaweah ophiolite belt underwent two distinct phases of abyssal MORB magma genesis. The first phase was at 484 ± 18 Ma (Early Ordovician), which generated a complete abyssal crust and depleted upper mantle sequence probably along a fast-spreading ridge in the Panthalassa ocean basin. The second phase is constrained by 295 ± 15 U/Pb zircon ages on rare felsic intrusives, and by a 299 ± 32 Ma Sm-Nd isochron age on a wide range of mafic to rare felsic rocks. This Permo-Carboniferous phase of abyssal magmatism occurred along a large offset transform fracture zone. During this phase of magmatism and tectonism a part of the Early Ordovician abyssal lithosphere that was proximal to the fracture zone was disrupted into an oceanic metamorphic core complex and was cut into a series of elongate slabs by transform-related ductile shear zones. Deformation progressed within the transform zone to the state of producing mélange. Mélange mixing was facilitated by copious serpentinization and related diapiric mobilization, some of which surfaced onto the seafloor. Pillowed abyssal tholeiite eruptions, ophicalcites, and radiolarian oozes mingled with serpentinite debris along fault scarps and debris aprons. As deformation and pelagic sedimentation progressed, biogenic oozes were mixed and ultimately replaced by siliceous argillite derived from terrigenous material and distally derived volcanic ashes. The hemipelagic deposits were mobilized by submarine mass wasting and accumulated along axial troughs within the transform system.

Regional tectonic relations of the SW Cordillera indicating a late Paleozoic transform truncation of the Neoproterozoic-Paleozoic passive margin may be directly linked to the transform history of the Kings-Kaweah ophiolite belt. Direct kinematic linkage between the oceanic transform system and the passive margin truncation zone led to the juxtaposition of the ophiolite belt with a veneer of para-autochthonous strike-slip ribbons that together were accreted along the truncation locus. Emplacement of the ophiolite belt occurred by its en masse accretion to the hanging wall of a new subduction zone along the preexisting transform juncture starting at ca. 255 Ma. Related arc magmatism began in the eastern Sierra by ca. 248 Ma. Fragments of high-pressure oceanic metamorphic rocks that formed along the new subduction zone were locally entrained by serpentinite diapirs that intruded up into the overlying ophiolite belt, which introduced the exotic blocks into the mélange assemblage. In Late Triassic to earliest Jurassic time, fluid-assisted melting of depleted peridotites accreted to the hanging wall of the subduction zone rendered boninitic to arc-tholeiitic mafic magmas that were erupted within and above the ophiolite belts' hemipelagic cover strata. Later in the Jurassic, siliciclastic turbidites spread across the Kings-Kaweah ophiolite belt as the forearc region matured. Detritus for the turbidites was supplied mainly by exhumed early Paleozoic passive margin–related strata and by early Mesozoic arc rocks of the eastern Sierra Nevada region. By late Middle to Late Jurassic time (170–148 Ma) small calc-alkaline plutons and dike swarms were emplaced into the Kings-Kaweah ophiolite belt within a transtensional deformation field, and by ca. 125 Ma copious gabbroic to tonalitic plutons of the Sierra Nevada batholith intruded and pervasively contact metamorphosed the ophiolite belt.

Regional relations of the SW Cordilleran truncation and subduction initiation event, as well as the geologic history of the Kings-Kaweah ophiolite belt, suggest that subduction initiation was driven primarily by far-field plate tectonic forces and involved, first, highly oblique subduction whose tangential components were directly inherited from the prior transform phase of motion. Once subduction had been ongoing, and as the subduction trajectory evolved to a stronger normal component, aged cold, early Paleozoic abyssal lithosphere that was entering the trench began to founder, leading to a distinct slab rollback phase. This resulted in regional extension across the arc and forearc environment, leading to a reorganization of arc magmatism to scattered large-volume submarine calderas and to dispersed boninitic-arc tholeiitic volcanism in the forearc region. In this context the early Mesozoic SW Cordilleran subduction initiation event resembles a hybridization between far-field-controlled "induced subduction initiation" and a more local buoyancy force–controlled "spontaneous subduction initiation," as defined by Stern (2004).

ACKNOWLEDGMENTS

The author is indebted to C.A. Hopson for decades of inspiration in pursuit of addressing the ophiolite problem. Conversations with P.D. Asimow, J.M. Eiler, M.C. Gurnis, J.W. Hawkins, C. Şengor, J.W. Shervais, and R.J. Stern were of great value for the data interpretation presented. Direct assistance, acquisition of spikes and standards, and helpful tips in radiogenic isotopic geochemistry from J.G. Wasserburg, D.A. Papanastassiou, H. Ngo, and J.C. Chen are kindly acknowledged. Additional assistance in various aspects of the geochemical analytical work presented here by T. Bunch, A. Chapman, and M. Ducea are kindly acknowledged. Assistance in database compilation of Great Valley basement cores and technical drafting by Z.A. Saleeby is acknowledged. Assistance in mineral separation procedures by M. Chaudhry and I. Saleeby was essential for this study. The author thanks Harvey and Bobby Ruth for their hospitality while doing fieldwork, and their assistance in fieldwork logistics. Critical reviews by E.A. Miranda, K.D. Putirka, and J. Wakabayashi were a great asset. A grant from the Gordon and Betty Moore Foundation helped bring this study to completion. (Caltech Tectonics Observatory Contribution no. 119.)

REFERENCES CITED

Ague, J.J., and Brimhall, G.H., 1988, Magmatic arc asymmetry and distribution of anomalous plutonic belts in the batholiths of California: Effects of assimilation, crustal thickness, and depth of crystallization: Geological Society of America Bulletin, v. 100, p. 912–927, doi:10.1130/0016-7606(1988)100<0912:MAAADO>2.3.CO;2.

Anczkiewicz, R., Platt, J.P., Thirlwall, M.F., and Wakabayashi, J., 2004, Franciscan subduction off to a slow start: Evidence from high precision Lu-Hf garnet ages on high grade blocks: Earth and Planetary Science Letters, v. 225, p. 147–161, doi:10.1016/j.epsl.2004.06.003.

Anderson, T.H., and Silver, L.T., 1979, The role of the Mojave-Sonora megashear in the tectonic evolution of northern Sonora, *in* Anderson, T.H., and Roldan-Quintana, J., eds., Geology of Northern Sonora: Hermosillo, Sonora, Sonora Instituto de Geologia, Universidad Autonoma de Mexico, p. 59–68.

Aumento, F., Loncarevic, B.D., and Ross, D.I., 1971, Hudson geotraverse: Geology of the Mid-Atlantic Ridge at 45°N: Royal Society of London Philosophical Transactions, ser. A, v. 268, p. 623–650.

Babcock, J.M., Harding, A.J., Kent, G.M., and Orcutt, J.A., 1998, An examination of along-axis variation of magma chamber width and crustal structure on the East Pacific Rise between 13°30′N and 12°20′N: Journal of Geophysical Research, v. 103, p. 30,451–30,467, doi:10.1029/98JB01979.

Baines, A.G., Cheadle, M.J., Dick, H.J.B., Scheirer, A.H., John, B.E., Kusznir, N.J., and Matsumoto, T., 2003, Mechanism for generating the anomalous uplift of oceanic core complexes: Atlantis Bank, Southwest Indian Ridge: Geology, v. 31, p. 1105–1108, doi:10.1130/G19829.1.

Baines, A.G., Cheadle, M.J., John, B.E., and Schwartz, J.J., 2008, The rate of oceanic detachment faulting at Atlantis Bank, SW Indian Ridge: Earth and Planetary Science Letters, v. 273, p. 105–114.

Barbeau, D.L., Ducea, M.N., Gehrels, G.E., Kidder, S., Whitmore, P.H., and Saleeby, J.B., 2005, The origin of Salinia, California: New evidence from U-Pb detrital zircon geochronology of basement and cover rocks: Geological Society of America Bulletin, v. 117, p. 466–481, doi:10.1130/B25496.1.

Barrow, W.M., and Metcalf, R.V., 2006, A reevaluation of the paleotectonic significance of the Paleozoic Central Metamorphic terrane, eastern Klamath Mountains, California: New constraints from trace element geochemistry and $^{40}Ar/^{39}Ar$ thermochronology, *in* Snoke, A.W., and Barnes, C.G., eds., Geological Studies in the Klamath Mountains Province, California and Oregon: A Volume in Honor of William P. Irwin: Geological Society of America Special Paper 410, p. 393–410.

Barth, A.P., Tosdal, R.M., Wooden, J.L., and Howard, K.A., 1997, Triassic plutonism in southern California: Southward younging of arc initiation along a truncated continental margin: Tectonics, v. 16, p. 290–304, doi:10.1029/96TC03596.

Bebout, G.E., and Barton, M.D., 2002, Tectonic and metasomatic mixing in a high-T, subduction zone melange—Insights into the geochemical evolution of the slab-mantle interface: Chemical Geology, v. 187, p. 79–106, doi:10.1016/S0009-2541(02)00019-0.

Behrman, P.S., and Parkison, G.A., 1978, Pre-Callovian rocks, west of the Melones fault, central Sierra Nevada Foothills, *in* Howell, D.G., and McDougall, K.A., eds., Mesozoic Paleogeography of the Western United States: Society of Economic Paleontologists and Mineralogists, Pacific Section, 2nd Pacific Coast Paleogeography Symposium, p. 337–348.

Bloomer, S.H., Natland, J.H., and Fisher, R.L., 1989, Mineral relationships in gabbroic rocks from fracture zones of Indian Ocean ridges: Evidence for extensive fractionation, parental diversity and boundary-layer recrystallization, *in* Saunders, A.D., and Norry, M.J., eds., Magmatism in the Ocean Basins: Geological Society [London] Special Publication 42, p. 107–124.

Bloomer, S.H., Taylor, B., and MacLeod, C.J., 1995, Early arc volcanism and the ophiolite problem: A perspective from drilling in the western Pacific, *in* Taylor, B., and Natland, J., eds., Active Margins and Marginal Basins of the Western Pacific: Washington, D.C., American Geophysical Union, p. 67–96.

Bonatti, E., and Honnorez, J., 1976, Sections of the Earth's crust in the equatorial Atlantic: Journal of Geophysical Research, v. 81, p. 4104–4116, doi:10.1029/JB081i023p04104.

Bonatti, E., Honnorez, J., and Ferrara, G., 1971, Peridotite-gabbro-basalt complex from the equatorial Mid-Atlantic Ridge: Royal Society of London Philosophical Transactions, ser. A, v. 268, p. 385–402.

Bonatti, E., Honnorez, J., and Gartner, S., Jr., 1973, Sedimentary serpentinites from the Mid-Atlantic Ridge: Journal of Sedimentary Petrology, v. 43, p. 728–735.

Bonatti, E., Emiliani, C., Ferrara, G., Honnorez, J., and Rydell, H., 1974, Ultramafic-carbonate breccias from the equatorial Mid-Atlantic Ridge: Marine Geology, v. 16, p. 83–102, doi:10.1016/0025-3227(74)90057-7.

Boudier, F., and Coleman, R.G., 1981, Cross section through the peridotite in the Samail ophiolite, southeastern Oman Mountains: Journal of Geophysical Research, v. 86, p. 2573–2592, doi:10.1029/JB086iB04p02573.

British Antarctic Survey, 1985, Tectonic Map of the Scotia Arc: Cambridge, UK, British Antarctic Survey, scale 1:3,000,000, 1 sheet.

Busby-Spera, C.J., 1984, Large-volume rhyolite ash flow eruptions and submarine caldera collapse in lower Mesozoic Sierra Nevada, California: Journal of Geophysical Research, v. 89, p. 8417–8427, doi:10.1029/JB089iB10p08417.

Busby-Spera, C.J., 1988, Speculative tectonic model for the lower Mesozoic arc of the southwest Cordilleran United States: Geology, v. 16, p. 1121–1125, doi:10.1130/0091-7613(1988)016<1121:STMFTE>2.3.CO;2.

Canales, J.P., Tucholke, B.E., and Collins, J.A., 2004, Seismic reflection imaging of an oceanic detachment fault: Atlantis megmullion (Mid-Atlantic Ridge, 30°10′): Earth and Planetary Science Letters, v. 222, p. 543–560, doi:10.1016/j.epsl.2004.02.023.

Cannat, M., 1996, How thick is the magmatic crust at slow spreading oceanic ridges?: Journal of Geophysical Research, v. 101, p. 2847–2857, doi:10.1029/95JB03116.

Carter, N.L., and Ave Lallemant, H.G., 1970, High temperature flow of dunite and peridotite: Geological Society of America Bulletin, v. 81, p. 2181–2202, doi:10.1130/0016-7606(1970)81[2181:HTFODA]2.0.CO;2.

Casey, J.F., and Dewey, J.F., 1984, Initiation of subduction zones along transform and accreting plate boundaries, triple junction evolution, and forearc spreading centers—Implications for ophiolite geology and obduction, *in* Gass, I.G., Lippard, S.J., and Shelton, A.W., eds., Ophiolites and Oceanic Lithosphere: Geological Society [London] Special Publication 13, p. 269–290.

CAYTROUGH, 1978, Geological and geophysical investigation of the Mid-Cayman Rise spreading center: Initial results and observations, *in* Talwani, M., Harrison, C.G., and Hayes, D.E., eds., Deep Sea Drilling Results in the Atlantic Ocean: Oceanic Crust, Maurice Ewing Series, v. 2: Washington, D.C., American Geophysical Union, p. 66–93.

Chapman, A.D., Saleeby, J., Wood, D.J., Piasecki, A., and Farley, K., 2011, Regional displacement analysis and palinspastic restoration of dispersed crustal fragments in the southern Sierra Nevada, California: Geosphere (in press).

Chen, J.H., and Moore, J.G., 1982, Uranium-lead isotopic ages from the Sierra Nevada batholith: Journal of Geophysical Research, v. 87, p. 4761–4784, doi:10.1029/JB087iB06p04761.

Chen, J.H., and Tilton, G.R., 1991, Application of lead and strontium isotopic relationships to the petrogenesis of granitic rocks, central Sierra Nevada batholith, California: Geological Society of America Bulletin, v. 103, p. 439–447, doi:10.1130/0016-7606(1991)103<0439:AOLASI>2.3.CO;2.

Cipriani, A., Bonatti, E., Seyler, M., Brueckner, H.K., Brunelli, D., Dallai, L., Hemming, S.R., Ligi, M., Ottolini, L., and Turrin, B.D., 2009, A 19 to 17 Ma amagmatic extension event at the Mid-Atlantic Ridge: Ultramafic mylonites from the Vema Lithospheric Section: Geochemistry Geophysics Geosystems, v. 10, doi:10.1029/2009GC002534.

Clemens-Knott, D., and Saleeby, J.B., 1999, Impinging ring dike complexes in the Sierra Nevada batholith, California: Roots of the Early Cretaceous volcanic arc: Geological Society of America Bulletin, v. 111, p. 484–496, doi:10.1130/0016-7606(1999)111<0484:IRDCIT>2.3.CO;2.

Clemens-Knott, D., Saleeby, J.B., Taylor, H.P., Jr., and Chappell, B., 2011, Geochemistry of the western Sierra Nevada batholith: Multiple pathways of mafic magma differentiation in the Early Cretaceous arc: Contributions to Mineralogy and Petrology (in press).

Cocks, L.R.M., and Torsvik, T.H., 2002, Earth geology from 500 to 400 million years ago: A faunal and paleomagnetic review: Journal of the Geological Society [London], v. 159, p. 631–644, doi:10.1144/0016-764901-118.

Coleman, R.G., 1977, Ophiolites, Ancient Oceanic Lithosphere?: New York, Springer-Verlag, 240 p.

Coleman, R.G., and Peterman, Z.E., 1975, Oceanic plagiogranite: Journal of Geophysical Research, v. 80, p. 1099–1108, doi:10.1029/JB080i008p01099.

Constantin, M., Hekinian, R., Bideau, D., and Hebert, R., 1996, Construction of the oceanic lithosphere by magmatic intrusions: Petrologic evidence from plutonic rocks formed along the fast-spreading East Pacific Rise: Geology, v. 24, p. 731–734, doi:10.1130/0091-7613(1996)024<0731:COTOLB>2.3.CO;2.

Cox, D.P., and Pratt, W.P., 1973, Submarine chert-argillite slide breccia of Paleozoic age in southern Klamath Mountains, California: Geological Society of America Bulletin, v. 84, p. 1423–1438, doi:10.1130/0016-7606(1973)84<1423:SCSOPA>2.0.CO;2.

D'Allura, J.A., Moores, E.M., and Robinson, L., 1977, Paleozoic rocks of the northern Sierra Nevada: Their structural and paleogeographic implications, *in* Stewart, J.H., and Stevens, C.H., eds., Paleozoic Paleogeography of the Western United States: Society of Economic Paleontologists and Mineralogists, Pacific Section, p. 395–408.

Davis, G.A., Monger, J.W.H., and Burchfiel, B.C., 1978, Mesozoic construction of the Cordilleran "collage," central British Columbia to central California, *in* Howell, D.G., and McDougall, K.A., eds., Mesozoic Paleogeography of the Western United States: Society of Economic Paleontologists and Mineralogists, Pacific Section, Pacific Coast Paleogeography Symposium, 2nd, p. 1–32.

DeBari, S.M., Taylor, B., Spencer, K., and Fujioka, K., 1999, A trapped Philippine Sea plate origin for MORB from the inner slope of the Izu-Bonin trench: Earth and Planetary Science Letters, v. 174, p. 183–197, doi:10.1016/S0012-821X(99)00252-6.

DeLong, S.E., Dewey, J.F., and Fox, P.J., 1977, Displacement history of oceanic fracture zones: Geology, v. 5, p. 199–202, doi:10.1130/0091-7613(1977)5<199:DHOOFZ>2.0.CO;2.

DePaolo, D.J., 1981, A neodymium and strontium isotopic study of the Mesozoic calc-alkaline granitic batholiths of the Sierra Nevada and Peninsular Ranges, California: Journal of Geophysical Research, v. 86, p. 10,470–10,488, doi:10.1029/JB086iB11p10470.

Deplus, C., LeFriant, A., Boudon, G., Komorowski, J., Villemant, B., Harford, C., Segoufin, J., and Cheminee, J., 2001, Submarine evidence for large-scale debris avalanches in the Lesser Antilles arc: Earth and Planetary Science Letters, v. 192, p. 145–157, doi:10.1016/S0012-821X(01)00444-7.

Dickinson, W.R., and Gehrels, G.E., 2003, U-Pb ages of detrital zircons from Permian and Jurassic eolian sandstones of the Colorado Plateau, U.S.A., paleogeographic implications: Sedimentary Geology, v. 163, p. 29–66, doi:10.1016/S0037-0738(03)00158-1.

Dickinson, W.R., and Lawton, T.F., 2001, Carboniferous to Cretaceous assembly and fragmentation of Mexico: Geological Society of America Bulletin, v. 113, p. 1142–1160, doi:10.1130/0016-7606(2001)113<1142:CTCAAF>2.0.CO;2.

Ducea, M., 2001, The California Arc: Thick granitic batholiths, eclogitic residues, lithospheric-scale thrusting, and magmatic flare-ups: GSA Today, v. 11, no. 11, p. 4–10, doi:10.1130/1052-5173(2001)011<0004:TCATGB>2.0.CO;2.

Dunne, G.C., Gulliver, R., and Sylvester, A., 1978, Mesozoic evolution of the Inyo, Argus, and Slate Ranges, eastern California, *in* Howell, D., ed., Mesozoic Paleogeography of the Western United States: Society of Economic Paleontologists and Mineralogists, Pacific Section, p. 189–206.

Engle, C.G., and Fisher, R.L., 1975, Granitic to ultramafic rock complexes of the Indian Ridge system, western Indian Ocean: Geological Society of America Bulletin, v. 86, p. 1553–1578, doi: 10.1130/0016-7606(1975)86<1553:GTURCO>2.0.CO;2.

Ernst, W.G., Saleeby, J.B., and Snow, C.A., 2009, Guadalupe pluton–Mariposa Formation age relationships in the Sierran Foothills: Onset of Mesozoic subduction in northern California: Journal of Geophysical Research, v. 114, B11204, doi:10.1029/2009JB006607.

Fiske, R.S., and Tobisch, O.T., 1978, Paleogeographic significance of volcanic rocks in the Ritter Range pendant, central Sierra Nevada, California, *in* Howell, D.G., and McDougall, K.A., eds., Mesozoic Paleogeography of the Western United States: Society of Economic Paleontologists and Mineralogists, Pacific Section, Pacific Coast Paleogeography Symposium, 2nd, p. 209–222.

Fox, P.J., Schreiber, E., Rowlett, H., and McCamy, K., 1976, The geology of the Oceanographer fracture zone: A model for fracture zones: Journal of Geophysical Research, v. 81, p. 4117–4128, doi:10.1029/JB081i023p04117.

Fryer, P., Lockwood, J.P., Becker, N., Phipps, S., and Todd, C.S., 2000, Significance of serpentine mud volcanism in convergent margins, *in* Dilek, Y., Moores, E.M., Elthon, D., and Nicolas, A., eds., Ophiolites and Oceanic Crust: New Insights from Field Studies and the Ocean Drilling Program: Geological Society of America Special Paper 349, p. 35–51.

Getty, R.G., Selverstone, J., Wernicke, B.P., Jacobsen, S.B., Aliberti, E., and Lux, D.R., 1993, Sm-Nd dating of multiple garnet growth events in an arc-continent collision zone, northwestern U.S. Cordillera: Contributions to Mineralogy and Petrology, v. 115, p. 45–57, doi:10.1007/BF00712977.

Gilbert, H., Jones, C., Owens, T.J., and Zandt, G., 2007, Imaging Sierra Nevada lithosphere sinking: Eos (Transactions, American Geophysical Union), v. 88, p. 225–229, doi:10.1029/2007EO210001.

Glazner, A.F., Lee, J., Bartley, J.M., Coleman, D.S., Kylander-Clark, A., Greene, D.C., and Le, K., 2005, Large dextral offset across Owens Valley, California, from 148 Ma to 1872 A.D., *in* Stevens, C., and Cooper, J., eds., Western Great Basin Geology: Fieldtrip Guidebook and Volume Prepared for Joint Meeting of the Cordilleran Section, GSA, and Pacific Section, AAPG, San Jose, California, p. 1–35.

Grasse, S.W., Gehrels, G.E., Lahren, M.M., Schweickert, R.A., and Barth, A.P., 2001, U-Pb geochronology of detrital zircons form the Snow Lake pendant, central Sierra Nevada—Implications for Late Jurassic–Early Cretaceous dextral-slip faulting: Geology, v. 29, p. 307–310, doi:10.1130/0091-7613(2001)029<0307:UPGODZ>2.0.CO;2.

Greene, D.C., Stevens, C.H., and Wise, J.M., 1997, The Laurel-Convect fault, eastern Sierra Nevada, California: A Permo-Triassic left-lateral fault, not a Cretaceous intrabatholithic break: Geological Society of America Bulletin, v. 109, p. 483–488, doi:10.1130/0016-7606(1997)109<0483:TLCFES>2.3.CO;2.

Gu, S., Zhang, M., Gui, B., and Lu, X., 2007, An attempt to quantitatively reconstruct the paleo-primary productivity by counting the radiolarian fossils in cherts from the latest Permian Dalong Formation in southwestern China: Frontiers of Earth Science in China, v. 1, p. 412–416, doi:10.1007/s11707-007-0050-1.

Hall, C.E., Gurnis, M., Sdrolias, M., Lavier, L.L., and Muellar, D.R., 2003, Catastrophic initiation of subduction following forced convergence across a fracture zone: Earth and Planetary Science Letters, v. 212, p. 15–30, doi:10.1016/S0012-821X(03)00242-5.

Harding, J.P., Gehrels, G.E., Harwood, D.S., and Girty, G.H., 2000, Detrital zircon geochronology of the Shoo Fly complex, northern Sierra terrane, northeastern California, *in* Soreghan, M.J., and Gehrels, G.E., eds., Paleozoic and Triassic Paleogeography and Tectonics of Western Nevada and Northern California: Geological Society of America Special Paper 347, p. 43–55.

Harper, G.D., Saleeby, J.B., and Heizler, M., 1994, Isotopic age of emplacement of the Josephine ophiolite and overlying flysch during the Late Jurassic Nevadan Orogeny, Klamath Mountains, Oregon-California: Journal of Geophysical Research, v. 99, p. 4293–4321, doi:10.1029/93JB02061.

Hilde, T.W.C., Uyeda, S., and Kroenke, L., 1977, Evolution of the western Pacific and its margin: Tectonophysics, v. 38, p. 145–165.

Hoffman, A.W., 2004, Sampling mantle heterogeneity through oceanic basalts: Isotopes and trace elements, *in* Carson, R.W., ed., Treatise on Geochemistry, v. 2, The Mantle and Core: Amsterdam, Elsevier Pergamon, p. 61–101.

Holland, T.J.B., and Powell, R., 1998, An internally consistent thermodynamic data set for phases of petrological interest: Journal of Metamorphic Geology, v. 16, p. 309–343, doi:10.1111/j.1525-1314.1998.00140.x.

Honnorez, J., Mevel, C., and Montigny, R., 1984, Geotectonic significance of gneissic amphibolites from the Vema fracture zone, equatorial Mid-Atlantic Ridge: Journal of Geophysical Research, v. 89, p. 11,379–11,400, doi:10.1029/JB089iB13p11379.

Hopson, C.A., Mattinson, J.M., and Pessagno, E.A., Jr., 1981, Coast Range ophiolite, western California, *in* Ernst, W.G., ed., The Geotectonic Development of California, Ruby Volume I: Englewood Cliffs, New Jersey, Prentice Hall, p. 418–510.

Hopson, C.A., Mattinson, J.M., Pessagno, E.A., Jr., and Luyendyk, B.P., 2008, California Coast Range ophiolite: Composite Middle and Late Jurassic oceanic lithosphere, *in* Wright, J.E., and Shervais, J.W., eds., Ophiolites, Arcs, and Batholiths: A Tribute to Cliff Hopson: Geological Society of America Special Paper 438, p. 1–102, doi:10.1130/2008.2438(01).

Hsü, K.J., 1968, Principles of mélanges and their bearing on the Franciscan-Knoxville paradox: Geological Society of America Bulletin, v. 79, p. 1063–1074, doi:10.1130/0016-7606(1968)79[1063:POMATB]2.0.CO;2.

Humphris, S.E., and Thompson, G., 1978, Hydrothermal alteration of oceanic basalts by seawater: Geochimica et Cosmochimica Acta, v. 42, p. 107–125, doi:10.1016/0016-7037(78)90221-1.

Ildefonse, B., Blackman, D.K., John, B.E., Ohara, Y., Miller, D.J., and MacLeod, C.J., 2007, Oceanic core complexes and crustal accretion at slow-spreading ridges: Geology, v. 35, p. 623–626, doi:10.1130/G23531A.1.

Ingall, E.D., Schroeder, P.A., and Berner, R.A., 1990, The nature of organic phosphorus in marine sediments: New insights from ^{31}P NMR: Geochimica et Cosmochimica Acta, v. 54, p. 2617–2620, doi:10.1016/0016-7037(90)90248-J.

Irwin, W.P., 1977, Review of Paleozoic rocks of the Klamath Mountains, *in* Stewart, J.H., and Stevens, C.H., eds., Paleozoic Paleogeography of the Western United States: Society of Economic Paleontologists and Mineralogists, Pacific Section, p. 441–455.

Jacobi, R.D., 1976, Sediment slides on the northwestern continental margin of Africa: Marine Geology, v. 22, p. 157–173, doi:10.1016/0025-3227(76)90045-1.

Jacobsen, S.B., Quick, J.E., and Wasserburg, G.J., 1984, A Nd and Sr isotopic study of the Trinity peridotite: Implications for mantle evolution: Earth and Planetary Science Letters, v. 68, p. 361–378, doi:10.1016/0012-821X(84)90122-5.

Johnson, K.T., and Dick, H.B., 1992, Open system melting and temporal and spatial variation of peridotite and basalt at the Atlantis II fracture zone: Journal of Geophysical Research, v. 97, p. 9219–9241, doi:10.1029/92JB00701.

Karson, J.A., and Dick, H.J.B., 1983, Tectonics of ridge-transform intersections at the Kane Fracture Zone: Marine Geophysical Researches, v. 6, p. 51–98, doi:10.1007/BF00300398.

Kistler, R.W., 1990, Two different types of lithosphere in the Sierra Nevada, California, *in* Anderson, J.L., ed., The Nature and Origin of Cordilleran Magmatism: Geological Society of America Memoir 174, p. 271–282.

Kokelaar, B.P., 1982, Fluidization of wet sediments during the emplacement and cooling of various igneous bodies: Journal of the Geological Society [London], v. 139, p. 21–33, doi:10.1144/gsjgs.139.1.0021.

Lackey, J.S., Valley, J.W., and Saleeby, J., 2005, Supracrustal input to magmas in the deep crust of Sierra Nevada batholith: Evidence from high-$\delta^{18}O$ zircon: Earth and Planetary Science Letters, v. 235, p. 315–330, doi:10.1016/j.epsl.2005.04.003.

Lahren, M.M., and Schweickert, R.A., 1989, Proterozoic and Lower Cambrian miogeoclinal rocks of Snow Lake pendant, Yosemite-Emigrant Wilderness, Sierra Nevada, California: Evidence for major Early Cretaceous dextral translation: Geology, v. 17, p. 156–160, doi:10.1130/0091-7613(1989)017<0156:PALCMR>2.3.CO;2.

Le Pourhiet, L., Gurnis, M., and Saleeby, J., 2006, Mantle instability beneath the Sierra Nevada Mountains in California and Death Valley extension: Earth and Planetary Science Letters, v. 251, p. 104–119, doi:10.1016/j.epsl.2006.08.028.

Lee, C.T.A., Luffi, P., Plank, T., Dalton, H., and Leeman, W.P., 2009, Constraints on the depths and temperatures of basaltic magma generation of Earth and other terrestrial planets using new thermobarometers for mafic magmas: Earth and Planetary Science Letters, v. 279, p. 20–33, doi:10.1016/j.epsl.2008.12.020.

Li, Z.A., and Lee, C.A., 2006, Geochemical investigation of serpentinized oceanic lithosphere mantle in the Feather River ophiolite, California: Implications for the recycling rate of water by subduction: Chemical Geology, v. 235, p. 161–185, doi:10.1016/j.chemgeo.2006.06.011.

Liggett, D.L., 1990, Geochemistry of the garnet-bearing Tharps Peak granodiorite and its relation to other members of the Lake Kaweah intrusive suite, southwestern Sierra Nevada, California, *in* Anderson, J.L., ed., The Nature and Origin of Cordilleran Magmatism: Geological Society of America Memoir 174, p. 225–236.

Lockwood, J.P., 1971, Sedimentary and gravity-slide emplacement of serpentinite: Geological Society of America Bulletin, v. 82, p. 919–936, doi:10.1130/0016-7606(1971)82[919:SAGEOS]2.0.CO;2.

Ludwig, K.R., 2001, Users Manual for Isoplot/Ex (rev. 2.49): A Geological Toolkit for Microsoft Excel: Berkeley Geochronology Center Special Publication 1a, 56 p.

Mack, S., Saleeby, J.B. and Farrell, J.E., 1979, Origin and emplacement of the Academy pluton, Fresno County, California: Geological Society of America Bulletin Part I, v. 90, p. 321–323; Part II, v. 90, p. 633–694.

Manning, C.G., 1997, Coupled reaction and flow in subduction zones: Silica metasomatism in the mantle wedge, *in* Jamtveit, B., and Yardley, B.W.D., eds., Fluid Flow and Transport in Rocks, Mechanisms and Effects: London, Chapman and Hall, p. 139–146.

Mattinson, J.M., 1976, Ages of zircons from the Bay of Islands ophiolite complex, western Newfoundland: Geology, v. 4, p. 393–394, doi:10.1130/0091-7613(1976)4<393:AOZFTB>2.0.CO;2.

Mattinson, J.M., 1994, A study of complex discordance in zircons using step-wise dissolution techniques: Contributions to Mineralogy and Petrology, v. 116, p. 117–129, doi:10.1007/BF00310694.

May, J.C., and Hewitt, R.L., 1948, The basement complex in well samples from Sacramento and San Joaquin Valleys, California: California Division of Mines and Geology Journal, v. 44, p. 129–158.

McClelland, W.C., Gehrels, G.E., and Saleeby, J.B., 1992, Upper Jurassic–Lower Cretaceous basinal strata along the Cordilleran margin: Implications for the accretionary history of the Alexander-Wrangellia-Peninsular terrane: Tectonics, v. 11, p. 823–835, doi:10.1029/92TC00241.

Melson, W.G., and Thompson, G., 1971, Petrology of a transform fault zone and adjacent ridge segments: Royal Society of London Philosophical Transactions, ser. A, v. 263, p. 423–442.

Melson, W.G., Hart, S.R., and Thompson, G., 1972, St. Paul's Rocks, equatorial Atlantic: Petrogenesis, radiometric ages, and implications on sea-floor spreading, *in* Shagam, R., et al., eds., Studies in Earth and Space Sciences: A Memoir in Honor of Harry Hammond Hess: Geological Society of America Memoir 132, p. 241–272.

Metcalf, R.V., Wallin, E.T., Willse, K.R., and Muller, E.R., 2000, Geology and geochemistry of the Trinity terrane, California: Evidence of middle Paleozoic depleted supra-subduction zone magmatism in a proto-arc setting, *in* Dilek, Y., Moores, E.M., Elthon, D., and Nicolas, A., eds., Ophiolites and Oceanic Crust: New Insights from Field Studies and the Ocean Drilling Program: Geological Society of America Special Paper 349, p. 403–418.

Miller, E.L., and Sutter, J.F., 1982, Structural geology and $^{40}Ar/^{39}Ar$ geochronology of the Goldstone–Lane Mountain area, Mojave Desert, California: Geological Society of America Bulletin, v. 93, p. 1191–1207, doi:10.1130/0016-7606(1982)93<1191:SGAAGO>2.0.CO;2.

Miller, K.C., and Mooney, W.D., 1994, Crustal structure and composition of the southern Foothills metamorphic belt, Sierra Nevada, California, from seismic data: Journal of Geophysical Research, v. 99, p. 6865–6880, doi:10.1029/93JB02755.

Moiseyev, A.N., 1970, Late serpentinite movements in the California Coast Ranges: New evidence and implications: Geological Society of America Bulletin, v. 81, p. 1721–1732, doi:10.1130/0016-7606(1970)81[1721:LSMITC]2.0.CO;2.

Moore, D.G., Curray, J.R., and Emmel, F.J., 1976, Large submarine slide (olistostrome) associated with Sunda arc subduction zone, northeast Indian Ocean: Marine Geology, v. 21, p. 211–226, doi:10.1016/0025-3227(76)90060-8.

Moore, J.N., and Foster, C.T., Jr., 1980, Lower Paleozoic metasedimentary rocks in the east-central Sierra Nevada, California: Correlations with Great Basin formations: Geological Society of America Bulletin, v. 91, p. 37–43, doi:10.1130/0016-7606(1980)91<37:LPMRIT>2.0.CO;2.

Moore, T.C., Jr., Van Andel, T.H., Blow, W.H., and Heath, G.R., 1970, Large submarine slide off northeastern continental margin of Brazil: American Association of Petroleum Geologists Bulletin, v. 54, p. 125–128.

Mottana, A., and Bocohio, R., 1975, Superferric eclogites of the Voltri Group (Pennidic Belt, Apennines): Contributions to Mineralogy and Petrology, v. 49, no. 3, 201–210, doi:10.1007/BF00376588.

Mottl, M.J., 1983, Metabasalts, axial hot springs, and the structure of hydrothermal systems at mid-ocean ridges: Geological Society of America Bulletin, v. 94, p. 161–180, doi:10.1130/0016-7606(1983)94<161:MAHSAT>2.0.CO;2.

Murphy, J.B., and Nance, R.D., 2008, The Pangea conundrum: Geology, v. 36, p. 703–706, doi:10.1130/G24966A.1.

Nadin, E.S., and Saleeby, J., 2008, Disruption of regional primary structure of the Sierra Nevada batholith by the Kern Canyon fault system, California, *in* Wright, J.E., and Shervais, J.W., eds., Ophiolites, Arcs, and Batholiths: A Tribute to Cliff Hopson: Geological Society of America Special Paper 438, p. 429–454.

Nance, R.D., and Linnemann U., 2008, The Rheic Ocean: Origin, evolution and significance: GSA Today, v. 18, p. 4–12, doi:10.1130/GSATG24A.1.

Ogg, J.G., and Smith, A.G., 2004, The geomagnetic polarity time scale, *in* Gradstein, F.M., Ogg, J.G., and Smith, A.G., eds., A Geologic Time Scale 2004: Cambridge, UK, Cambridge University Press, p. 63–86.

Oliver, H.W., and Robbins, S.L., 1978, Bouguer Gravity Map of California, Fresno Sheet: California Division of Mines and Geology, scale 1:250,000, 1 sheet.

Pearce, J.A., 1982, Trace element characteristics of lavas from destructive plate boundaries, *in* Thorpe, R.S., ed., Andesites: New York, Wiley and Sons, p. 525–548.

Pearce, J.A., Baker, P.E., Harvey, P.K., and Luff, I.W., 1995, Geochemical evidence for subduction fluxes, mantle melting and fractional crystallization beneath the South Sandwich island arc: Journal of Petrology, v. 36, p. 1073–1109.

Pickett, D.A., and Saleeby, J.B., 1994, Nd, Sr, and Pb isotopic characteristics of Cretaceous intrusive rocks from deep levels of the Sierra Nevada batholith, Tehachapi Mountains, California: Contributions to Mineralogy and Petrology, v. 118, p. 198–215, doi:10.1007/BF01052869.

Pockalny, R.A., Detrick, R.S., and Fox, P.J., 1988, Morphology and tectonics of the Kane transform from Sea Beam bathymetry data: Journal of Geophysical Research, v. 93, p. 3179–3193, doi:10.1029/JB093iB04p03179.

Powell, R., and Holland, T., 1994, Optimal geothermometry and geobarometry: American Mineralogist, v. 79, p. 120–133.

Putman, G.W., and Alfors, J.T., 1969, Geochemistry and Petrology of the Rocky Hill Stock, Tulare County, California: Geological Society of America Special Paper 120, 109 p.

Quick, J.E., 1981, Petrology and petrogenesis of the Trinity peridotite, and upper mantle diapir in the eastern Klamath Mountains, California: Journal of Geophysical Research, v. 86, p. 11,837–11,863, doi:10.1029/JB086iB12p11837.

Reagan, M.K., and Meijer, A., 1984, Geology and geochemistry of early arc-volcanic rocks from Guam: Geological Society of America Bulletin, v. 95, p. 701–713, doi:10.1130/0016-7606(1984)95<701:GAGOEA>2.0.CO;2.

Reynolds, J.R., Langmuir, C.H., Bender, J.F., Kastens, K.A., and Ryan, F., 1992, Spatial and temporal variability in the geochemistry of basalts from the East Pacific Rise: Nature, v. 359, p. 493–499, doi:10.1038/359493a0.

Robinson, P.T., Malpas, J., Dilek, Y., and Zhou, M., 2008, The significance of sheeted dike complexes in ophiolites: GSA Today, v. 18, no. 11, p. 4–10, doi:10.1130/GSATG22A.1.

Rogers, R.D., Mann, P., and Emmet, P.A., 2007, Tectonic terranes of the Chortis block based on integration of regional aeromagnetic and geologic data, *in* Mann, P., ed., Geologic and Tectonic Development of the Caribbean Plate in Northern Central America: Geological Society of America Special Paper 428, p. 65–88.

Rommevaux-Jestin, C., Deplus, C., and Patriat, P., 1997, Mantle Bouguer anomaly along an ultra slow-spreading ridge: Implications for accretionary processes and comparison from central Mid-Atlantic Ridge: Marine Geophysical Researches, v. 19, p. 481–503, doi:10.1023/A:1004269003009.

Rosencrantz, E., Malcolm, I.R., and Sclater, J.G., 1988, Age and spreading history of the Cayman Trough as determined from depth, heat flow, and magnetic anomalies: Journal of Geophysical Research, v. 93, p. 2141–2157, doi:10.1029/JB093iB03p02141.

Ross, C.A., and Ross, J.R.P., 1983, Late Paleozoic accreted terranes of western North America, *in* Stevens, C.H., ed., Pre-Jurassic Rocks in Western North America Suspect Terranes: Society of Economic Paleontologists and Mineralogists, Pacific Section, p. 7–22.

Rubin, C.M., Miller, M.M., and Smith, G.M., 1990, Tectonic development of Cordilleran mid-Paleozoic volcano-plutonic complexes: Evidence for convergent margin tectonism, *in* Howard, D.S., and Miller, M.M., eds., Paleozoic and Early Mesozoic Paleogeographic Relations in the Klamath Mountains, Sierra Nevada, and Related Terranes: Geological Society of America Special Paper 255, p. 1–16.

Saleeby, J.B., 1975, Structure, petrology and geochronology of the Kings-Kaweah mafic-ultramafic belt, southwestern Sierra Nevada Foothills, California [Ph.D. thesis]: Santa Barbara, University of California, Santa Barbara, 286 p.

Saleeby, J.B., 1977, Fracture zone tectonics, continental margin fragmentation, and emplacement of the Kings-Kaweah ophiolite belt, southwest Sierra Nevada, California, *in* Coleman, R.G., and Irwin, W.P., eds., North American Ophiolites: Oregon Department of Geology and Mineral Industries Bulletin 95, p. 141–160.

Saleeby, J.B., 1978, Kings River ophiolite, southwest Sierra Nevada Foothills, California: Geological Society of America Bulletin, v. 89, p. 617–636, doi:10.1130/0016-7606(1978)89<617:KROSSN>2.0.CO;2.

Saleeby, J.B., 1979, Kaweah serpentinite melange, southwest Sierra Nevada Foothills, California: Geological Society of America Bulletin, v. 90, p. 29–46, doi:10.1130/0016-7606(1979)90<29:KSMSSN>2.0.CO;2.

Saleeby, J.B., 1982, Polygenetic ophiolite belt of the California Sierra Nevada, geochronological and tectonostratigraphic development: Journal of Geophysical Research, v. 87, p. 1802–1824.

Saleeby, J.B., 1990, Geochronological and tectonostratigraphic framework of Sierran-Klamath ophiolitic assemblages, *in* Howard, D.S., and Miller, M.M., eds., Paleozoic and Early Mesozoic Paleogeographic Relations in the Klamath Mountains, Sierra Nevada, and Related Terranes: Geological Society of America Special Paper 255, p. 93–114.

Saleeby, J., 2007, Western extent of the Sierra Nevada batholith in the Great Valley Basement: Eos (Transactions, American Geophysical Union), v. 88, F2186.

Saleeby, J.B., and Busby, C., 1993, Paleogeographic and tectonic setting of axial and western metamorphic framework rocks of the southern Sierra Nevada, California, *in* Dunne, G., and McDougall, K., eds., Mesozoic Paleogeography of the Western United States—II: Society of Economic Paleontologists and Mineralogists, Pacific Section, Book 71, p. 197–226.

Saleeby, J., and Dunne, G.C., 2011, Temporal and structural relations of early Mesozoic arc plutonism, southern Sierra Nevada, California: Geological Society of America Bulletin (in press).

Saleeby, J.B., and Sharp, W.D., 1980, Chronology of the structural and petrologic development of the southwest Sierra Nevada Foothills, California: Geological Society of America Bulletin, pt. 1, v. 91, p. 317–320; pt. 2, v. 91, p. 1416–1535.

Saleeby, J.B., Busby, C., Goodin, W.D., and Sharp, W.D., 1978, Early Mesozoic paleotectonic-paleogeographic reconstruction of the southern Sierra Nevada region, California, *in* Howell, D., ed., Mesozoic Paleogeography of the Western United States: Society of Economic Paleontologists and Mineralogists, Pacific Section, p. 311–336.

Saleeby, J.B., Hannah, J.L., and Varga, R.J., 1987, Isotopic age constraints on middle Paleozoic deformation in the northern Sierra Nevada, California: Geology, v. 15, p. 757–760, doi:10.1130/0091-7613(1987)15<757:IACOMP>2.0.CO;2.

Saleeby, J.B., Busby-Spera, C., Oldow, J.S., Dunne, G.C., Wright, J.E., Cowan, D.S., Walker, N.W., and Allmendinger, R.W., 1992, Early Mesozoic tectonic evolution of the western U.S. Cordillera, *in* Burchfiel, B.C., Lipman, P.W., and Zoback, M.L., eds., The Cordilleran Orogen: Conterminous U.S.: Boulder, Colorado, Geological Society of America, Geology of North America, v. G-3, p. 107–168.

Saleeby, J., Ducea, M., and Clemens-Knott, D., 2003, Production and loss of high-density batholithic root, southern Sierra Nevada region: Tectonics, v. 22, no. 6, p. 1–24, doi:10.1029/2002TC001374.

Saleeby, J., Farley, K., Kistler, R.W., and Fleck, R., 2007, Thermal evolution and exhumation of deep level batholithic exposures, southernmost Sierra Nevada, California, *in* Cloos, M., Carlson, W.D., Gilbert, M.C., Liou, J.G., and Sorensen, S.S., eds., Convergent Margin Terranes and Associated Regions: A Tribute to W.G. Ernst: Geological Society of America Special Paper 419, p. 39–66, doi:10.1130/2007.2419(02).

Schreiber, E., and Fox, P.J., 1977, Density and P-wave velocity of rocks from the FAMOUS region and their implication to the structure of the oceanic crust: Geological Society of America Bulletin, v. 88, p. 600–608, doi:10.1130/0016-7606(1977)88<600:DAPVOR>2.0.CO;2.

Schroeder, T., and John, B.E., 2004, Strain localization on an oceanic detachment fault system, Atlantis Massif, 30 degrees north, Mid-Atlantic Ridge: Geochemistry Geophysics Geosystems, v. 5, Q11007, doi:10.1029/2004GC000728.

Schroeder, T., Cheadle, M.J., Dick, H.J.B., Faul, U., Casey, J.F., and Keleman, P.B., 2007, Nonvolcanic seafloor spreading and corner-flow rotation accommodated by extensional faulting at 15°N on the Mid-Atlantic Ridge: A structural synthesis of ODP Leg 209: Geochemistry Geophysics Geosystems, v. 8, Q06015, doi:10.1029/2006GC001567.

Schweickert, R.A., and Lahren, M.M., 1989, Triassic caldera at Tioga Pass, Yosemite National Park, CA: Structural relations and significance: Geological Society of America Abstracts with Programs, v. 21, no. 5, p. 141.

Schweickert, R.A., Saleeby, J.B., and Tobisch, O.T., 1977, Paleotectonic and paleogeographic significance of the Calaveras complex, western Sierra Nevada, California, *in* Stewart, J.H., and Stevens, C.H., eds., Paleozoic Paleogeography of the Western United States: Society of Economic Paleontologists and Mineralogists, Pacific Section, p. 381–394.

Shaw, H.F., Chen, J.H., Saleeby, J.B., and Wasserburg, G.J., 1987, Nd-Sr-Pb systematics and age of the Kings River ophiolite, California: Contributions to Mineralogy and Petrology, v. 96, p. 281–290, doi:10.1007/BF00371249.

Shervais, J.W., 1982, Ti-V plots and the petrogenesis of modern and ophiolitic lavas: Earth and Planetary Science Letters, v. 59, p. 101–118, doi:10.1016/0012-821X(82)90120-0.

Shervais, J.W., Murchy, B.L., Kimbrough, D.L., Renne, P.R., and Hanan, B., 2005, Radioisotopic and biostratigraphic age relations in the Coast Range ophiolite, northern California: Implications for the tectonic evolution of the western Cordillera: Geological Society of America Bulletin, v. 117, p. 633–653, doi:10.1130/B25443.1.

Smith, D.L., and Miller, E.L., 1990, Late Paleozoic extension in the Great Basin, western United States: Geology, v. 18, p. 712–715, doi:10.1130/0091-7613(1990)018<0712:LPEITG>2.3.CO;2.

Snoke, A.W., Sharp, W.D., Wright, J.E., and Saleeby, J.B., 1982, Significance of mid-Mesozoic peridotitic to dioritic intrusive complexes, Klamath Mountains–western Sierra Nevada: Geology, v. 10, p. 160–166, doi:10.1130/0091-7613(1982)10<160:SOMPTD>2.0.CO;2.

Snow, C.A., 2007, Petrotectonic evolution and melt modeling of the Penon Blanco arc, central Sierra Nevada foothills, California: Geological Society of America Bulletin, v. 119, p. 1014–1024, doi:10.1130/B25972.1.

Spear, F.S., 1993, Metamorphic Phase Equilibria and Pressure-Temperature-Time Paths: Mineralogical Society of America Monograph, 799 p.

Stern, R.J., 2004, Subduction initiation: Spontaneous and induced: Earth and Planetary Science Letters, v. 226, p. 275–292.

Stern, R.J., and Bloomer, S.H., 1992, Subduction zone infancy: Examples from the Eocene Izu-Bonin-Mariana and Jurassic California: Geological Society of America Bulletin, v. 104, p. 1621–1636, doi:10.1130/0016-7606(1992)104<1621:SZIEFT>2.3.CO;2.

Stern, T.W., Bateman, P.C., Morgan, B.S., Newell, M.F., and Peck, D.L., 1981, Isotopic U-Pb Ages of Zircon from the Granitoids of the Central Sierra Nevada, California: U.S. Geological Survey Professional Paper 1185, 17 p.

Stern, R.J., Morris, J., Bloomer, S.H., and Hawkins, J.W., Jr., 1991, The source of the subduction component in convergent margin magmas: Trace element and radiogenic isotope evidence from Eocene boninites, Mariana forearc: Geochimica et Cosmochimica Acta, v. 55, p. 1467–1481, doi:10.1016/0016-7037(91)90321-U.

Stevens, C.H., 2009, New Occurrences of Permian Corals from the McCloud Belt in Western North America: Palaeontologia Electronica, v. 12, I. 2A, 16 p.

Stevens, C.H., and Greene, D.C., 2000, Geology of Paleozoic rocks in eastern Sierra Nevada roof pendants, California, *in* Lageson, D.R., Peters, S.G., and Lahren, M.M., eds., Great Basin and Sierra Nevada: Geological Society of America Field Guide 2, p. 237–254.

Stevens, C.H., and Stone, P., 2005, Structure and regional significance of the Late Permian(?) Sierra Nevada–Death Valley thrust system, east-central California: Earth-Science Reviews, v. 73, p. 103–113, doi:10.1016/j.earscirev.2005.04.006.

Stevens, C.H., Stone, P., and Miller, J.S., 2005, A new reconstruction of the Paleozoic continental margin of southwestern North America: Implications for the nature and timing of continental truncation and the possible role of the Mojave-Sonora megashear, *in* Anderson, T.H., Nourse, J.A., McKee, J.W., and Steiner, M.B., eds., The Mojave-Sonora Megashear Hypothesis: Development, Assessment, and Alternatives: Geological Society of America Special Paper 393, p. 597–618.

Stone, P., and Stevens, Ch., 1988, Pennsylvanian and Early Permian Paleogeography of east-central California; implications for the shape of the continental margin and the timing of continental truncation: Geology, v. 16, p. 330–333, doi:10.1130/0091-7613(1988)016<0330:PAEPPO>2.3.CO;2.

Sun, S., and McDonough, W.F., 1989, Chemical and isotopic systematics of oceanic basalts: Implications for mantle composition and processes, *in* Saunders, A.D., and Norry, M.J., eds., Magmatism in the Ocean Basins: Geological Society [London] Special Publication 42, p. 313–345.

Taylor, R.N., Nesbitt, R.W., Vidal, P., Harmon, R.S., Auvray, B., and Croudace, I.W., 1994, Mineralogy, chemistry, and genesis of boninite series volcanics, Chichijima, Bonin Islands, Japan: Journal of Petrology, v. 35, p. 577–617.

Terra, F., and Wasserburg, J.G., 1972, U/Pb systematics in lunar basalts: Earth and Planetary Science Letters, v. 17, p. 65–78.

Tilton, G.R., Hopson, C.A., and Wright, J.W., 1981, Uranium-lead isotopic ages of the Samail ophiolite, Oman, with applications to Tethyan ocean ridge tectonics: Journal of Geophysical Research, v. 86, p. 2763–2775, doi:10.1029/JB086iB04p02763.

Tucholke, B.E., Behn, M.D., Buck, W.R., and Lin, J., 2008, Role of melt supply in oceanic detachment faulting and formation of megamullions: Geology, v. 36, p. 455–458, doi:10.1130/G24639A.1.

Van Andel, T.H., von Herzen, R.P., and Phillips, J.D., 1971, The Vema fracture zone and the tectonics of transverse shear zones in oceanic plates: Marine Geophysical Research, v. 1, p. 261–283.

Varne, R., and Rubenach, M.J., 1972, The geology of Macquarie Island and its relationship to oceanic crust, *in* Hayes, D.E., ed., Antarctic Oceanology II, The Australian–New Zealand Section: Washington, D.C., American Geophysical Union, p. 251–266.

Wakabayashi, J., 1990, Counterclockwise P-T-t paths from amphibolites, Franciscan complex, California: Relics from the early stages of subduction zone metamorphism: Journal of Geology, v. 98, p. 657–680, doi:10.1086/629432.

Walker, J.D., 1988, Permian and Triassic rocks of the Mojave Desert and their implications for timing and mechanisms of continental truncation: Tectonics, v. 7, p. 685–709, doi:10.1029/TC007i003p00685.

Wallin, E.T., and Metcalf, R.V., 1998, Supra-subduction zone ophiolite formed in an extensional forearc: Trinity terrane, Klamath Mountains, California: Journal of Geology, v. 106, p. 591–608.

Watkins, R., Reinheimer, C.E., Wallace, J.W., and Nestell, M.K., 1987, Paleogeographic significance of a Permian sedimentary megabreccia in the central belt of the northern Sierra Nevada: Geological Society of America Abstracts with Programs, v. 19, p. 771.

Wentworth, C.M., Fisher, G.R., Levine, P., and Jachens, R.C., 1995, The surface of crystalline basement, Great Valley and Sierra Nevada, California: A digital map database: U.S. Geological Survey Open-File Report 95-96.

Wolf, M.B., and Saleeby, J.B., 1995, Late Jurassic dike swarms in the southwestern Sierra Nevada Foothills terrane, California: Implications for the Nevadan orogeny and North American plate motion, *in* Miller, D.M., and Busby, C., eds., Jurassic Magmatism and Tectonics of the North American Cordillera: Geological Society of America Special Paper 299, p. 203–228.

Zandt, G., Gilbert, H., Owens, T., Ducea, M., Saleeby, J., and Jones, C., 2004, Active foundering of a continental arc root beneath the southern Sierra Nevada, California: Nature, v. 431, p. 41–46, doi:10.1038/nature02847.

Zindler, A., and Hart, S., 1986, Chemical Geodynamics: Annual Review of Earth and Planetary Sciences, v. 14, p. 493–571, doi:10.1146/annurev.ea.14.050186.002425.

Manuscript Accepted by the Society 21 December 2010